NTNU – Trondheim
Norwegian University of
Science and Technology

Submicron Particles and Inflammation

Dessislava Dimitrova Mihaylova

Chemical Engineering and Biotechnology
Submission date: June 2012
Supervisor: Gudmund Skjåk-Bræk, IBT
Co-supervisor: Asbjørn Magne Nilsen, NTNU, Det Medisinske Fakultet, Institutt for Kreftforskning og Molekylær medisin

Norwegian University of Science and Technology
Department of Biotechnology

Acknowledgements

This work was carried out at the Institute of Cancer Research and Molecular Biology at NTNU, Trondheim.

The author would like to thank her supervisors Professor Asbjørn Nilsen and Professor Gudmund Skjåk-Bræk for helpful discussions regarding this work. Both my supervisors have guided me through this year with enthusiasm and constructive criticism.

Further, the author would like to thank Chief Engineer Liv Ryan for excellent technical assistance and Bioengineer Bjørg Steinkjer for her help regarding the work with whole blood. Senior Engineer Kjartan W. Egeberg is thanked for his help with the confocal microscopy. A last thank to my fellow Master student Linn Elise Gulliksen for support and excellent collaboration at the lab during this last year's work.

Trondheim, June 9th, 2012

Dessislava D. Mihaylova

Summary

Iron nanoparticles occur naturally in the environment, but their exposure increases dramatically due to the field of nanotechnology and –medicine. It is poorly understood how the intracellular cooperative mechanisms of submicron particles and microorganisms function on mammalian immune system. In this study, superparamagnetic iron oxide (SPIO) submicron particles will be used to benefit the research within environmental diseases, addressing the biocompatibility of these particles.

The size-dependent effects in the immune system of two carboxyl coated SPIO particles with stated sizes 100 nm and 1 μm will be studied *in vitro*. It would be interesting to determine whether these particles were able to activate the inflammasome, but still, the precise molecular mechanisms for the activation remain unknown. In order to reveal the biocompatibility of these particles, tests were performed as a function of particle concentration ranging from 0.01 to 100 μg/mL using both whole blood and peripheral blood mononuclear cells (PBMC) isolated from healthy donors. The monocytes were first primed with Lipopolysaccharide from *Escherichia coli* 0111:B4 strain, followed by stimulation with increasing concentrations of the submicron particles.

Flow cytometry on whole blood samples identified up-regulation of CD11b monocytes and granulocytes by the particles. In addition, Terminal Complement Complex analyses proved activation of the complement system. It is possible that the particles have been coated with C3b by the complement and phagocytized by the monocytes through CD11b/CD18 receptor. Cytokine secretion from monocytes and whole blood was measured with sandwich ELISA and Bio-plex.

The smaller particles seemed to induce higher inflammatory responses than the larger ones. It was, however, interesting to find that the particles themselves caused secretion of active IL-1β without being primed in advance. The mechanisms of the NLRP3 inflammasome activation might be explained by ROS production due to iron imbalance in the cytoplasm. Toxicity of the particles was seen at 10 μg/mL, suggesting their potentially low biocompatibility above this concentration. However, it is suggested better biocompatibility of the silica coated 1 μm particles than the polysaccharide coated 100 nm particles.

Sammendrag

Jernpartikler eksisterer naturlig i miljøet, men eksponeringen for disse øker i takt med økende bruk av slike partikler innen blant annet medisinsk teknologi. Det er liten kjennskap til hvordan mikro- og nanopartikler påvirker det mammalske immunsystemet. Hensikten med dette prosjektet er derfor å bruke superparamagnetiske jernoksid (SPIO) sub-micron partikler i korrelasjon med bakterielle komponenter for å bedre forståelse av hvordan immunsystemet påvirkes av disse.

To typer partikler vil bli brukt til denne studien, én med hydrodynamisk diameter på 100 nm og én på 1 µm. Hensikten er å blant annet undersøke om disse aktiverer NLRP3 inflammasomet i monocytter *in vitro*, ved å forhåndsaktivere monocyttene med LPS fra *E. coli* og deretter stimulere med økende konsentrasjon av partiklene. Selv om det fortsatt er usikkerhet rundt de molekylære aktiveringsmekanismene for inflammasomet er det ved hjelp av denne studien blitt foreslått en dose-responskurve for begge partiklene. Partikkelkonsentrasjonene har variert fra 0.01 µg/mL til 100 µg/mL, og liknende stimuleringer har blitt utført i både monocytt- og fullblodsforsøk. Cytokinresponsen i begge typer forsøk har blitt analysert med både ELISA og multivariat cytokinanalyse.

Flowcytometri på fullblodsprøver har detektert en oppregulering av CD11b monocytter og granulocytter. I tillegg har C5b-9 analyser vist at partiklene i seg selv aktiverer komplementsystemet. Det foreslås at partiklene har blitt merket med C3b av komplementsystemet og deretter fanget opp av CD11b/CR3.

De minste partiklene ser ut til å fremkalle en høyere inflammatorisk respons sammenliknet med de større partiklene. Videre funn viste, overraskende nok, at partiklene i seg selv var i stand til å aktivere inflammasomet uten forhåndsaktivering av monocyttene med LPS. ROS-dannelse er en foreslått aktiveringsmekanisme for inflammasomet. Det ble observert en toksisitet for partiklene fra 10 µg/mL. Disse resultatene foreslår at partiklene er biologisk anvendbare for konsentrasjoner under 10 µg/mL, hvor 1 µm partiklene generelt gir lavere aktivering av inflammatoriske reaksjoner enn 100 nm partiklene.

Table of contents

Abbreviations

Ab	Antibody
Ag	Antigen
Ala	Alanine
Asp	Aspartate
ATP	Adenosine-5'-triphosphate
AU	Arbitrary Units
BSA	Bovine Serum Albumine
C	Complement components
CD	Cluster of Differentiation
CR	Complement Receptor
DIC	Differential Interference Contrast
DNA	Deoxyribonucleic acid
EDTA	Ethylenediaminetetraacetic acid
ELISA	Enzyme-Linked ImmunoSorbent Assay
FBS	Fetal Bovine Serum
fl	Femtoliters
Gly	Glycine
G-CSF	Granulocyte Colony-Stimulating Factor
GM-CSF	Granulocyte-Macrophage Colony-Stimulating Factor
H_2O_2	Hydrogen Peroxide
H_2SO_4	Sulfuric acid
HI	Heat Inactivated
Ig	Immunoglobulin
IL	Interleukin
IFN	Interferon
IRAK	IL-1 Receptor Kinases
LPS	Lipopolysaccharide
LRR	Leucine-Rich Regions
M	Medium
MAC	Membrane Attack Complex
Mal	MyD88 Adapter Like

MBL	Mannose-Binding Lectin
MCP	Monocyte Chemotactic Protein
MD	Lymphocyte antigen 96 (cell surface protein)
MIP	Macrophage Inflammatory Protein
mM	milliMolar
MO	Monocyte
MyD	Myeloid Differentiation primary response gene
NF	Nuclear Factor
NK	Natural Killer cells
NLRP	NOD-Like Receptor Protein
NOD	Nucleotide Oligomerization Domain
PAMP	Pathogen-Associated Molecular Patterns
PBMC	Peripheral Blood Mononuclear Cells
PBS	Phosphate Buffered Saline
PFA	Paraformaldehyde
PMT	Photomultiplier
PRR	Pattern Recognition Receptors
ROS	Reactive Oxygen Species
rpm	Rounds per minute
RPMI	Roswell Park Memorial Institute
SPION	SuperParamagnetic Iron Oxide Nanoparticles
TACE	TNF-α converting enzyme
TCC	Terminal Complement Complex
Th	T helper cells
TIR	Toll/IL-1 Receptor
TLR	Toll-Like Receptor
TMB	Tetramethylbenzidine
TNF	Tumour Necrosis Factor
TRAM	TRIF-Related Adaptor Molecule
TRIF	Toll/IL-1R domain-containing adaptor-inducing interferon

1 Introduction

1.1 Background

Inflammation is an underlying condition of many diseases that represent important public health problems. It is believed that cytokines, that are signaling substances of the immune system and important regulators of the inflammatory process, are affected by exposure from environmental particles. Particles administered alone may induce production of one set of cytokines that is different from the one produced after co-existing exposure to microorganisms. Thus, particles may influence upon the immune responses against bacteria.

Airway diseases are often associated with exposure to microbial products through the inhalation of bacterial fragments such as Lipopolysaccharide (LPS). It is known that high administration of LPS can induce fever, increase heart rate, and lead to septic shock and organ dysfunction (Parrillo, 1993). It is also shown that levels of LPS within the environment can correlate with severity of asthma. LPS can often coexist with pollutant exposure, which causes inhalation of small particulate matter to become an additional cause of airway inflammation (Chaudhuri et al., 2010). It is also proven that there is an increased incidence of respiratory diseases with the increased use of nanoparticles (Yazdi Amir et al., 2010).

General background theory throughout this chapter is obtained from the educational literature books (Kindt et al., 2007, Madigan et al., 2009).

1.2 Blood

1.2.1 Blood plasma and serum

Blood serum is commonly used as the primary nutritive supplement for cell cultures. Addition of serum to culture medium provides hormones, growth factors, essential fatty acids and other agents that are necessary for cell survival and growth.

The complement system is a heat-labile bactericidal factor in serum which is required along with heat-stable antibody (Gasque, 2004). It is therefore possible to heat inactivate complement at 56°C for 30 minutes.

1.2.2 Monocytes

Monocytes are mononucleated, white blood cells (leukocytes) and are part of the innate immune system. The progenitors of the monocytes are produced in the bone marrow by a process known as hematopoiesis. The differentiated pro-monocytes leave the bone marrow and enter the blood, where they further differentiate into mature monocytes. Monocytes spend some time circulating in the bloodstream during which they enlarge, after which they migrate into the tissues and differentiate into specific tissue macrophages. Here, macrophages are activated by a variety of stimuli in the course of an immune response.

1.2.3 Granulocytes

Granulocytes are leukocytes with granules in their cytoplasm. This type of cells can be divided into three sub-types, known as the neutrophils, basophils and eosinophils. Their general functions are to phagocytize foreign material coated with antibody (Ab) or complement.

1.3 Cytokines

Cytokines are low-molecular-weight regulatory proteins. They are secreted by various types of cells in the body, including monocytes and granulocytes, and function as messenger molecules acting between cells. Cytokine production is generally induced in response to stimuli from an infection. The cytokines exercise their effect in cells via specific high affinity cell-surface cytokine receptors. Because cytokines and their optimum receptors exhibit so high affinities for each other, cytokines can mediate biological effects at picomolar concentrations.

Upon activation, cells generate intracellular processes leading to changes in gene transcription (Meager, 1998). These proteins also stimulate growth and differentiation of cells. Many cytokines are referred to as interleukins (ILs).

Seventeen cytokines have been briefly described in the following sections.

1.3.1 IL-1β

Interleukin-1 includes both IL-1α and IL-1β, and is produced mainly by monocytes. The latter form has many biological effects and needs therefore to be tightly regulated. Like many other cytokines, IL-1β is transcriptionally regulated (Latz, 2010). Once it is released, it activates the inflammatory response at the site of infection (Franchi et al.,

2009). It is, as one of many things, the primary cause of chronic and acute inflammation. In addition, it is a pyrogenic cytokine causing fever as one of the symptoms for septic shock (Nilsen, 2011). An IL-1β converting enzyme (caspace-1) cleaves this cytokine's pro-form at two sequence-related sites: Asp-27-Gly-28 and Asp-116-Ala-117, but it does not cleave IL-1α. This is described in further details in chapter 1.6.3.

In combination with other interleukins such as IL-3 and IL-6, IL-1 probably stimulates proliferation and differentiation of the various haematopoietic cell lineages. In addition, IL-1 has a synergetic effect with IL-6 on IL-2 synthesis by activated T lymphocytes. IL-1 also has synergetic effect with IL-4 on B-cell activation and immunoglobulin isotype regulation, and with IL-2 or IFN on augmenting natural killer (NK) cell activity (Meager, 1998).

1.3.2 IL-2

Interleukin-2 binds to high-affinity receptors expressed mainly by CD4+ T lymphocytes, and stimulates proliferation of these cells. It also acts on NK cells, B lymphocytes and macrophages. When acting on B cells, their proliferation is stimulated, as well as the induction of immunoglobulin (Ig) synthesis. IL-2 also stimulates T cells to synthesize and secrete several other cytokines, including IFN-γ and IL-4 (Meager, 1998).

Although CD4+ T lymphocytes are the main source of IL-2 production, it has been shown that murine dendritic cells that have been activated by LPS, for instance, have detectable production of IL-2. In contrast, no production of this cytokine can be detected in macrophages (Thomson and Lotze, 2003).

1.3.3 IL-4 and IL-13

Human IL-4 is shown to encode a precursor polypeptide which, following cleavage yields the mature protein IL-4. It is produced by cells of the T-lymphoid lineage, principally by activated T-helper 2 (Th2) cells and mast cells (Meager, 1998). It stimulates or aids proliferation of B lymphocytes, where it promotes Ig class switching and induces IgE and IgG secretion *in vitro* (Nuesslein and Spiegelberg, 1990). IL-4 is required for virtually all primary IgE responses in mice (Snapper, 1996). IL-4 belongs to a subset of cytokines that include IL-3, IL-5 and GM-CSF.

IL-13 is an IL-4 like regulator of inflammatory and immune responses. Both are produced by CD4+ T cells and at low levels by CD8+ T cells. Detectable levels of IL-13

protein are, however, produced after two hours of activation. Ongoing IL-13 protein production can still be observed 72 hours after activation of human T-cell. On the contrary, no detectable levels of IL-4 can be observed 24 hours after activation of human T-cell. This gives reason to believe that IL-13 is produced early, and in contrast to IL-4, over prolonged periods of time (Snapper, 1996).

Both IL-4 and IL-13 have comparable effects on monocytes and proliferation of human B lymphocytes (Meager, 1998). They both inhibit the production of pro-inflammatory cytokines, IL-10, IL-12, and IFN-α by monocytes (Snapper, 1996).

1.3.4 IL-5

Eosinophil progenitors are phagocytic granulocytes that can migrate from blood to tissue space and their proliferation and differentiation is induced by IL-5. Eosinophils are thought to play a role in the defense against parasitic organisms, as well as in allergic responses (Kindt et al., 2007). IL-5 is also produced by T lymphocytes (Thomson and Lotze, 2003).

1.3.5 IL-6

Cytokine IL-6 is known to induce the acute-phase response and other transcriptionally inflammatory responses. Still, it is less toxic than IL-1β and TNF-α. IL-6 is a late-acting differentiation factor in mature B lymphocytes. It also functions in the activation of T cells, in addition to enhancing Ig secretion by B cells (Meager, 1998). IL-6 is characterized as the chief stimulator of the production of most acute phase proteins in response to varied stimuli (Gabay, 2006). This cytokine is important to the transition between acute and chronic inflammation by the recruitment of monocytes to the area of inflammation (Gabay, 2006).

LPS, as well as IL-1 and TNF, enhances IL-6 synthesis by monocytes and fibroblasts. IFN-γ induces IL-6 production by macrophages and endothelial cells. IL-4 stimulates IL-6 synthesis in keratinocytes and endothelial cells, whereas it inhibits IL-6 (and IL-1 and TNF-α) production in monocytes and fibroblasts. IL-10 and IL-13 are potent inhibitors of IL-6 production by macrophages and monocytes (Snapper, 1996).

1.3.6 IL-7

IL-7 receptors are present on B cell progenitors, but not on mature B cells, meaning that IL-7 supports growth of immature B cells. IL-7 receptors are also present on early and mature T cells (Meager, 1998).

1.3.7 IL-8

IL-8 is a member of the small chemokine superfamily. It is a chemotactic cytokine with specificity mainly for neutrophils and T lymphocytes. Raised levels of IL-8 may inflict on harmful cell-mediated toxicity by inappropriately attracting activated neutrophils, monocytes and lymphocytes into tissues and organs (Meager, 1998).

1.3.8 IL-10

Interleukin 10 is known as a cytokine synthesis suppressing factor produced by human T cells, monocytes and carcinoma cells. For instance, it inhibits cytokine synthesis of IFN-γ by Th1 cells, as well as the production of the pro-inflammatory cytokines IL-1, IL-6 and TNF-α by monocytes. In contrast to IL-8, elevated levels of IL-10 may be the organism's attempt to down-regulate cytokine overproduction (Meager, 1998, Thèze, 1999). Human IL-10 appears to be produced by activated CD8+ cytotoxic T lymphocytes, B cell lymphomas, and LPS-activated monocytes, amongst others. In possible synergetic activity with IL-4, IL-10 blocks the production of IL-1, IL-6, IL-8, TNF-α, G-CSF, GM-CSF by LPS-activated monocytes. In addition, the production of chemokines like IL-8 and MIP-1α is blocked by IL-10 in macrophages (Meager, 1998). In monocytes, IL-10 is produced later than pro-inflammatory cytokines (Thèze, 1999).

1.3.9 IL-12

IL-12 is mainly produced by B lymphocytes and is known as both a stimulatory factor and a cytotoxic lymphocyte maturation factor (Meager, 1998). There are indications that IL-12 stimulates IFN-γ production by T cells and NK cells by cooperation with IL-1 or TNF-α. The presence of IFN-γ may favor the development of the Th1 subset by inhibiting the production of IL-10 by macrophages (Thèze, 1999).

Upon activation of phagocytic cells with LPS, accumulation of IL-12 is observed within two to four hours, after which it subsides after several hours (Thèze, 1999).

1.3.10 IL-17

This cytokine is an activator of T cell-dependent inflammatory reaction. It appears to act like IL-1 and TNF-α by inducing IL-6 and IL-8 production and enhancing cell-surface expression of adhesion molecules (Meager, 1998).

1.3.11 G-CSF

Granulocyte colony-stimulating factor (G-CSF) mainly stimulates proliferation and differentiation of granulocytes. G-CSF is one of the four classic haemotapoietic growth factors, the others being GM-CSF, M-CSF and IL-3 (Meager, 1998).

1.3.12 GM-CSF

Granulocyte-macrophage colony-stimulating factor (GM-CSF) stimulates proliferation and activation of mainly granulocytes and monocytes. GM-CSF can be produced by many cell types, including monocytes and T lymphocytes (Meager, 1998). GM-CSF appears to share biological activities with IL-3, and there is reason to believe that these two cytokines act synergetically with IFN-γ (Snapper, 1996).

1.3.13 IFN-γ

In general, interferon is not a single protein but a heterogeneous group of molecules. The IFNs can be divided into three types, where type 1 includes IFN-α and –β, type 2 includes IFN-γ, and type 3 includes IFN-λ (Mogensen, 2009). IFN-γ is a single protein in all animal species, and it is glycosylated and proteolytically processed in variable ways at the C terminal end, producing different heterogeneous molecular species of IFN-γ. This specific cytokine has antiviral activity, and is a macrophage-activating factor. In addition, IFN-γ is a co-stimulator for proliferation of B lymphocytes, where it enhances IgG secretion. IFN-γ induces the production of the pro-inflammatory cytokines IL-1, IL-6 and TNF-α by monocytes, which IL-10 inhibits. High levels of IFN-γ is not acutely toxic, but it may potentiate certain TNF-α actions (Meager, 1998).

1.3.14 MCP-1

When monocyte chemotactic protein-1 (MCP-1) is up-regulated, for instance by LPS, monocytes, NK-cells and T lymphocytes are recruited and activated. This may often cause glomerular damage (Gu et al., 2007). MCP-1 induces expression of CD11b, CD11c, IL-1 and IL-6. MCP-1 can activate as well as attracts monocytes, but has not the ability to differentiate them into macrophages (Allavena et al., 1999).

1.3.15 MIP-1β

Macrophage inflammatory protein-1β (MIP-1β) is a chemoattractant cytokine which attracts and causes migration of CD4+ T lymphocytes and monocytes (Schall et al., 1993). Its expression is induced by pro-inflammatory stimuli, such as LPS (Ziegler et al., 1991).

1.3.16 TNF-α

Human Tumor Necrosis Factor α (TNF-α) is synthesized as a larger precursor and is mainly produced by activated macrophages in response to inflammation and other environmental stresses. TNF-α is an inducer of cytokines and cell adhesion molecules, in addition to regulating proliferation and differentiation in lymphocytes and haemopoietic progenitors (Meager, 1998). TNF-α accumulates within two hours after stimulation of phagocytic cells with LPS (Thèze, 1999).

TNF-α converting enzyme (TACE) is a protease that processes pro-TNF-α to the mature and secreted component TNF-α (McGeehan et al., 1994, Newton et al., 2001). It is shown that several proteases have the ability to process the pro-inflammatory TNF-α, but TACE is the one with the highest efficiency (Newton et al., 2001).

1.3.17 Cytokines in allergic responses

Human CD4+ Th cells can be divided into at least three major subsets according to their cytokine production profiles. Th1 cells produce, among other cytokines, relatively high levels of IL-2, IFN-γ, but no IL-4 or IL-5. On the other hand, following Ag-specific stimulation, Th2 cells generally synthesize high levels of IL-4, IL-5, IL-6, IL-9, IL-10 and IL-13 and no or low levels of IL-2 and IFN-γ. Th0, produces both Th1 and Th2 cytokines (Snapper, 1996, Thèze, 1999).

Th1 cells are predominantly involved in delayed hypersensitivity reactions and, through the production of IFN-γ, in the activation of macrophages to eliminate intracellular pathogens. Th2 cells are efficient in giving help to B cells for antibody production (Snapper, 1996).

1.4 Complement system

The complement system is a protein-based defense in blood serum, and plays a key role in both innate and adaptive immunity. A major role for this system is the recognition

and destruction of pathogens. After initial activation, the various complement components interact in a highly regulated cascade to carry out functions such as lysis of foreign bacteria, cells and viruses. In addition, the complement system promotes phagocytosis of particular antigens. This action is known as opsonization. The complement also induces inflammation, as well as it clears and removes immune complexes from the circulation.

There are three distinct pathways through which complement can be activated on pathogen surface. These pathways are known as the classical-, the alternative- and the mannose-binding lectin pathway. Each depend on different molecules for its initiation, but they converge to generate the same set of effector molecules in the common final pathway (Janeway et al., 2001). All three pathways are presented in chapters 1.4.1-1.4.3, and are presented in figure 1.1.

In mammals, the liver is the major source of most complement proteins, and many cell types including monocytes and endothelial cells also synthesize most of the complement components (Morgan and Gasque, 1997). The ultimate goal for the activation of the complement system is the formation of the Terminal Complement Complex (TCC), and complement activation can thus be measured in terms of TCC.

1.4.1 The classical pathway

The classical pathway begins with the formation of soluble Ag-Ab complexes, also termed immune complexes, on a suitable target such as a bacterial cell.

This pathway is initiated by activation of the C1 complex. This is followed by cleaving the next two components of the classical pathway, C4 and C2, generating C4b and C2b, respectively. Together, these large fragments form a C3 convertase from a C4bC2 complex. Its function is to cleave C3 molecules to C3a and C3b molecules. The anaphylatoxin C3a initiates a local inflammatory response while C3b coats the surface of pathogens (Janeway et al., 2001).

1.4.2 The alternative pathway

The alternative pathway is Ab-independent. Here, active products similar to those of the classical pathway are generated, but no Ag-Ab complexes are required for initiation. This pathway is rather initiated by cell surface constituents that are foreign to the host through the spontaneous hydrolysis of C3 (Janeway et al., 2001).

1.4.3 The mannose-binding lectin pathway

As for the alternative pathway, activation of the lectine pathway is Ab-independent. This pathway is activated by the binding of mannose-binding lectin (MBL) to mannose residues on the surface of microorganisms. The concentration of MBL, which is an acute phase protein, increases during inflammatory responses (Kindt et al., 2007).

The MBL pathway is homologous to the classical pathway in way of using MBL to trigger the complement cascade. MBL is a similar protein to C1, and following its binding to a pathogen surface, C4 and C2 are cleaved forming the C3 convertase (Janeway et al., 2001).

1.4.4 Common final pathway

The next step in the cascade is the generation of the C5 convertase. A C5 convertase is formed by the binding of C3b to C4b2b to yield C4b2b3b. C5 is captured by the C5 convertase complex through binding to an acceptor site on C3b, generating C5b and C5a. Opsonization of pathogens is a major function of C3b and its proteolytic derivatives.

After enzymatic cleavage of C3 and C5, two fragments known as anaphylatoxin (C3a and C5a) are released in the fluid phase (Ward, 2004, Strainic et al., 2008). C5a is regarded as the most potent chemoattractant for neutrophils and monocytes. It contributes to a rapid mobilization of phagocytic cells at the site of injury to promote clearance of pathogens (Gasque, 2004). Both C3a and C5a have the ability to induce gene expression and protein synthesis of TNF-α and IL-1β in monocytes and macrophages (Schindler et al., 1990).

The opsonization of bacteria by complement also facilitates the binding of the bacteria to the adherence Complement Receptor 1 (CR1) and the integrin and phagocytosis receptor CR3 (CD11b/CD18) on blood leukocytes (Gasque, 2004). CD11b will be further described in chapter 1.5.2. Complement activation in the fluid phase with the release of C5a up-regulates CD11b rapidly and induces oxidative burst (Mollnes et al., 2002b). C5a also enhances synthesis of inflammatory mediators and degranulation of granulocytes (Ward, 2004).

CR3 on macrophages, monocytes and leukocytes bind to inactivated forms of C3b that remain attached to the pathogen surface. This binding stimulates phagocytosis of the pathogen (Janeway et al., 2001).

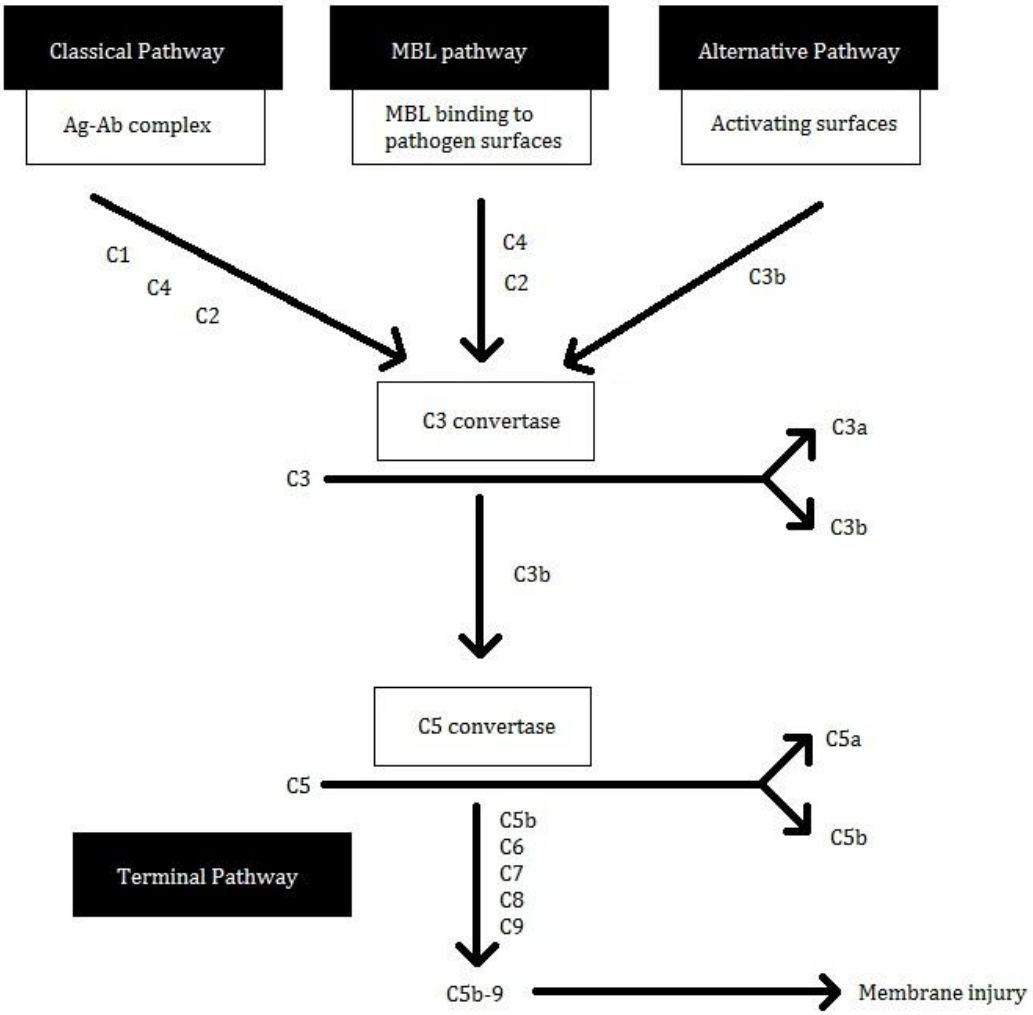

Figure 1.1 Pathways of complement system (Zhou et al., 2001). Complement is activated through the classical-, MBL- and alternative pathway, all described in sections 1.4.1 – 1.4.4.

1.4.5 Terminal complement complex

In the membrane attack pathway, five soluble plasma proteins (shown in figure 1.1) assemble into a multimolecular complex that is inserted into and through the targeted membrane. This creates a functional pore which enables ions and small molecules to diffuse freely across the membrane. As a result, the cell is not able to maintain its osmotic balance and the cell is killed by lysis (Morgan, 1999, Janeway et al., 2001, Kindt et al., 2007).

The complex is formed as part of the complement activation. The first step in the formation is the cleavage of C5 by its convertase to release C5b. One molecule of C5b binds one molecule of C6, which further facilitates binding of C7. This C5b6b7 complex then binds one molecule of C8, after which a variable number of C9 molecules associate with the C5b678 complex, creating the C5b-9 complex. This TCC molecule exists in one

active membrane form known as Membrane Attack Complex (MAC) and as the soluble C5b-9 complex (Morgan, 1989).

1.5 Foreign materials to the body

1.5.1 LPS and PAMPs

A great part of a gram-negative bacteria's cell membrane is associated with its toxicity to animals, in particular a hydrophobic component known as lipid A. This toxic component is the main inducer of immunological responses to Lipopolysaccharide (LPS). Common to all microbial species are the conserved structural motifs known as Pathogen-Associated Molecular Patterns (PAMPs), such as LPS. These are usually necessary for the microbe's survival, and are absent from eukaryotic hosts. That is why the release of LPS into the host's blood circulation causes the activation of several immune cells.

The immune system's first line of defense against pathogens is generally phagocytes and includes both monocytes and granulocytes. Phagocytes interact directly with PAMPs using specialized Pattern Recognition Receptors (PRRs), which are a group of soluble and membrane-bound host proteins. The interaction between PAMPs and PRRs most often leads to lysis of the targeted cell or opsonization.

1.5.2 Cell surface receptors

Cluster of differentiation (CD) is a group of Ag on the surface of leukocytes. CDs are also known as PRRs.

CD11b

Main cellular expressions of CD11b are on monocytes, macrophages and granulocytes. This Ag is also mediating the uptake of complement coated particles. CD11b antibody can be used to identify and count CD11b+ (positive) cells by flow cytometry, amongst other methods.

CD11b forms CR3 in humans by association with CD18. CR3 is a PRR and is involved in phagocytosis of C3b-coated bacteria and LPS clearance. Up-regulation of CD11b/CR3 on human granulocytes has previously been shown to be complement dependent (Mollnes et al., 2002b, Sprong et al., 2003). When exposed to LPS, leukocytes exhibit increased expression of CD11b/CD18, and produce cytokines such as IL-1 and TNF-α (Surette et al., 1993).

CD14

CD14 is expressed mainly by macrophages and monocytes, but it is also expressed by granulocytes and dendritic cells at a lesser extent. CD14 acts as a co-receptor along with the TLR-4 for the detection of LPS, although it is capable of recognizing other PAMPs also (Zanoni et al., 2011). It is an anchored protein, but a soluble form of CD14 has been detected on plasma, suggesting that it can be secreted (Simmons et al., 1989). This soluble form has been reported to act as an acute phase protein and may regulate T cell activation and trigger mitogenesis of B cells (Kindt et al., 2007).

In contrast to granulocytes, monocytes are highly dependent on CD14 for up-regulation of CD11b at low LPS concentrations (Duchow et al., 1993). There have been done experiments showing that the LPS induced granulocyte activation was more dependent on complement, and monocyte activation was more dependent on CD14 (Brekke et al., 2007).

1.5.3 Submicron particles

Inhalation of micro particles of silica and asbestos fibers, or diesel particles in very small quantities over time, can lead to chronic inflammation (Chaudhuri et al., 2010). Other environmental irritants, such as silica and asbestos micro particles, activate the NLRP3 inflammasome (explained in chapter 1.6.3) by disrupting the phagosome membrane (Pelka and Latz, 2011).

Nanoparticles are defined as single particles with a diameter less than 100 nm. Such particles are frequently used in many everyday products such as paper, white paint, plastics and especially in cosmetics (Yazdi Amir et al., 2010), as well as in medicine. The diameter of submicron particles is defined as less than 1 μm.

Superparamagnetic iron oxide nanoparticles (SPION), both with and without surface coatings, are being widely used for biomedical applications that can identify potential cellular damage. SPIONs are the only clinically approved metal oxide nanoparticles, where they can be used as tools for drug delivery. The small size of these particles yields large surface area to mass ratio and this has been associated with inflammation and generation of reactive oxygen species (ROS) (Singh et al., 2010). Medical therapy utilizes the ability of iron particle suspensions to interact with an external magnetic field. By doing this the particles can be coated with drugs, for instance, and be positioned to a

specific area in the body. After removal of magnetic field, the SPIONs do not retain any magnetism (Bonnemain, 1998).

Iron particles include maghemite (Fe_2O_3) and magnetite (Fe_3O_4). These may occur naturally as particulate matter in the environment. The exposure level of such particles is rapidly increasing, and it is therefore wanted to investigate the risks associated with their exposure. The iron oxide core of SPION can be synthesized chemically, and its surface may thereafter be coated with biocompatible molecule such as carboxyl groups.

Two types of particles are used in this study. Their hydrodynamic diameters are 1 µm and 100 nm, respectively. The former is an aqueous dispersion of magnetic fluorescent non-porous particles with maghemite core and a silica-consisting coating. The latter is an aqueous dispersion of magnetic fluorescent nanoparticles with magnetite core. Its coating consists of an unspecified polysaccharide. Carboxyl is the functional group in both particles (Chemicell100nm, Chemicell1µm). Silica and other coatings with inorganic molecules provide stability to the nanoparticle in solution. It also helps in binding biological ligands at the particle's surface for various medical applications (Qhobosheane et al., 2001, Gupta Ajay and Gupta, 2005). Previous experiments have shown that silica nanoparticles are a good biocompatible solid support (Qhobosheane et al., 2001). The datasheets for the particles are given in attachment O, and an illustration of each particle is shown in figure 1.2.

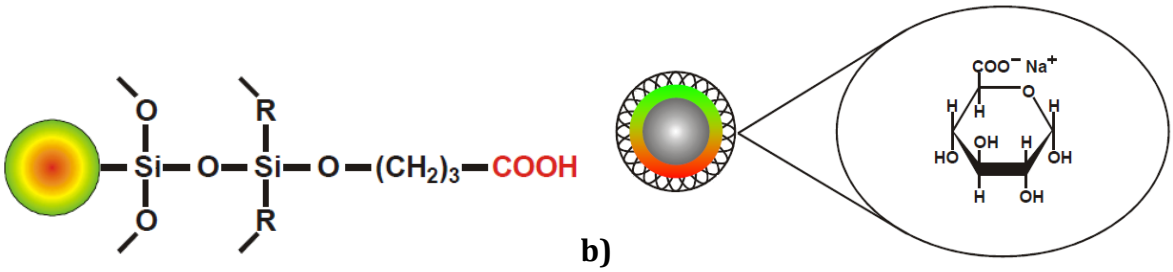

a) **b)**

Figure 1.2 Particles: **a)** screenMAG/B-Carboxyl (1 µm), **b)** nano-screenMAG/B-ARA (100 nm).

In a study, it was discovered that large particles had relatively low carcinogenic activity at the same instilled dose as smaller particles (Borm and Driscoll, 1996). However, another study suggested that smaller particles could be taken up by the cells as agglomerates and therefore considered as bigger than the largest particles (Grassian et al., 2007). Further, surface chemistry needs to be taken in consideration in order to predict cell uptake mechanisms (Grassian et al., 2007, Singh et al., 2010).

Previous studies have revealed that the magnetite nanoparticles coated with a bipolar surfactant is concentration dependent. One study showed that these particles were non-toxic in the concentration range of 0.1-10 μg/mL while toxicity could be seen at 100 μg/mL (Ankamwar et al., 2010).

1.6 Cellular receptors and intracellular components

1.6.1 TLRs

Among the PRRs are the Toll-Like Receptors (TLRs). These contain Leucine-Rich Regions (LRRs) in the extracellular domain that detect cellular products such as PAMPs. Ten TLRs in humans are known to react with specific PAMPs from bacteria and other microorganisms (Mogensen, 2009, Takeuchi and Akira, 2010). LPS is known to be recognized by Toll-like receptor 4 (TLR-4), a LPS receptor found on the surface of many immune cells, among them monocytes (Wang and Quinn, 2010). However, relatively small amounts of TLR-4 are found on the plasma membrane of human monocytes. There are, on the other hand, detected considerable amounts of TLR-4 in intracellular compartments, such as endosomes (Husebye et al., 2010).

TLR-4 consists of three distinct protein domains, each with a separate function, known as the TLR-4/MD-2/CD14 complex. The external domain of the receptor contains a binding site for LPS complexed with CD14, a high-affinity, non-transmembrane protein on the surface of phagocytes. Further, CD14 concentrates LPS for binding to the TLR-4/MD-2 complex (Park et al., 2009). The binding of LPS to TLR-4 starts a cascade of reactions that activates transcription factors such as nuclear factor kappa B (NF-κB). This is a protein which binds to specific regulatory sites on DNA, initiating transcription of downstream genes. This process will not be further emphasized here except that it is responsible for the induction of inflammatory responses. An overview of the cascade reaction which happens after TLR-4 has responded to LPS is shown in figure 1.3.

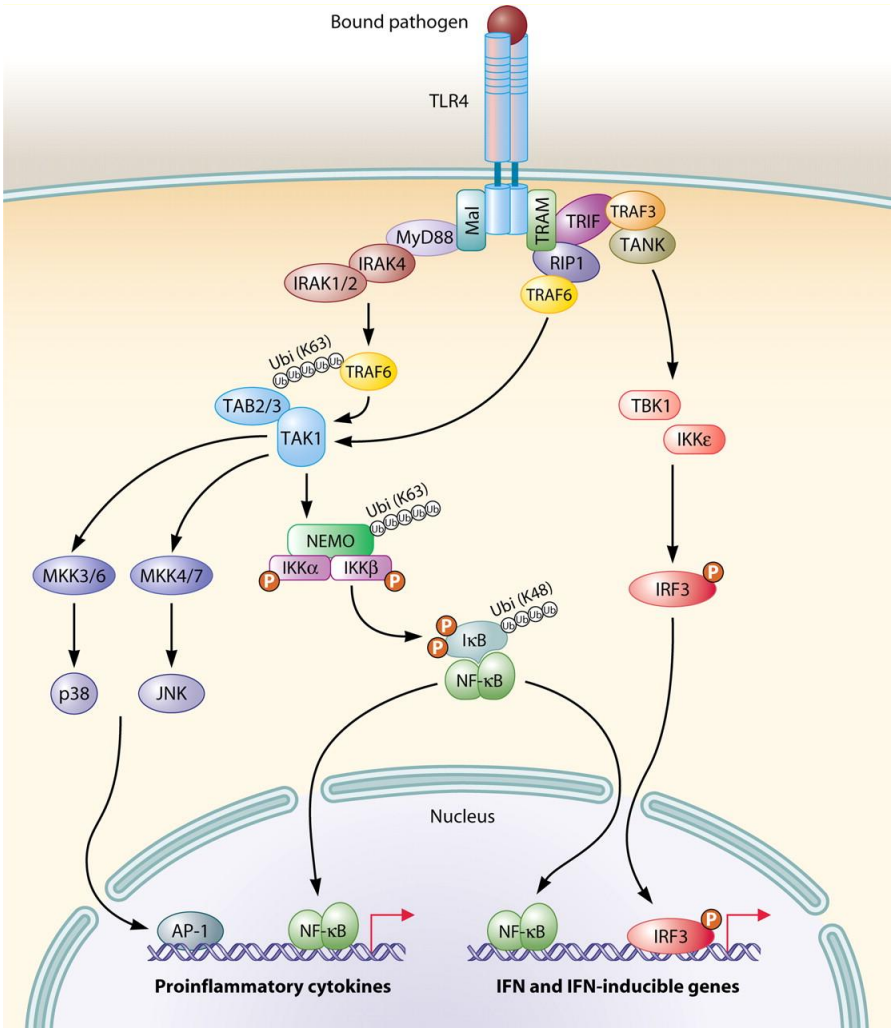

Figure 1.3 TLR-4 on a cell, for instance a monocyte, responding to a pathogen with LPS (Mogensen, 2009). This binding triggers a downstream signaling pathway including both MyD88 dependent and –independent pathway. These are described later in chapter 1. The outcome is an induced inflammatory response caused by the initiated transcription of genes encoding different sets of cytokines.

Figure 1.3 shows several cytoplasmic Toll/IL-1 receptor (TIR) domain-containing adaptors that are thought to play an important role in TLR signaling pathways. Among these are MyD88, Mal, TRIF, and TRAM, and all are associated with TLR through homophilic interaction of TIR domains (Uematsu and Akira, 2006). The Myeloid Differentiation primary response gene (88) (MyD88) is a common adaptor that is essential for the downstream signaling of TLRs and the pro-inflammatory cytokine production (Yamamoto et al., 2003).

There are two types of MyD88 associated pathways. It is previously suggested that these two pathways are activated by TLR-4 in a sequential manner (Kagan et al., 2008). The author proposed that TLR-4 first induces MyD88-dependent signaling at the plasma membrane, after which the TLR-4 complex becomes endocytosed. This internalization,

which is apparent to be induced by LPS, would thereafter activate MyD88-independent pathway from endosomal compartments. These pathways are briefly described in the following two sections.

1.6.1.1 MyD88-dependent pathway

The MyD88-dependent signaling pathway is essential for the early activation of pro-inflammatory cytokine genes, including those encoding TNF-α and IL-1β. MyD88 recruits IL-1 receptor kinases (IRAK) to TLRs upon stimulation at the plasma membrane. Several IRAK molecules are activated by phosphorylation which causes further downstream signaling. These reactions lead to the early activation of the transcription factor NF-κB, which finally induces target genes (Palsson-McDermott and O'Neill, 2004, Uematsu and Akira, 2006, Mogensen, 2009).

1.6.1.2 MyD88-independent pathway

Endosomes are compartments inside eukaryotic cells. TLR-4 inside an endosome has the ability to induce IFN-inducible genes in a MyD88-independent manner. A late response to LPS makes use of TRIF and TRAM which are the adaptors responsible for signaling and activation of NF-κB. This pathway induces the so-called late activation of NF-κB (Palsson-McDermott and O'Neill, 2004, Uematsu and Akira, 2006, Mogensen, 2009).

1.6.2 Caspase

Intracellular cysteinyl aspartate-specific proteases (caspases) have essential, catalytic roles in inflammation. The mechanism involved in the activation of pro-inflammatory caspases involve an autocatalytic processing of pro-caspase-1 to generate two subunits (p20 and p10) (Eisenbarth Stephanie et al., 2008).

Caspases are known to cleave substrates present after aspartic acid (Asp) residues in other proteins (Franchi et al., 2009). Inflammatory caspases include Caspase-1, -4 and -5 in humans, and they are essential for the activation of specific cytokines. Caspase-1, for instance, has the enzymatic function of cleaving pro-IL-1β at its Asp-116 amino acid to generate the mature and active IL-1β (Martinon et al., 2002).

1.6.3 Inflammasomes

The inflammasome is a complex of proteins in the cytosol of a cell that mediates the activation of caspase-1, which thereafter promotes secretion of IL-1β, as well as IL-18 (Franchi et al., 2009, Chen and Pedra, 2010). Four different receptors have been shown

to form an inflammasome, three of which belong to the NOD-like receptor (NLR) family of proteins. These are NLRP1 and 3, NLRC4, and AIM2, the latter being a receptor of the HIN family of proteins (Gross et al., 2011).

The NLRP3 inflammasome's function is to convert inactive pro-caspase-1 to active caspase-1, which then cleaves accumulated cytokine precursors to an active form that can be secreted. Materials like crystal fibers, submicron particles and several other environmental pollutants, in addition to ATP, are all shown to activate NLRP3 (Bauernfeind et al., 2011).

Normal baseline for NLRP3 expression is not sufficient for caspase-1 cleavage in unprimed macrophages. To be able to sense danger signals in their environment via the activation of the NLRP3 inflammasome, it is believed that the cells need to acquire a signal that indicates the presence of infection (Bauernfeind et al., 2011). This is achieved by the activation of PRRs by microbial products, for instance LPS from *Escherichia coli*. It is therefore required to perform a priming procedure via TLRs, later to be able to cleave pro-caspase-1 with particulate stimuli. Upon activation, caspase-1 is able to cleave cytosolic pro-IL-1β and pro-IL-18 to their active forms (Martinon et al., 2002, Chen and Pedra, 2010, Pelka and Latz, 2011). The two stimuli must be sensed by the same cell for effective immune activation (Eisenbarth Stephanie et al., 2008). These series of events are presented in figure 1.4 exemplified with the activation of IL-1β.

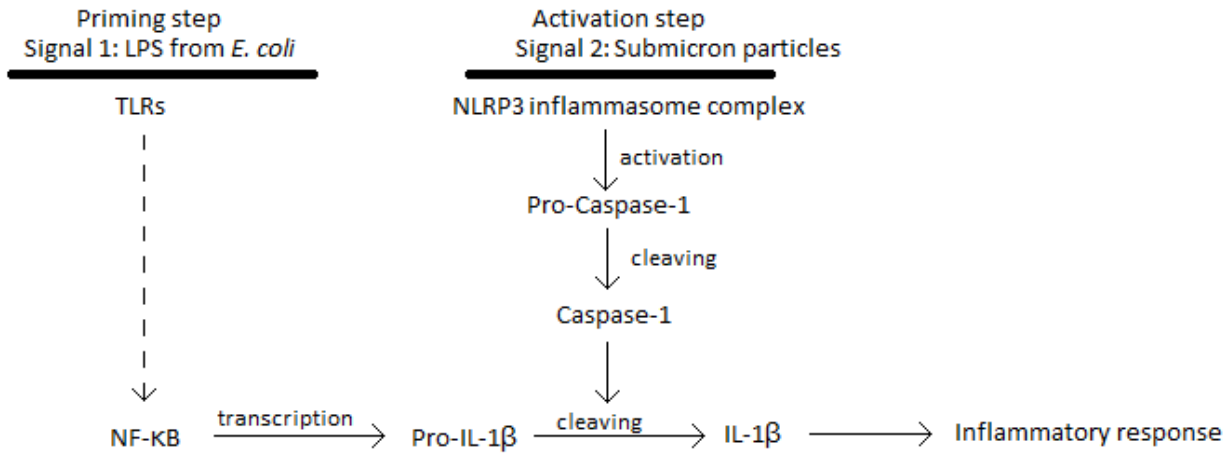

Figure 1.4 TLR mediates NF-κB activation and pro-IL-1β in response to a priming step. The generation of IL-1β via cleavage of its pro-form requires the activity of caspase-1. Illustration inspired by Bauernfeind (Bauernfeind et al., 2011).

The inflammasome and IL-1β are both tightly regulated due to the severe effects caused by overproduction of active IL-1β (Bauernfeind et al., 2011). There are different

signaling pathways that have been proposed to engage the NRLP3 inflammasome (Tschopp and Schroder, 2010). Among these, there is one proposing the intracellular generation of Reactive Oxygen Species (ROS) as the crucial element for NLRP3 activation. ROS may be produced during phagocytosis of particles or activated inflammatory cells. This model is presented in figure 1.5.

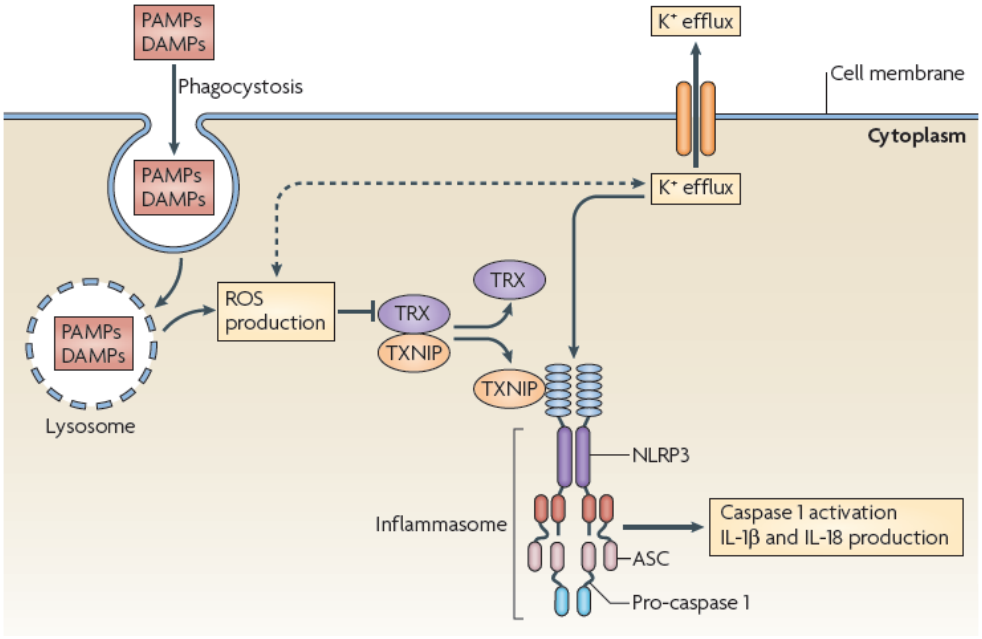

Figure 1.5 The ROS model of NLRP3 inflammasome activation (Tschopp and Schroder, 2010).

1.7 Aims for the thesis

Since it still is poorly understood how the intracellular cooperative mechanisms of particles and microorganisms function, it would be interesting to study their impact on the immune system *in vitro*. The submicron particles presented in chapter 1.5.3 will be studied for their ability to activate the inflammasome in isolated monocytes. These cells are initially thought to be primed with LPS from *E. coli*, after which they will be stimulated with the particles. Whole blood from healthy donors will not be primed with LPS, only stimulated with particles.

Inflammatory responses will be measured with ELISA and Bio-plex. Flow cytometry will be used to measure up-regulation of CD11b on monocytes and granulocytes from whole blood. Further, complement activation will be measured in terms of TCC in whole blood serum.

Confocal microscopy will be used to verify the stated sizes of the particles, as well as to study their tendencies to agglomerate.

2 Materials and methods

The Regional Research Committee has given the Institute of Cancer Research and Molecular Medicine permission to use donated blood and serum with written consent from healthy individuals at the Blood bank at St. Olav's Hospital in Trondheim.

All reagents and equipment that are used during the experimental procedures are listed alphabetically with their associated manufacturer and catalog number in attachment A.

2.1 PBMC and monocytes

2.1.1 Isolation of PBMC and monocytes

Peripheral blood mononuclear cells (PBMC) were isolated from A+ buffy coat of healthy blood donors. Buffy coat is a component prepared from a single whole blood donation by separation of part of the plasma and the erythrocytes. The majority of the platelets have been removed, but the buffy coat still consists of leukocytes, thrombocytes, some erythrocytes and plasma (Council_of_Europe, 2007).

Human monocytes were isolated by adherence after Ficoll-Hypaque purification of PBMC as previously described by Bøyum (Boyum, 1976). However, some modifications have been done. Approximately 45 mL A+ buffy coat was diluted in 80 mL Phosphate Buffered Saline (PBS). Lymphoprep was the density gradient used for the isolation of PBMC. This was due to the lower density than 1.077 g/mL of mononucleated cells such as monocytes, where 1.077 g/mL is the density of Lymphoprep. Thus, these cells could be isolated by centrifugation for 20 minutes at 1800 rpm with no brakes, at 20°C. The Lymphoprep allowed the erythrocytes to sediment through the medium while retaining the mononuclear cells at the medium interface (Axis-Shield). This is illustrated in figure 2.1.

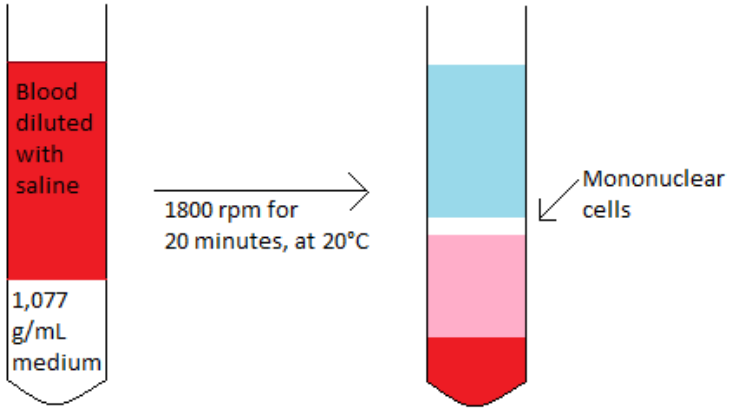

Figure 2.1 Isolation of PBMC by the use of Lymphoprep and centrifugation (Axis-Shield).

After centrifugation, the contamination of erythrocytes in the mononuclear cell suspension is usually 3-10% of the total cell number (Axis-Shield). As previously proposed, Zap-oglobin can be added to the cell suspension to completely lyse red blood cells (Iwamoto and Nagai, 1981). 20 µL of the cell suspension was added to 10 mL of an isotonic solution with two droplets of Zap-oglobin. The amount of PBMC in the cell suspension was counted by an electronic cell counter in the range from 30 000 to 32 000 fl.

Approximately 100 mL of the mononuclear cell suspension shown in figure 2.1 was collected into new tubes and spun down by centrifugation for 10 minutes at 2000 rpm with full brakes (20°C).

Hanks' Balanced Salt Solution was used for the following washing procedure. This was repeated three times by decanting the supernatants and resuspending the pellet in Hanks' solution, followed by centrifugation for 8 minutes at 800 rpm (20°C). The essential function of the Hanks' salt solution was to maintain the optimum physiological pH (roughly 7.0-7.4) and osmotic balance for cellular growth, as well as to provide the cells with water and essential ions (Invitrogen, 2011).

The bicarbonate buffering system RPMI-1640 was added 1.7 mL L-glutamine and 0.25 mL Gentamicin prior to use. Active A+ serum was prepared to 5% concentration in RPMI-1640 due to this medium's growth support of several types of cultured cells (Sigma-Aldrich, 2011a).

After the last washing procedure, the pellet was resuspended in RPMI-1640 with 5% active A+ serum. Cells ($4 \cdot 10^6$ cells/mL) were cultured in 24 well plates, with 0.5 mL per well, and incubated with 5% CO_2 for 90 minutes (37°C). The adhered monocytes were thereafter purified by washing three times with Hank's solution to eliminate contaminating cells such as non-adherent lymphocytes (Bennett and Breit, 1994). Finally, the isolated monocytes were added the respective volumes listed in table 2.1 of either heat inactivated or active 5% A+ serum in RPMI-1640 medium.

2.1.2 Stimulation of monocytes

Dilutions with the particles, LPS and ATP were prepared in Milli-Q water which was additionally filtered with 0.20 µm syringe filter. The submicron particles with stated average sizes of 100 nm and 1 µm were used as received from the manufacturer and stored at 4°C. A 1 mg/mL stock solution of LPS was prepared and stored at 4°C. The ATP was made with concentration 42.5 mM and stored at -20°C in 300 µl aliquots.

Ultra-Pure LPS from *E. coli* 0111-B4 strain was the priming agent. The given volumes of LPS listed in table 2.1 were added to the respective wells, after which the plates were incubated with 5% CO_2 for 2 hours (37°C).

Table 2.1 Concentrations with respective volumes of medium, LPS, ATP and particles in each well.

Content in well	Volume of medium added [µL]	Volume of LPS added [µL]	Conc. of LPS in wells	Volume of ATP added [µL]	Conc. of ATP in wells [mM]	Volume of particles added [µL]
M ÷ MO	500	-	-	-	-	-
M+MO	500	-	-	-	-	-
Positive control, LPS	498.65	1.35	27 ng/mL	-	-	-
Positive control, ATP	480	10	100 pg/mL	37	3	
0.01 µg/mL-100 µg/mL	480	10	100 pg/mL	-	-	10

The respective volumes of particles given in table 2.1 were added to the samples. Two positive controls were added, the first one was 27 ng/mL LPS and the second one 3 mM ATP. In addition, two negative controls were used, with and without monocytes, designated M+MO and M ÷ MO, respectively. The plates were incubated with 5% CO_2 for 6 hours (37°C). Finally, the cell plates were centrifuged and cell-free supernatants were stored in 96 wells plates at -20 °C.

2.2 Whole blood

Whole blood was used for TCC, cytokine and flow cytometric analyses. Particles, LPS, ATP and Zymosan were all diluted in sterile Dulbecco's PBS in small CryoTubes. Zymosan is a protein-carbohydrate complex prepared from yeast cell wall. It is often used to induce inflammatory responses, which include the production of pro-inflammatory cytokines in macrophages, amongst other phagocytes (Sigma_Aldrich). Final concentration of Zymosan was 10 µg/mL, and 100 ng/mL for LPS. The final particle- and ATP concentrations were the same as for the monocyte stimulation, except the lowest concentration. Thus, the concentrations ranged from 0.1 µg/mL to 100 µg/mL for the particles and 3 mM for ATP. The whole blood analyses were not primed with LPS prior to particle stimulation.

Venous blood was drained from healthy donors and collected into polypropylene tubes containing 80 µL Refludan per 4 mL of blood as previously described (Mollnes et al., 2002a). Vacuum was made in the tubes by extracting 19 mL of air with a syringe and cannula. The whole blood model is based on anticoagulation with lepirudin which is a highly specific thrombin inhibitor not influencing complement activation (Brekke et al., 2007). Particle samples, LPS, ATP, and Zymosan were added directly to the blood and the time zero baseline sample (T_0) was processed immediately. The remaining samples were thereafter incubated at 37°C depending on the type of analysis they were predicted for. For flow analysis, the incubation period was 15 minutes (T15), 1 hour for TCC samples (T60), and 6 hours for cytokine analyses (T360), respectively.

At T15, the whole blood was fixed using 50 µL 1% PFA solution per 50 µl blood sample and incubated for 4 minutes (37°C). 25 µL of fixed blood was stained with the nuclear dye LDS-751 to discriminate leukocytes from red blood cells. Further, the cells were stained with antibodies for CD14 to distinguish between monocytes and granulocytes, and finally with anti-CD11b. The stained samples were incubated in the dark for 15 minutes at room temperature. Thereafter, they were resuspended in 400 µL PBS and analyzed with a flow cytometer as described in section 2.5.

Immediately after the second incubation period (T60), further complement activation was stopped by adding 5 µL EDTA per sample. The blood samples were centrifuged for 15 minutes at 3 000 rpm (4°C), and the plasma was collected and stored at -20°C until it

was analyzed. The blood samples at T360 were handled the same way, only without addition of EDTA.

2.3 ELISA

Amounts of IL-1β and TNF-α were determined by means of sandwich Enzyme-linked Immunosorbent assay (ELISA). This is a procedure where an enzyme conjugated with an antibody reacts with a chromogenic substrate, generating a colored reaction product. A standard curve based on known concentrations of Ag is prepared, from which the unknown concentration of the samples can be determined.

Volumes are calculated in attachment B.2-B.4.

2.3.1 IL-1β

IL-1β levels in supernatants were measured with IL-1β ELISA kit according to the recommendations of the manufacturer, but with some modifications. All volumes were halved compared to the recommended working volumes. Coating Buffer was prepared by dissolving 10 PBS tablets in 1 L distilled water. This PBS solutions was used instead of the recommended 0.1 M Sodium Carbonate. Assay Diluent was prepared with 10% heat-inactivated Fetal Bovine Serum (FBS) in PBS. Standard curve of recombinant human IL-1β was constructed, ranging from 250 to 3.9 pg/mL, in addition to a blank sample.

The Wash Buffer used in the plate washer consisted of PBS with 0.05% Tween-20. The latter solution is a non-ionic detergent, useful for prevention of non-specific Ab binding (Sigma-Aldrich, 2011b). Together with PBS, it is useful for the washing procedures between each immunoreaction (Wikipedia, 2011).

The Substrate Solution used was a 1:1 mixture of color agent A and B. The active substances in these color agents are Hydrogen Peroxide and Tetramethylbenzidine (TMB), respectively. The color of the solution would change to blue and equation 2.1 describes the reaction that happened in the samples (Espevik et al., 2010).

$$H_2O_2 + \text{TMB} \rightarrow H_2O + \text{oxidized form of TMB} \quad (2.1)$$

The reaction was stopped by 1 M H_2SO_4. The color intensity quantifying the enzyme-bound Ab to the Ag was measured with a Microplate Absorbance Reader. Wavelength

correction was done by subtracting absorbance at 570 nm from absorbance at 450 nm. The results were processed by the software program Microplate Manager 6.

2.3.2 TNF-α

TNF-α levels in supernatants were measured with TNF-α ELISA kit as recommended by R&D Systems, but with some modifications. All volumes were halved compared to the recommended working volumes. Reagent Diluent was prepared with 1% heat-inactivated Bovine Serum Albumine (BSA) in PBS. Standard curve of recombinant human TNF-α was constructed, ranging from 8 to 0.125 ng/mL, in addition to a blank sample. Further reagents were applied as described in section 2.3.1, as well as by R&D Systems.

2.3.3 TCC-ELISA

Soluble C5b-9 complex in the samples from section 2.2 was measured using an enzyme immunoassay. This procedure was performed with some modifications compared to what is previously described (Mollnes et al., 1993). All samples were examined in singlets, and the standard in triplets. All working volumes were 50 µL per well.

Anti-C5b-9 was diluted in PBS and coating was done at 4°C over night in an ELISA plate. Any free binding seats in the wells were blocked for 45 minutes in room temperature with 0.1% BSA in PBS. The plate was washed three times with PBS containing 0.05% Tween-20 with a plate washer. This washing procedure was performed between each subsequent incubation.

The standard used in the assay, from which the standard curve was constructed, is previously described (Mollnes and Lachmann, 1987). It has been prepared from a normal human serum pool activated by 100 mg Zymosan per 10 ml serum. This has been incubated under continuous mixing for 30 minutes (37°C), and thereafter spun at 15 000 rpm for 30 minutes. The standards have been stored at -70°C in 100 µl aliquots.

The samples and standard were diluted in PBS containing 0.2% Tween-20 and 10 mM EDTA, and this solution was also used as negative control. The following incubation was for 2 hours in room temperature. The subsequent antibodies were diluted in PBS containing 0.1% Tween-20. The detection antibody was incubated for 1 hour, whereas the conjugate was incubated for 30 minutes, both in room temperature. The samples

were incubated with color agents A and B, and stopped with 1 M H_2SO_4 after 30 minutes, as described in section 2.3.1.

2.4 Bio-plex

Serum cytokines and chemokines were measured using a Bio-Plex Cytokine 17-Plex Panel. The Bio-plex procedure is similar to a sandwich ELISA, except the Bio-plex is run on a specialized dual-laser flow-based microplate detection system (Luminex, 2011). The xMAP Technology used 5.6 micron polystyrene microspheres. These are internally color coded with different intensities of two fluorescent dyes to create up to 100 possible individual bead sets, each with its own special signature. Because of all the different intensities, it is possible to analyze many cytokines in a single well of a 96-well microplate (Luminex, 2011). In this study, it was analyzed for 17 cytokines, and these are listed in table 2.2, as well as briefly described in chapter 1.3.

Table 2.2 Human Cytokine Standards in 17-plex, with their respective concentrations [pg/mL].

Cytokine	Concentration	Cytokine	Concentration
IL-1β	31 349	IL-13	35 832
IL-2	16 936	IL-17	22 256
IL-4	3 420	G-CSF	28 880
IL-5	29 507	GM-CSF	13 733
IL-6	25 171	IFN-γ	23 518
IL-7	27 558	MCP-1	19 992
IL-8	25 130	MIP-1β	14 995
IL-10	24 304	TNF-α	77 755
IL-12p70	35 952		

The 17-plex was used as recommended by the manufacturer, but with some modifications. The standard was diluted in 10% A+ serum, and the standard curves were constructed for the various cytokines according to the recommendations. All volumes were halved compared to the recommended working volumes.

The surface chemistry of the microspheres allowed chemical coupling of capture reagents such as Abs for a specific component. Detection of the multiplexed results was carried out using a system called Luminex. High-tech fluids based on the principles of flow cytometry caused the stream of suspended microspheres to line up in a single file prior to passing through the detection chamber. As a microsphere passed through the detection chamber, the internal dyes in the beads were excited and able to be classified. A second laser read the fluorescence intensity of the reporter molecule associated with

that bead. The intensity of fluorescence detected on the beads indicated the relative quantity of target molecules in the tested samples (Luminex, 2011).

2.5 Flow cytometer

Flow cytometry is used for studies of cell populations, amongst other. A flow cytometer uses a laser beam and light detector to count single intact cells in suspension. Those cells having a fluorescently tagged Ab conjugated onto their cell surface Ag demonstrate specific proteins on the cell surface. These cells are excited by a laser and emit light that is recorded by a second detector system. The flow cytometer is capable of sorting population of cells into different containers according to their fluorescent profile.

Here, deposition of complement components is studied by incubating submicron particles with whole blood. The expression of CD11b was analyzed on surfaces of granulocytes and CD14+ monocytes in whole blood. Data analysis was performed using a FACScan program on samples of 5000 events. Samples from section 2.2 were stored on ice in darkness before measurements. Samples stimulated with only PBS were used as negative control, and T_0 sample was used as an absolute negative control when the flow cytometer was adjusted. The results given in chapter 3 are reported as the mean of the distribution of cell fluorescent intensity, averaged between three independent experiments with no replicas each.

2.6 Determination of particle size by confocal laser scanning microscopy

The confocal microscope was used to capture images of the particles, both non-fluorescently and fluorescently. Samples with 100 nm particles were excited with 488 nm Argon laser lines, and images were captured, whereas 1 µm particle samples were excited with 405 nm laser lines.

A 1:10 dilution was prepared for the particles in room temperatured non-sterile water. Thus, for the 100 nm particles, a density of $1.8 \cdot 10^{14}$ particles/gram was prepared, whereas the particle density for the 1 µm particles was $1.8 \cdot 10^{11}$ particles/gram. The particle numbers were set to ensure a good visual particle density in the microscope. These dilutions were seeded onto a microscope slide and a cover slip was sealed onto it to avoid evaporation.

The optical section that fulfilled our criteria was <0.6 µm at both 23.2x and 63x magnification. The different particle sizes were optimized individually. By using

photomultipliers (PMTs), low levels of fluorescent light was detectable. An optical microscopy illumination technique known as differential interference contrast (DIC) was also used to enhance the contrast in unstained samples. DIC gained information about the optical path length of the sample, and because of the lighting, the object appeared black on a grey background.

2.7 Statistical analysis

The results from the experimental procedures are given as mean value ± SD (standard deviation). Two-sided Student's t-test with $p<0.05$ was considered statistically significant. Data were also analyzed by Analysis of Variance (ANOVA) in Excel with the same level of significance. ANOVA measures two sources of variation in the data, variations between groups and within groups, respectively. The p-value is determined from the F-statistics which is the ratio of the variation between groups divided by the variation within groups. A large F would indicate a small p-value, meaning that there is a larger difference between the groups than within.

3 Results

Statistical analyses are done mainly by ANOVA, but some point-analyses are in addition done with a Student's t-test at the same level of significance.

There are uncertainties whether there is a correlation between the points. Thus, the presented graphical results are treated as separate values.

3.1 Experiments with monocytes

Monocytes were isolated from healthy A+ blood donors by the Ficoll-Hypaque method as described in chapter 2. They were stimulated with particle concentrations ranging from 0.01 to 100 µg/mL. The particles had hydrodynamic diameters of 100 nm and 1 µm, respectively.

All average concentrations of isolated monocytes are given in table B.1 in attachment B. The secretions of cytokines were measured with standard ELISA and Bio-plex. The concentrations are listed in their respective tables in attachments C-H.

3.1.1 Primed versus unprimed monocytes

One part of the sample groups with monocytes were primed with 100 pg/mL LPS from *E. coli* prior to stimulation with particles, whereas the other part of the sample groups were not. These results represent three independent donors (D-F) with virtually identical results. The respective results are presented in attachments F-H.

There are three parameters for testing of significance. These are between primed and unprimed monocytes stimulated with 100 nm and 1 µm particles, respectively. Further, it is tested whether there is significance between the primed monocytes stimulated with the respective particles.

3.1.1.1 IL-1β

The average concentrations of IL-1β secretion measured with regular ELISA are listed in table I.2, as well as presented graphically in figure 3.1.

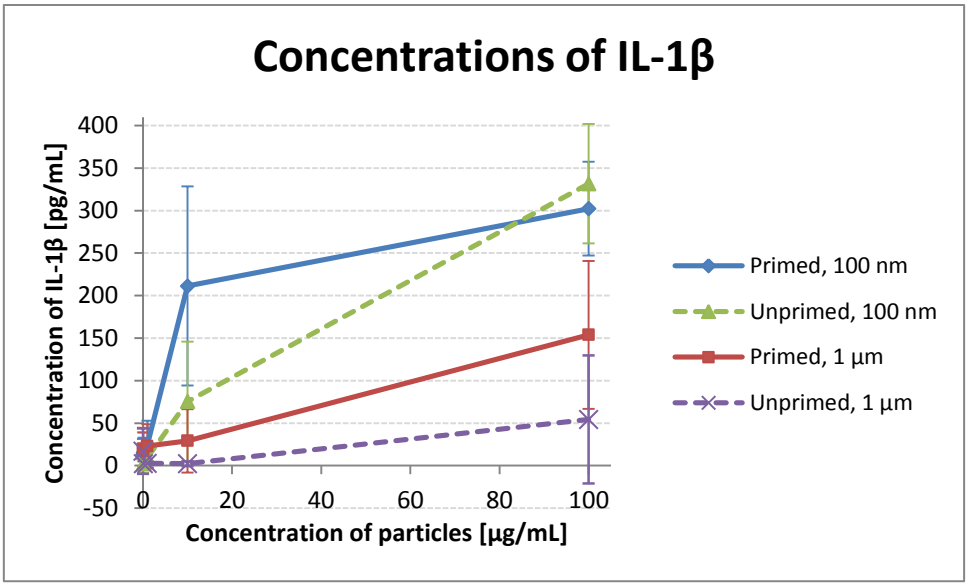

Figure 3.1 Secretion of IL-1β from monocytes (n=3), analyzed with ELISA.
Primed ATP control yields 302.9 ± 44.5 pg/mL, unprimed yields 186.2 ± 127.8 pg/mL.

It is seen from figure 3.1 that the unprimed sample groups show similar secretion responses as their respective primed sample groups, but with slightly lower cytokine concentrations. There is no significance between the primed and unprimed monocytes of the respective particle sizes. There is, in addition, no significance between the two primed samples.

3.1.1.2 TNF-α

The average concentrations of TNF-α secretion measured with ELISA are listed in table I.3, as well as presented graphically in figure 3.2.

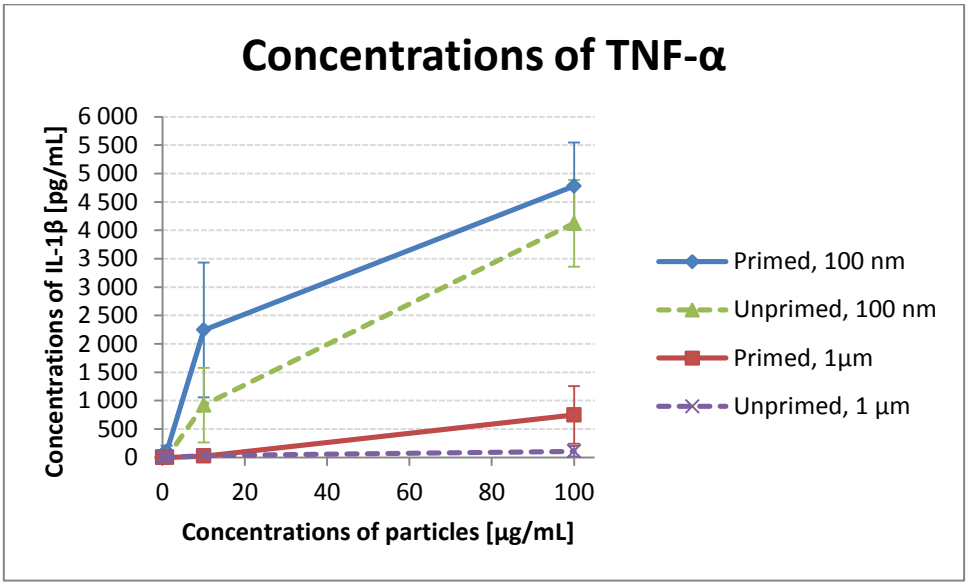

Figure 3.2 Secretion of TNF-α from monocytes (n=3), analyzed with ELISA.
Primed LPS control yields 728 ± 509 pg/mL, unprimed is undetectable.

As for IL-1β, the TNF-α concentrations secreted by the unprimed sample groups follow the same dose-response relationship as for the primed groups. Hence, there is no significance between the primed and unprimed monocytes of the respective particle sizes. However, there is significance in expression of TNF-α between the primed monocytes with 100 nm and 1 µm particles, respectively.

3.1.2 Bio-plex

This chapter presents five cytokines that gave some significant secretions after stimulation with the two particles. TNF-α resulted in values above the upper range of the standard curve and is therefore only presented graphically from ELISA measurements in figure 3.2. The results from Bio-plex are, however, listed in table I.9, attachment I. Attachment N presents the cytokines that did not show any significant responses after measurement with Bio-plex.

3.1.2.1 Il-1β

The average concentrations of IL-1β secretion measured with Bio-17-plex are listed in table I.4, as well as presented graphically in figure 3.3.

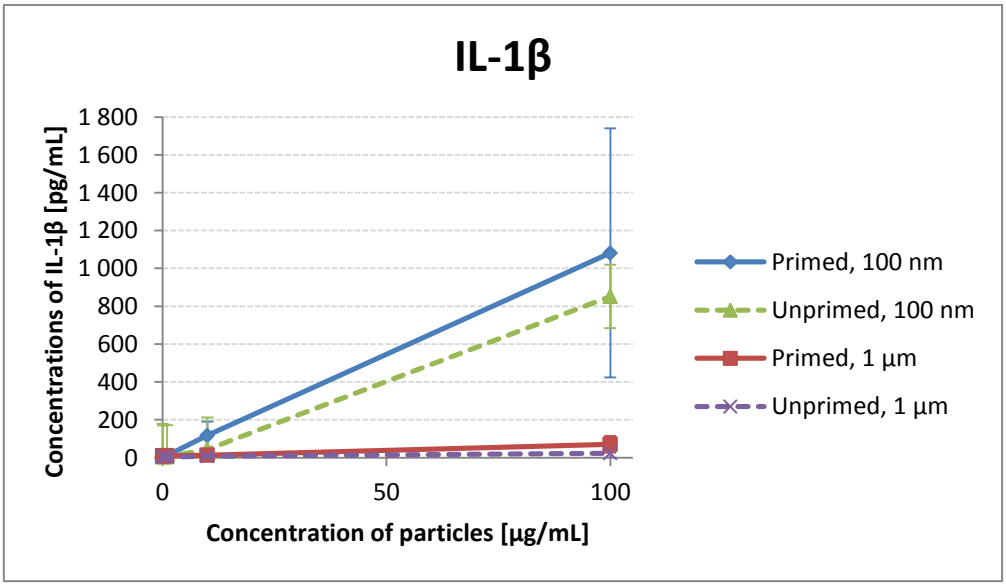

Figure 3.3 Secretion of IL-1β from monocytes (n=3), analyzed with Bio-plex. Primed ATP control gave 337.1 ± 188.3 pg/mL, and unprimed gave 92.4 ± 62.9 pg/mL.

The same trend is observed in figure 3.3 as in the previous two figures. There is no significance between any of the three testing parameters, except between the two primed sample groups at 10 µg/mL particle concentration. At 100 µg/mL particles, there is significance between the two primed groups at level $p<0.1$ (Student's t-test).

3.1.3.2 IL-2

The average concentrations of IL-2 secretion measured with Bio-plex are listed in table I.5, as well as presented graphically in figure 3.4.

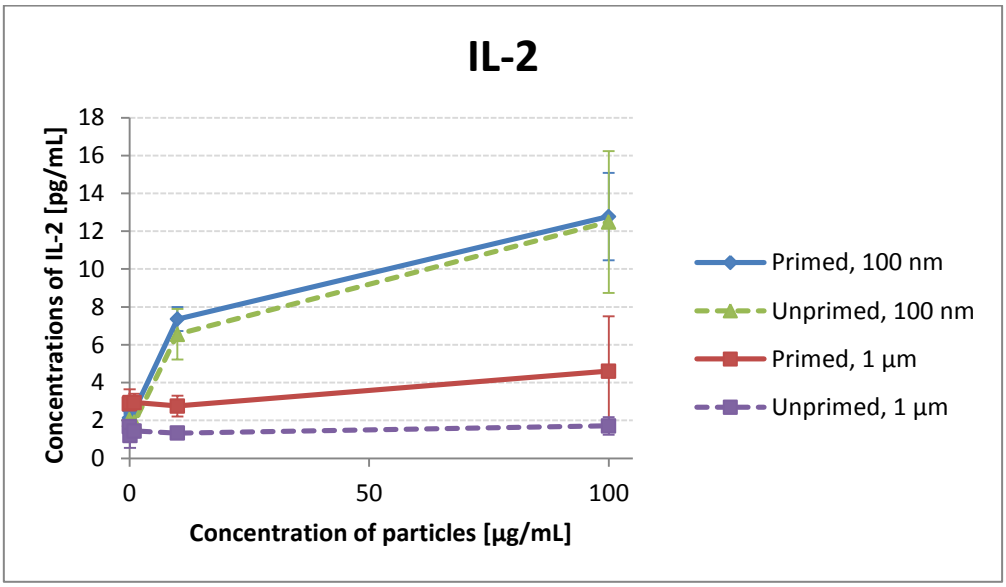

Figure 3.4 Secretion of IL-2 from monocytes (n=3), analyzed with Bio-plex. Primed LPS control yields 6.2 ± 1.5 pg/mL, unprimed is undetectable.

Yet again, unprimed sample groups follow a similar secretion trend as the primed groups. There is no significance between the primed monocytes with 100 nm particles and the respective unprimed monocytes. However, there is significance between the two respective parameters for the 1 µm particles. There is no significance between the two primed sample groups of monocytes. However, there is significance at 10 and 100 µg/mL particle concentration for the same level ($p<0,05$) tested with Student's t-test.

3.1.3.3 IL-6

The average concentrations of IL-6 secretion measured with Bio-plex are listed in table I.6, as well as presented graphically in figure 3.5.

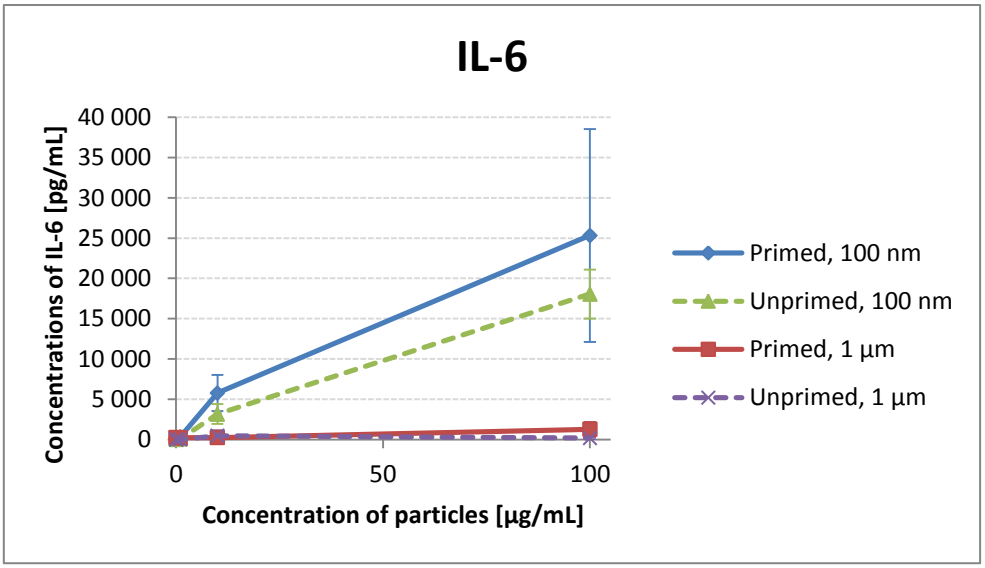

Figure 3.5 Secretion of IL-6 from monocytes (n=3), analyzed with Bio-plex. Primed LPS control yields 1 778.3 ± 993,4 pg/mL, unprimed is undetectable.

As described for previous cytokine results, the primed and unprimed samples of the respective sample groups show similar dose-responses. The primed monocytes stimulated with 1 µm particles secreted significantly higher concentrations of IL-6 than the respective unprimed cells. This is however not the case for the two groups with 100 nm. Further, there is significance between the two primed sample groups only at 10 and 100 µg/mL particle concentration.

3.1.3.4 GM-CSF

The average concentrations of GM-CSF secretion measured with Bio-plex are listed in table I.7, as well as presented graphically in figure 3.6.

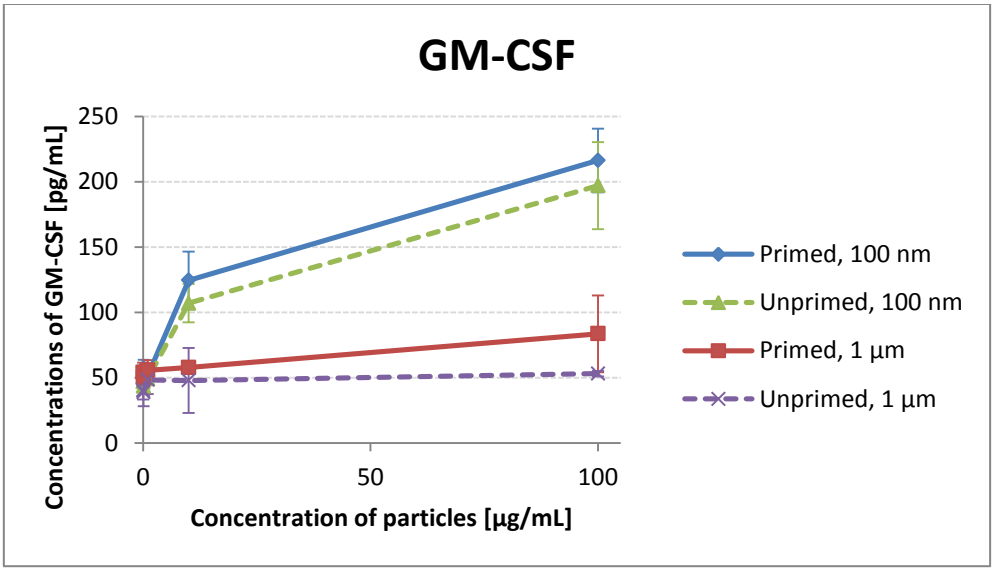

Figure 3.6 Secretion of GM-CF from monocytes (n=3), analyzed with Bio-plex. Primed LPS control yields 92.4 ± 7.2 pg/mL, unprimed is undetectable.

The primed and unprimed samples analyzed for GM-CSF show similar dose-responses as described for IL-2 and IL-6. The primed monocytes stimulated with 1 µm particles secreted significantly higher concentrations of GM-CSF than the respective unprimed cells. This is not the case for the two groups with 100 nm. Further, there is significance between the two primed sample groups only at 10 and 100 µg/mL particle concentration.

3.1.3.5 IFN-γ

The average concentrations of IFN-γ secretion measured with Bio-plex are listed in table I.8, as well as presented graphically in figure 3.7.

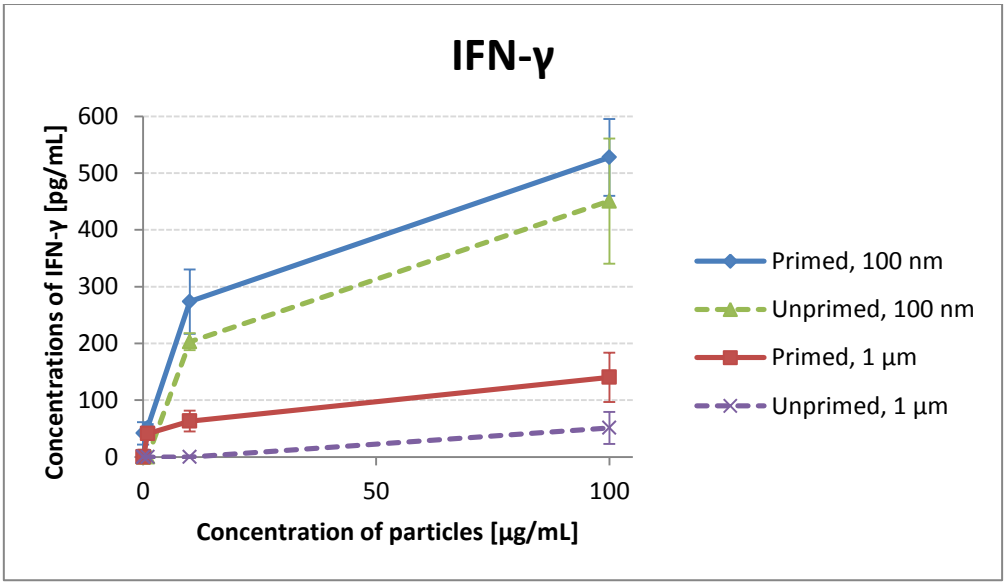

Figure 3.7 Secretion of IFN-γ from monocytes (n=3), analyzed with Bio-plex. Primed LPS control yields 163.9 ± 40.3 pg/mL, unprimed is undetectable.

The dose-responses for the primed sample groups analyzed for IFN-γ are similar to the respective unprimed groups. There is no significance between the groups for 100 nm particles, but there is between the primed and unprimed samples stimulated with 1 µm particles. There is, in addition, significance between the primed samples with the respective particles.

3.1.3 Active versus heat inactivated A+ serum

All samples presented in this section were primed with 100 pg/mL LPS prior to stimulation with particles and ATP. The following results illustrate the level of IL-1β secretion in active A+ serum compared to heat inactivated A+ serum. Results are given as the mean values of four independent donors (A-D), and these are independently

presented in attachments C-F. The results are given in table I.1, attachment I, in addition to graphical illustrations in figure 3.8.

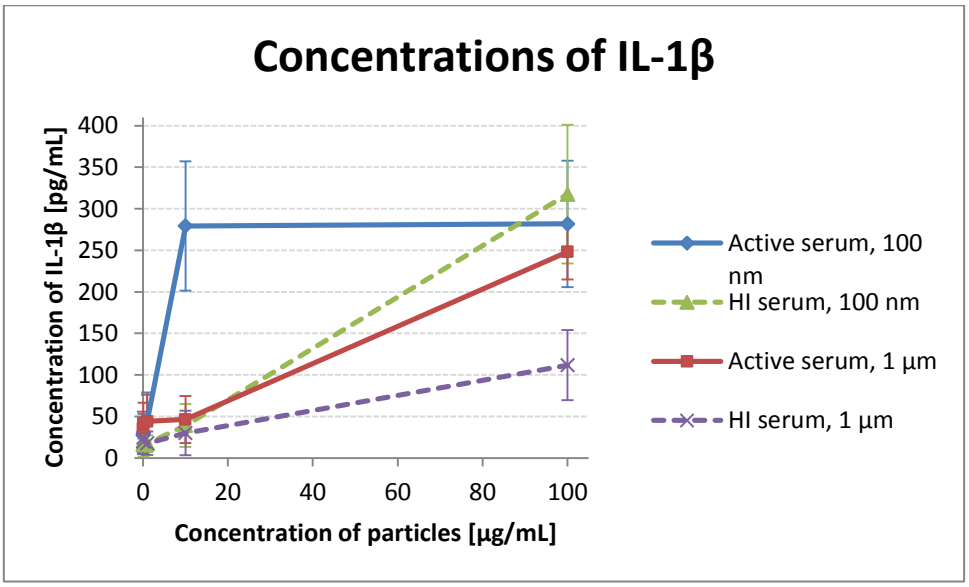

Figure 3.8 Comparison of IL-1β secretion from primed monocytes in active versus heat inactivated (HI) A+ serum (n=4), analyzed with ELISA.

Illustrated in the last figure are the differences in IL-1β secretion dependent on type of A+ serum the monocytes are stimulated in. It is seen that the dose-responses for the respective groups are similar, but the levels of secretion in HI serum are generally lower compared to secretion in active serum. There is a drastic increase in cytokine secretion at 10 µg/mL concentration of 100 nm particles in active serum. This yields a significantly higher IL-1β secretion at this particle concentration compared to the same group in HI serum. There is also significance between the two 1 µm sample groups at 100 µg/mL.

3.2 Whole blood studies

Whole blood from healthy donors was used for flow cytometric, TCC and cytokine analyses. Results are presented as mean values of three independent donors (G-I), and all are individually presented in attachments J-L. The average concentrations are listed in their respective tables in attachment M.

The positive control (Zymosan) and negative control (PBS) are only based on one measurement, but these values are prolonged and used as threshold value in the following figures. Zymosan was applied as positive control due to its known induction of

the inflammatory response. PBS, on the other hand, was the dilution medium, and it was therefore applied as negative control.

3.2.1 Flow studies

Leukocyte CD11b up-regulation in human whole blood was examined by flow cytometry on samples at T15. Purified LPS was included as control for the effect of pure fluid-phase complement activation, but these values are only given in table M.1.

The results for up-regulation of CD11b on CD14+ monocytes is illustrated in figure 3.9a), whereas the results for granulocytes is presented in figure 3.9b). It was tested whether there were any significant differences in up-regulation of CD11b on leukocytes after stimulation with the respective particles, and whether the 100 nm particles caused a significant up-regulation compared to PBS.

The average values which are presented graphically in figures 3.9a) and b) are listed in table M.1.

a)

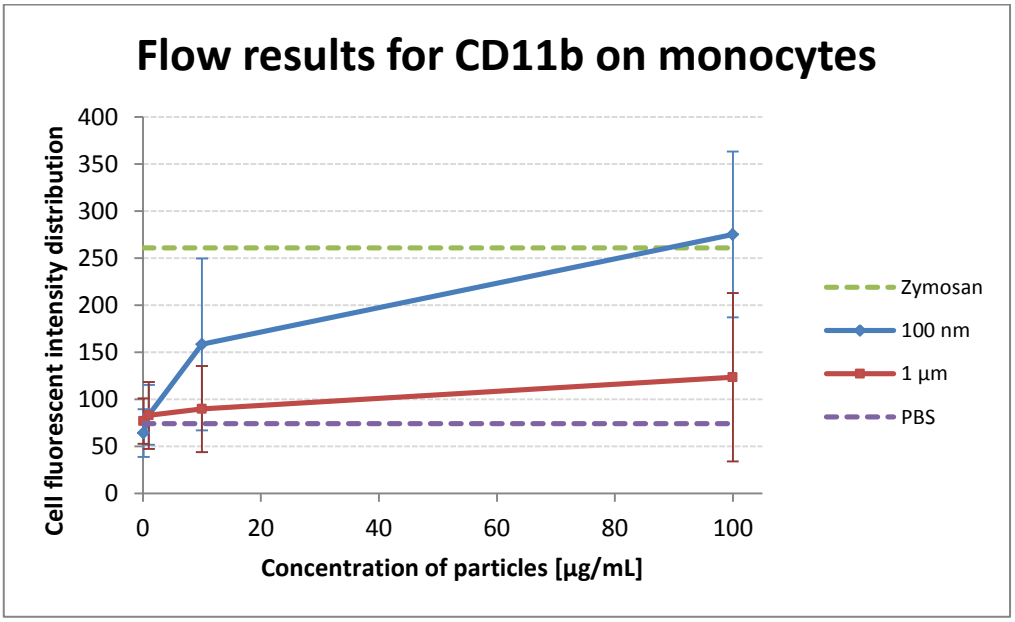

b)

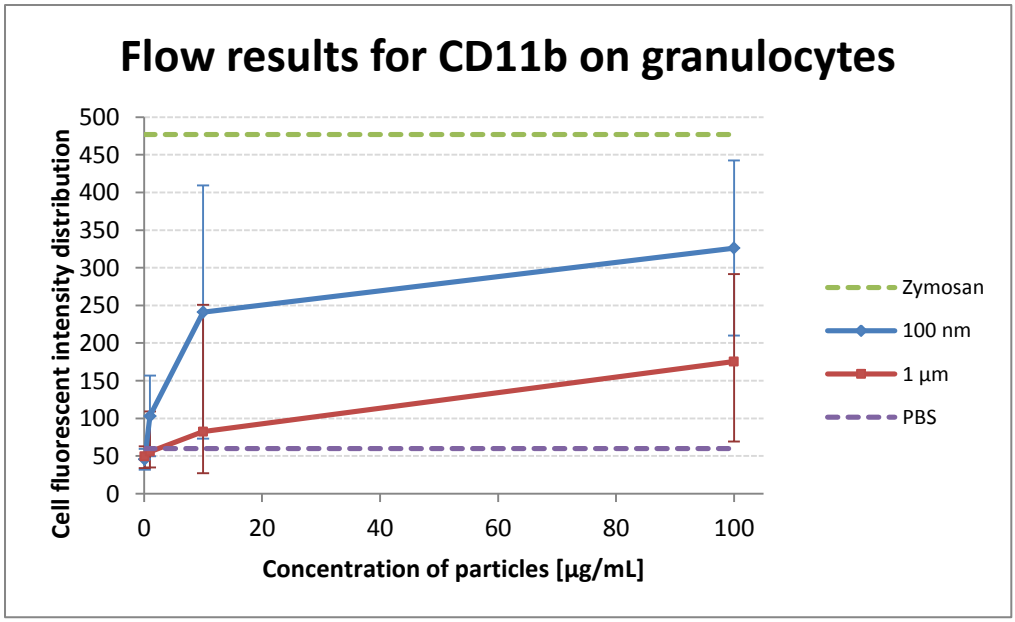

Figure 3.9 CD11b monocytes **(a)** and granulocytes **(b)**, with positive (Zymosan) and negative (PBS) controls, after gating for CD14+ cells. Zymosan resulted in 260.9 ± 34.2 in a) and 476.7 ± 42.0 in b). Data analyses for the mean of distribution of cell fluorescent intensity were performed on samples of 5000 events (n=3).

There was no significance between the two particles' up-regulation on neither monocytes nor granulocytes. However, there was a significant up-regulation of CD11b on both cells when stimulated with 100 nm particles compared to PBS control. In addition, it was found that there was a significant up-regulation from 0.1 to 100 µg/mL concentration of 100 nm particles, but not for 1 µm particles.

3.2.2 Terminal Complement Complex

Activated complement was measured in terms of TCC. The results from the soluble C5b-9 complex analyses in the whole blood samples are presented in figure 3.10 as the mean value of three independent donors, and listed in table M.2.

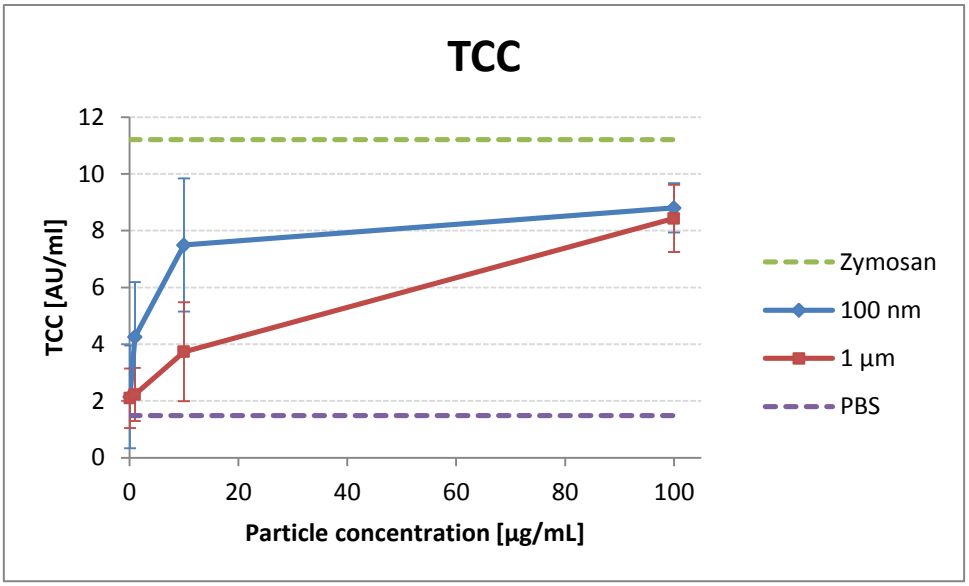

Figure 3.10 Average TCC results [AU/mL] based on three donors, with positive control (Zymosan) and negative control (PBS). Zymosan yielded 11.2 ± 1.3 AU/mL.

There is statistical significance between the respective particles and PBS control, but not between the two groups of particles. There is a significant increase in complement activation from 0.1 to 100 µg/mL for both the 100 nm and 1 µm particles, respectively. For the 100 nm particles there is in addition a significant increase in activation from 0.1 to 10 µg/mL. Additional testing with Student's t-test gave significant values between the two groups at 10 µg/mL particle concentration.

3.2.3 Cytokine analyses

Particles of 100 nm and 1 µm have been compared in human whole blood models ranging from 0.1 to 100 µg/mL particle concentrations.

In general, two statistical parameters were analyzed with ANOVA. The first one was whether there were any significant differences in cytokine secretion after stimulation with the two particles. Secondly, it was tested whether there were any secretion significances between 100 nm particles and PBS control.

Analysis with IL-1β ELISA

The average concentrations of IL-1β secretion measured with regular ELISA are listed in table M.3, as well as presented graphically in figure 3.11.

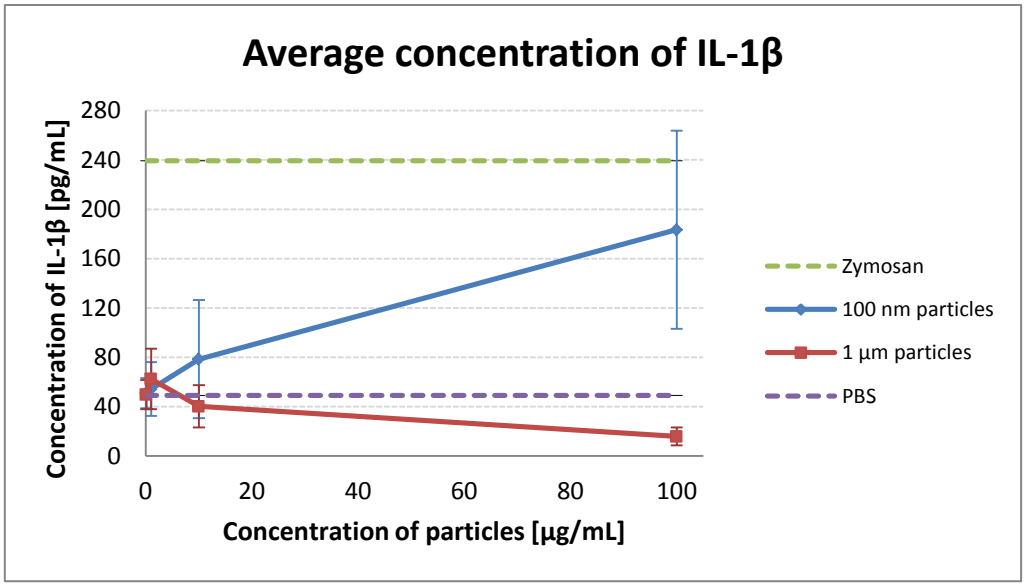

Figure 3.11 Average concentrations of IL-1β [pg/mL] from T360 analyzed with ELISA (n=3).

From figure 3.11 it is seen that there is significance between both particle stimulations as well as between 100 nm particles and PBS. Stimulations with 1 µm particles resulted in IL-1β secretion decreasing below the lower threshold with PBS control.

Bio-plex

This chapter presents four cytokines that gave significant secretion after stimulation of whole blood with the particles, including IL-1β. Attachment N presents the cytokines that did not give any significant responses with Bio-plex.

3.2.3.1 IL-1β

The average concentrations of IL-1β secretion measured with Bio-17-plex are listed in table M.4, as well as presented graphically in figure 3.12.

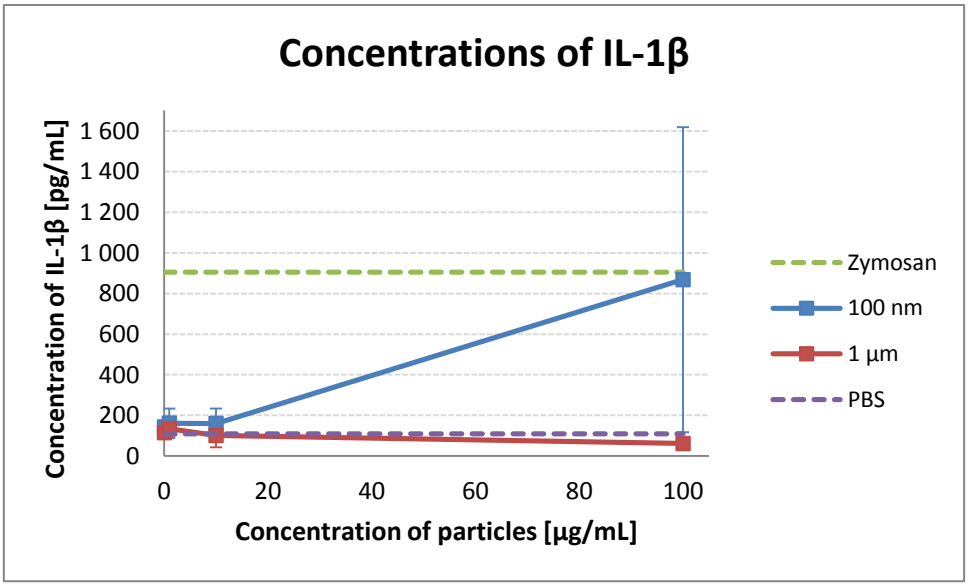

Figure 3.12 Average concentrations of IL-1β [pg/mL] from T360 analyzed with Bio-plex (n=3).

The last figure illustrates that 100 nm particles with concentration 100 µg/mL result in roughly the same secretion levels of IL-1β as Zymosan does. There is no significance for any of the tested parameters in figure 3.12.

3.2.3.2 IL-2

The average concentrations of IL-2 secretion measured with Bio-17-plex are listed in table M.5, as well as presented graphically in figure 3.13.

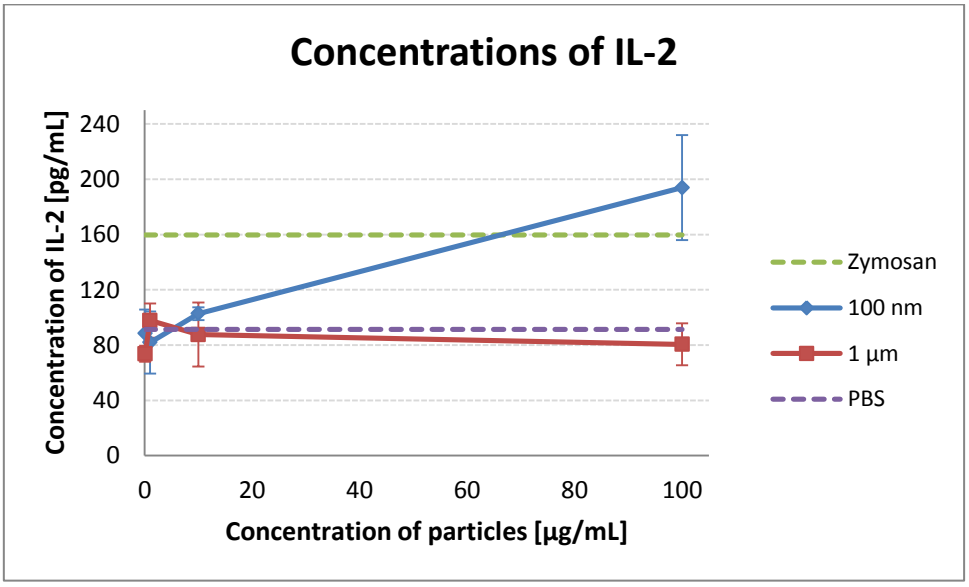

Figure 3.13 Average concentrations of IL-2 [pg/mL] from T360 analyzed with Bio-plex (n=3).

Analysis of IL-2 showed an increasing dose-dependence in cytokine secretion for the smaller particles and a slight decrease for the larger particles. There are significant

differences between 100 nm and 1 µm particles, as well as between 100 nm particles and PBS.

3.2.3.3 IL-6

The average concentrations of IL-6 secretion measured with Bio-17-plex are listed in table M.6, and presented graphically in figure 3.14.

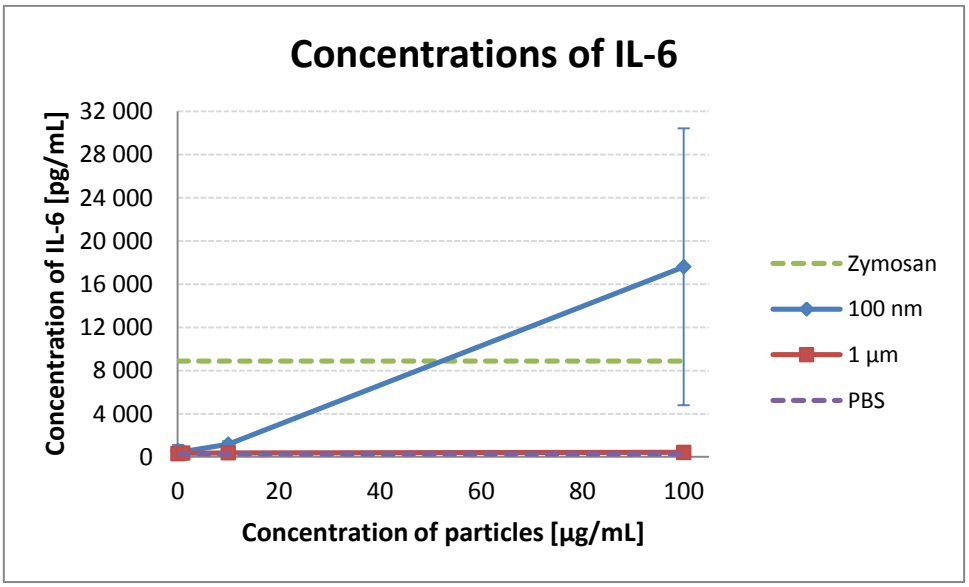

Figure 3.14 Average concentrations of IL-6 [pg/mL] from T360 analyzed with Bio-plex (n=3).

Secretion of IL-6 illustrated in figure 3.14 shows that there is a dose-dependent increase as a function of increasing 100 nm particle concentration. There is no significance for any of the tested parameters at level $p<0.05$, but Student's t-test resulted in $p<0.1$ for the differences between the two particles at 100 µg/mL concentration.

3.2.3.5 TNF-α

The average concentrations of TNF-α secretion measured with Bio-17-plex are listed in table M.7, and also presented graphically in figure 3.15.

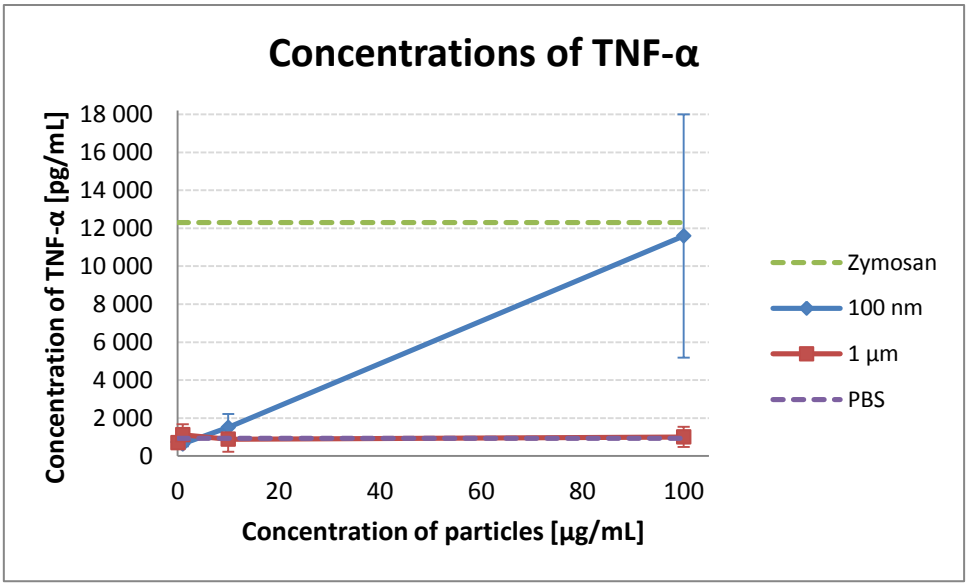

Figure 3.15 Average concentrations of TNF-α [pg/mL] from T360 analyzed with Bio-plex (n=3).

Similar results are seen for TNF-α secretion as for IL-6 described in section 3.2.3.3. There is a dose-dependent increase of cytokine secretion for the smaller particles, whereas the bigger particles do not seem to yield any higher secretion than the PBS control.

3.3 Dilution curves for LPS

Monocytes were isolated from healthy A+ PBMC donors in order to prepare dilution curves for LPS. These cells are stimulated two and six hours, respectively, and thereafter analyzed for cytokine secretion with IL-1β and TNF-α ELISAs. The results are presented in figures 3.16-3.18, and these values are all based on only one donor. The values are listed in tables I.10 and I.11 (attachment I). These tables present the results up to 25 000 pg/mL LPS, while the graphical illustrations are only up to 5 000 pg/mL.

3.3.1 Concentrations of IL-1β after two hours of stimulation with LPS

The following figure illustrates the dilution curve for LPS after two hours of stimulation when analyzed for IL-1β. The lower threshold (red line) in figures 3.16 and 3.18 is the negative control with medium and monocytes only.

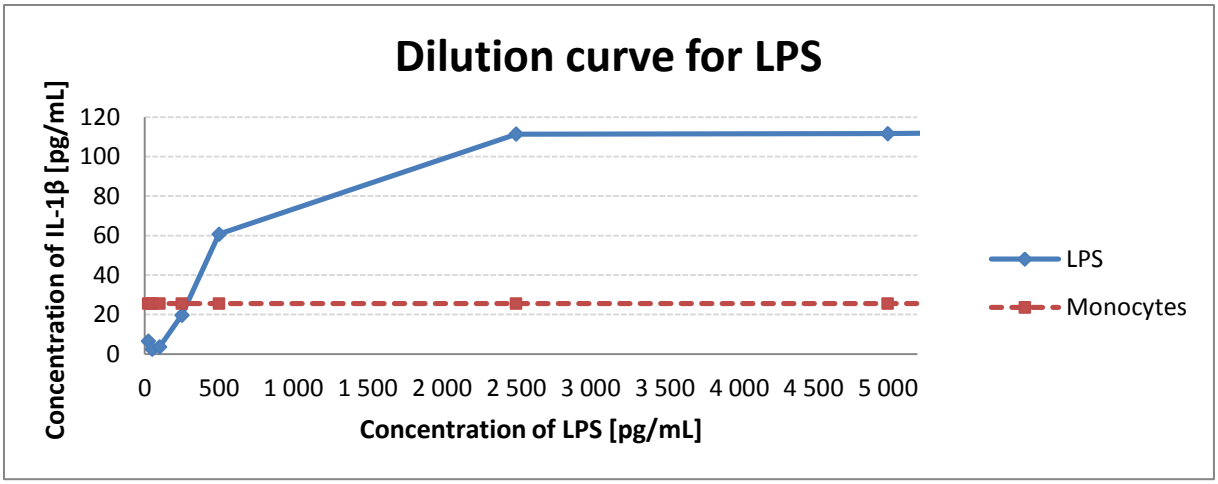

Figure 3.16 LPS dilution curve for secreted IL-1β [pg/mL] in response to increasing LPS concentration after two hours of stimulation (n=1).

Figure 3.16 shows that after two hours of stimulation, there is a dose-dependent increase in IL-1β secretion up to 2 500 pg/mL LPS, after which a plateau is observed. Negative controls with monocytes secrete even higher amounts of IL-1β than those stimulated with 250 pg/mL LPS.

3.3.2 Concentration of TNF-α after two hours of stimulation with LPS

Figure 3.17 illustrates the dilution curve for LPS after two hours of stimulation when analyzed for TNF-α levels in the cell-free supernatant.

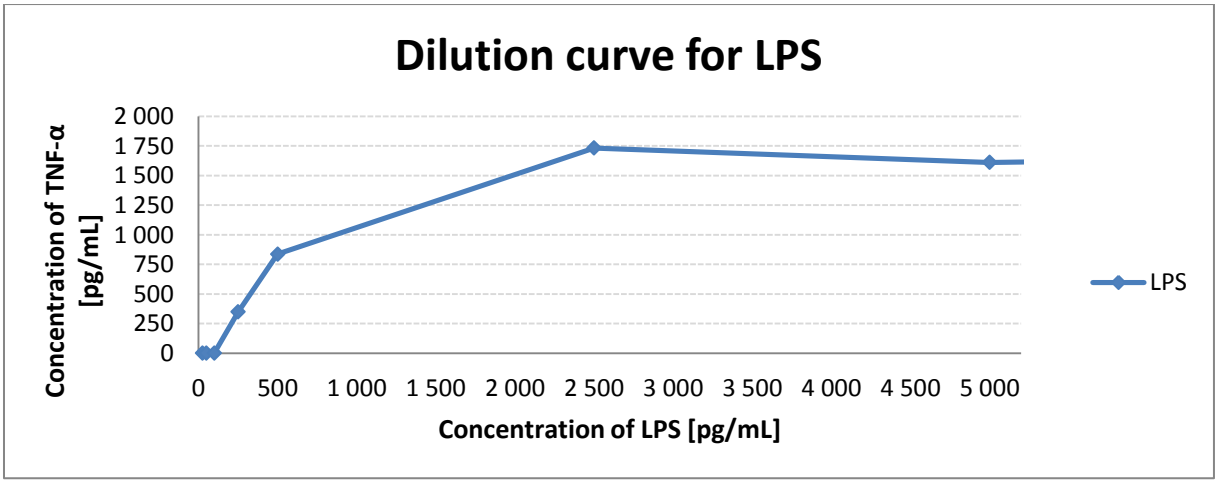

Figure 3.17 LPS dilution curve for secreted TNF-α [pg/mL] in response to increasing LPS concentration after two hours of stimulation (n=1).

The figure shows that after two hours of stimulation, there is a dose-dependent increase in TNF-α secretion up to 2 500 pg/mL LPS, after which a slight decrease and a plateau is observed. No secretion is detectable from the pure monocyte samples.

3.3.3 Concentration of IL-1β after six hours of stimulation with LPS

Figure 3.18 illustrates the dilution curve for LPS after six hours of stimulation when analyzed for IL-1β.

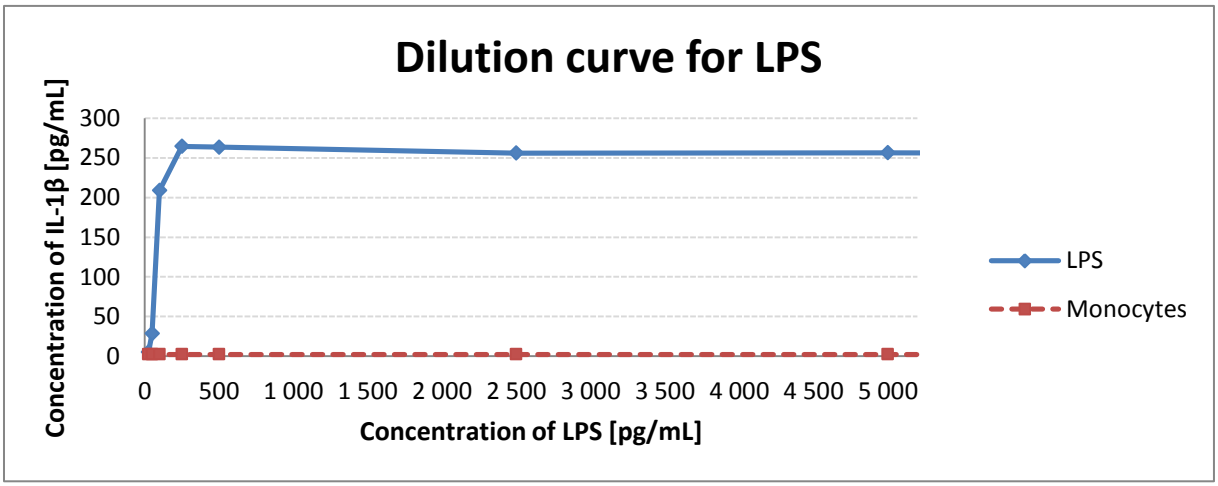

Figure 3.18 LPS dilution curve for secreted IL-1β [pg/mL] in response to increasing LPS concentration after six hours of stimulation (n=1).

Figure 3.18 shows that after six hours of stimulation, there is a dose-dependent increase in IL-1β secretion up to 250 pg/mL LPS, after which a plateau is seen. Monocytes themselves do not contribute much in IL-1β secretion.

3.3.4 Concentration of TNF-α after six hours of stimulation with LPS

Figure 3.19 illustrates the dilution curve for LPS after six hours of stimulation when analyzed for TNF-α cytokine.

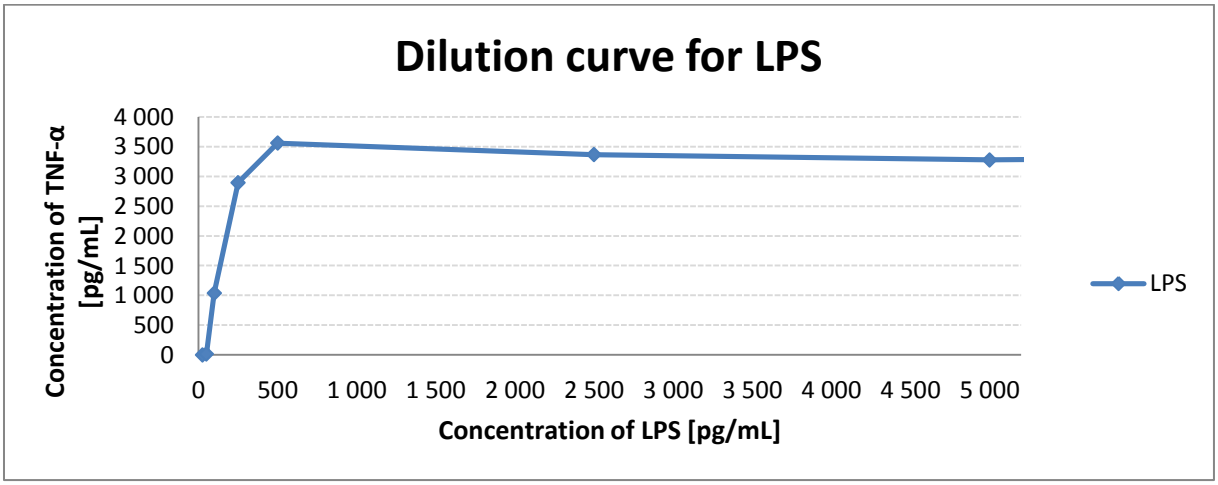

Figure 3.19 LPS dilution curve for secreted TNF-α [pg/mL] in response to increasing LPS concentration after six hours of stimulation (n=1).

Figure 3.19 shows that after six hours of stimulation, there is a dose-dependent increase in TNF-α secretion up to 500 pg/mL LPS, after which a slight decrease and a plateau is observed. No secretion is detected from the pure monocyte samples.

3.4 Confocal laser scanning microscopy

Images of the particles used in these experiments were captured with confocal microscopy.

3.4.1 Particles – 100 nm

Images were taken of the 100 nm particles at 63x magnification. Figure 3.20 illustrates the same optical section, but with three different illumination techniques. The image to the left was taken with PMT, while the image in the middle was taken with DIC. The one to the right is an overlap of the first two images.

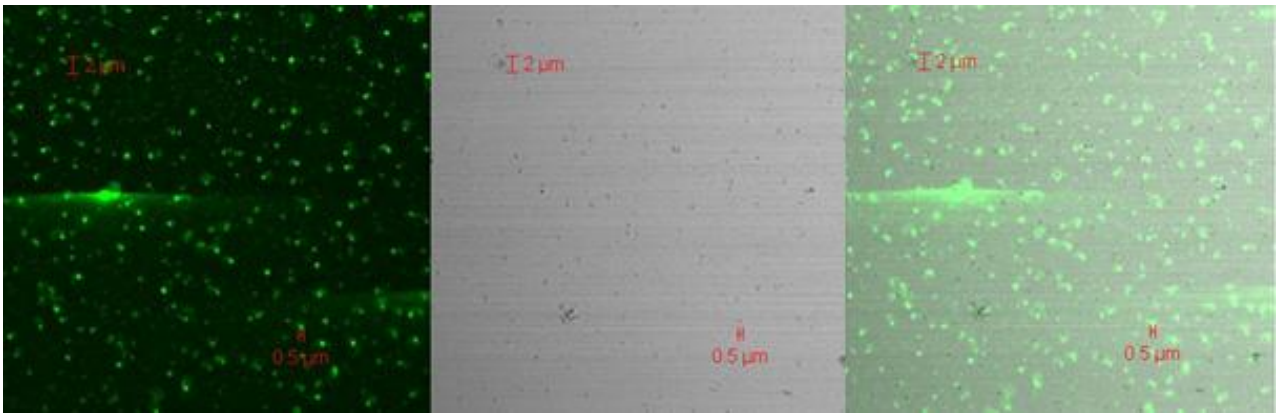

Figure 3.20 Images taken with a confocal microscope at 63x magnification. To the left: PMT imaging, in the middle: DIC imaging, to the right: combination of PMT and DIC.

In the last presented figure there are some particles that are smaller than 0.5 µm and others that are between 1-2 µm in diameter. The last ones are believed to be agglomerates of several 100 nm particles.

3.4.2 Particles - 1 µm

Images were taken of the 1 µm particles at both 23.2x and 63x magnification. Figure 3.21 illustrates a DIC image of a single 1 µm particle.

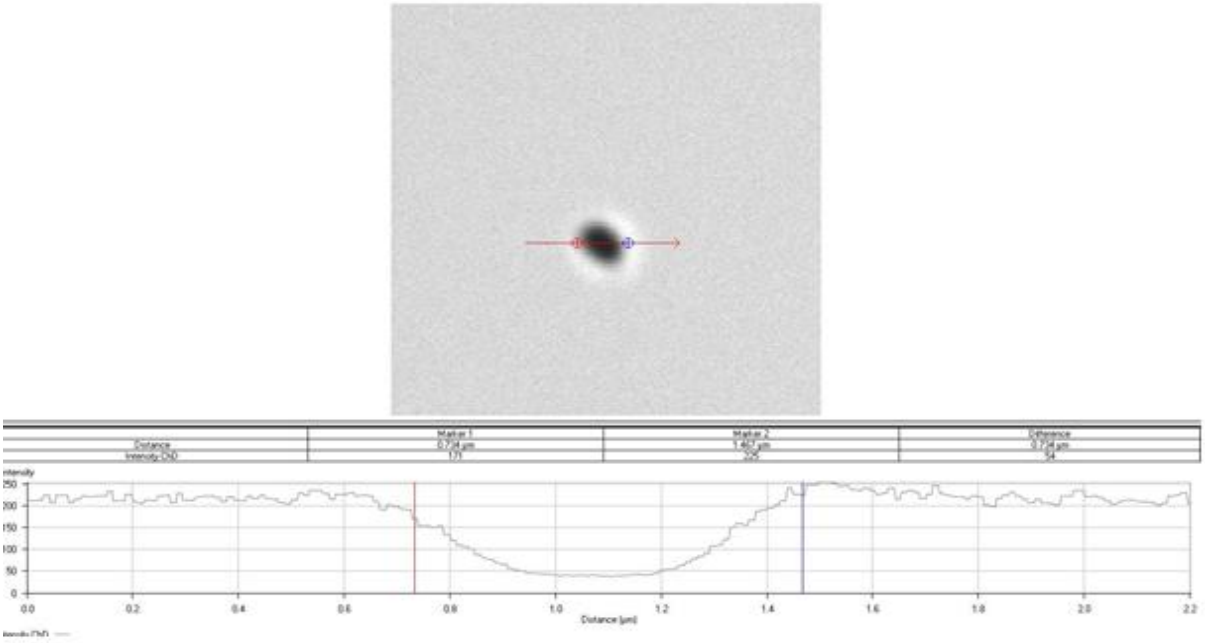

Figure 3.21 DIC image of a single 1 µm particle at 63x magnification. The scale shows distance [µm] at the x-axis, and intensity of transmitted light (ChD) at the y-axis.

The image above illustrates the distance and intensity of transmitted light between the two markers at the particle's diagonal. The measured diameter is 0.734 µm and the transmitted light intensity is 54 measured with the ChD channel.

Figure 3.22 illustrates a PMT image of a larger section with several 1 µm particles. The magnification was 23.2x.

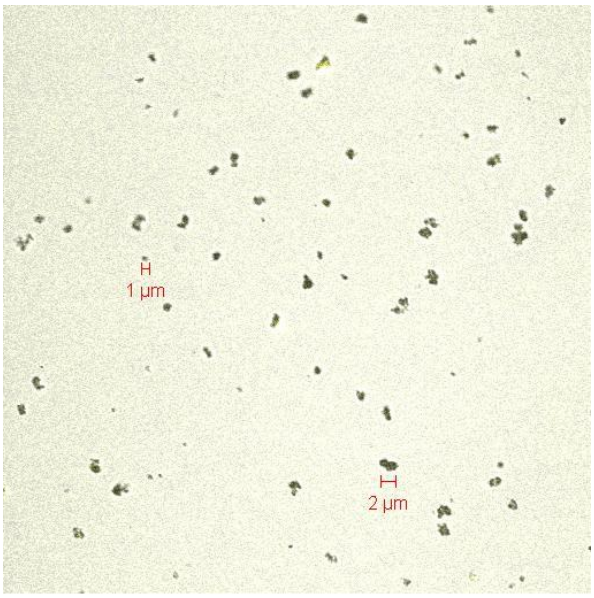

Figure 3.22 Larger section of 1 µm particle samples taken by PMT imaging at 23.2x magnification.

The last image shows that the sample with 1 µm particles contains both single particles as well as agglomerates with approximate sizes 2 µm.

4 Discussion

It is previously described that smaller particles result in higher inflammatory responses than larger ones. The experiences with exposure of monocytes and whole blood with particles of various sizes and concentrations (figures 3.1 to 3.15 in chapter 3) are consistent with this theory. All these results show that particle concentrations above 1.0 μg/mL result in higher secretion of cytokines for the 100 nm particles compared to the 1 μm particles.

4.1 Primed versus unprimed monocytes

The induction of inflammatory response from unprimed monocytes stimulated with only particles was tested and compared to monocytes that were primed with 100 pg/mL LPS prior to the same particle stimulations. According to the theory presented in chapter 1.6.3, pre-stimulation of monocytes with LPS was expected to raise pro-IL-1β levels prior to the inflammasome stimulation. The following particle stimulation would potentially activate the NLRP3 inflammasome leading to secretion of active IL-1β. However, figure 3.1 illustrates that there is no significance between the primed and unprimed monocytes of neither of the respective particle sizes. The unprimed monocytes secreted visibly lower amounts of IL-1β compared to the primed ones, but these differences are not significant. These findings are thus not consistent with the expected ones, where it was believed that the unprimed cells would not secrete detectable levels of IL-1β. The primed versus unprimed ATP controls show, however, that the inflammasome is activated by priming, because it is known that ATP itself is an activator of the NLRP3 inflammasome, but it is not engulfed by binding to TLR-4. This correlates with the findings, where unprimed ATP control cause less secretion of IL-1β compared to the primed control. The values are given in table I.2, attachment I.

There could be another uptake route within the monocytes that do not engage the NLRP3 inflammasome. Thus, the proposed mechanism in figure 1.5 would not be able to explain these results, unless presence of contaminating microbial ligands in the particles' storage buffers could activate the TLR-4. In this manner, pro-inflammatory IL-1β may be produced without any addition of external priming agents to the cell cultures. It may have happened that the bottles with the respective particles have been opened in an unsterile environment. As a result, this could have caused microbial growth in the storage buffers, although the manufacturer of the particles claims that the buffers have

been autoclaved, as stated on the enclosed datasheets in attachment O. This could explain the results shown in figure 3.1. At a particle concentration of 10 μg/mL, the unprimed monocytes secreted lower levels of IL-1β than the primed ones, although not significantly lower. It could be that the amount of unsterile storage buffer was not high enough to induce any high pro-inflammatory cytokine response from the cells. However, at 100 μg/mL, the unprimed monocytes stimulated with 100 nm particles secrete higher levels of active IL-1β than the primed ones. The same amount of storage buffer is added to both testing groups, but it is possible that the primed monocytes have reached their saturation point from the priming agent when the particles were added after two hours, and therefore, they did not produce higher levels of pro-cytokine.

Figures 3.2 to 3.7 show the same dose-response relationship for all testing groups as for IL-1β in figure 3.1. This indicates that particles themselves are causing inflammatory responses, where the smaller particles result in higher cytokine secretion of all the given cytokines compared to the bigger particles. Another possible explanation could be that the polysaccharide coated particles themselves were recognized as pathogens by the phagocytic cells. Thus, it could be proposed that some TLRs that are known to recognize bacteria were activated, causing an induction of an inflammatory response.

Comparing the given illustrations for IL-1β secretion measured with regular ELISA (figure 3.1) versus Bio-plex (figure 3.3) on the same samples, the multiplex shows as much as 3.7 times higher values for the smaller particles compared to ELISA. Bio-plex is a less sensitive analytical method than ELISA, and may for this reason detect incorrect levels of one cytokine. However, the same trend is seen in these two figures, except the sudden increase of IL-1β secretion from primed monocytes stimulated with 10 μg/mL 100 nm particles in figure 3.1.

Results presented in chapter 3.1.2 show that in total six cytokines secreted from monocytes (included TNF-α which had cytokine levels above range and are therefore not given), show similar dose-response relationships. These are IL-1β, IL-2, IL-6, GM-CSF, IFN-γ and TNF-α, and all are presented in chapter 1.3. IL-1β, IL-6 and TNF-α are pro-inflammatory cytokines that are produced by monocytes after stimulation with LPS. Cytokine IL-2 and IFN-γ induce the production of the other three cytokines in monocytes, which in addition are shown to produce GM-CSF. None of the stated cytokines are known to inhibit or down-regulate each other's activities.

Chapter 1.3.2 describes that no production of IL-2 has been detected in macrophages, only in dendritic cells. Here, secretion of IL-2 is however detected with multiplex analysis on samples from monocyte cultures. One of the major problems associated with the isolation of PBMC by the Ficoll-Hypaque gradient is the presence of contaminating lymphoid cells (Bennett and Breit, 1994, Boyum et al., 2002). Although the monocytes are positively selected for based on adherence to plastic, the purification procedure afterwards may not have been satisfying. The contaminating presence of lymphoid cells has the potential to influence experimental results. The secretion of IL-2 illustrated in figure 3.4 is so low (the maximum detected level is 13 pg/mL), and it is therefore believed that this cytokine has been secreted by contaminating dendritic or other lymphoid cells in the culturing plates.

4.2 Active versus heat inactivated A+ serum

Figure 3.8 illustrates the comparison between the same stimuli on monocytes, but in active and heat inactivated A+ serum, respectively. As described in 1.2.1, active serum contains nutritive supplements that are essential for cell growth. Although the results show that stimulation with 10 μg/mL of 100 nm particles yield approximately the same concentrations of IL-1β in both serums, the levels of secretion in heat inactivated serum are lower, all over. This is specially the case for sample groups stimulated with 1 μm. According to the theory, this would be expected since the inactive serum no longer contains nutrients supporting cell growth and survival. The monocytes will therefore not be able to produce comparable levels of cytokine as the ones in the active serum.

The drastic increase in IL-1β concentration between 1.0 and 10 μg/mL which is seen in figure 3.8 can be due to complement activity in active serum. As previously explained, complement is a heat-labile factor in serum, and can thus be heat inactivated. The heat inactivated A+ serum is therefore believed to contain no complement. Compared to the active serum, the heat inactivated A+ serum is causing a proportional increase of secreted IL-1β as a function of particle concentration. The active serum, however, show a sudden increase of secretion at 10 μg/mL particles. This can be due to opsonization of the LPS- and particle infected monocytes, resulting in a drastic release of cytokine from the cells when the particle concentration was ten times higher.

4.3 Flow studies in whole blood

Up-regulation of CD11b in monocytes and granulocytes is studied by flow analysis after gating for CD14 positive cells. The respective results are given in figures 3.9a) and b).

The effects of complement CD11b up-regulation was compared for the two separate particles. Here, the same increase in immune response is observed for the particles as from the experiments with monocytes. The smaller particles cause higher up-regulation of CD11b than the 1 μm particles on both leukocytes. The effect of particles was comparable on CD11b up-regulation on monocytes and granulocytes. It is notable that the negative control with PBS did not enhance up-regulation of the leukocytes, indicating that the dilution medium itself is not up-regulating CD11b. On the contrary, the positive control with Zymosan up-regulated CD11b granulocytes twice as much as CD11b monocytes.

This up-regulation of CD11b could imply that CR3 may be the receptor involved in the uptake of the particles, which eventually led to their endocytosis by the phagocytes.

4.4 TCC studies in whole blood

Activation of complement is shown in figure 3.10 as a measure of TCC in whole blood serum. Yet again, similar differences were found between the two particles it was stimulated with as described for earlier analyses. Both particles show an increasing activation of complement with increasing concentration of particles. However, 100 nm particles activate complement in a higher manner than the 1 μm particles up to stimulation with 100 μg/mL particles, where their activation was virtually the same. PBS control did not activate complement by itself and the particle-induced TCC level in the serum was 17.5 times higher compared to the TCC level induced by PBS alone. Zymosan, on the other hand, was activating complement in a higher degree than the particles.

Earlier reports have shown that CR3 on human granulocytes is complement dependent and is involved in phagocytosis of C3b-coated bacteria. It could be that the particles have been coated with this complement component and internalized by the phagocytic cells by recognition from CR3 on the cell membranes.

4.5 Cytokine analyses in whole blood

None of the whole blood samples were primed with LPS in advance to particle stimulation. This is because it was thought that the priming would inflict a lot in whole

blood. It was thought that the components in whole blood would already have reacted on LPS before the particles were added so that the resulting analyses of the blood would not show characteristic responses from the subsequent stimulation with particles. The priming procedure was, however, only thought to pre-stimulate monocytes in pure cell cultures.

Results from IL-1β specific ELISA on the whole blood samples show, yet again, similar dose-response relationship as the one found from the other analyses where the 100 nm particles induce higher cytokine secretion compared to the 1 μm particles. This is also true for the remaining three cytokines that were detected with Bio-plex. Results presented in chapter 3.2.3 show that in total four cytokines yield similar dose-response relationships after stimulation of whole blood. These are IL-1β, IL-2, IL-6 and TNF-α, and the cytokine diversity is less in whole blood than in pure monocyte cultures. This may be due to a higher complexity and diversity of cytokines that influence on each other.

The four cytokines that are found from whole blood studies are the same as from monocyte studies and have been discussed once already in section 4.1. Because there are monocytes in whole blood, it is not surprising that the same cytokines are detected in these axperiments. However, the level of secretion of IL-1β from whole blood (figure 3.12) is lower than from pure non-primed monocytes cultures (figure 3.1). The same is the case for IL-6 (figures 3.14 versus 3.5), but the opposite is true for TNF-α (figures 3.15 versus 3.2).

Chapter 1.3 describes that IL-4 is inhibitory on other cytokines such as IL-1, IL-6, and TNF-α. Attachment N.2 presents low and insignificant, however detectable levels of IL-4 in whole blood. Chapter 1.3 further described that cytokine IL-4 is a late-acting cytokine, and the given samples at T360 may thus not have been stimulated long enough to yield higher amounts of this cytokine. However, if the detectable levels of IL-4 are reliable, this cytokine may have inhibited some of the activity of IL-1β, IL-6 and TNF-α.

IL-4 is in addition inhibitory on cytokine IL-8. However, figure N.8 in attachment N shows that the secreted concentration of IL-8 is on nano-level, meaning that these findings are not in direct correlation with the theory. On the other hand, the low levels of IL-17 shown in figure N.12 may have up-regulated IL-8. In addition, there are many other cytokines and factors in whole blood that are not accounted for with 17-plex that

may have down-regulated for instance IL-4, and therefore resulted in higher secretion of IL-8.

GM-CSF was detected from pure monocyte cultures, but not in whole blood. This cytokine is also down-regulated by IL-4, and may thus be expected not to be excreted from monocytes in whole blood.

The activity of cytokine MCP-1 induces expression of IL-1 and IL-6, as described in section 1.3.14. When comparing figure N.16 in attachment N with figures 3.12 and 3.14, it is seen that a down-regulation of MCP-1 does not correlate with a down-regulation of IL-1 and IL-6. However, there are many other cells and cytokines in whole blood that activate the up-regulation of these two cytokines, so down-regulation of MCP-1 is not synonymous with down-regulation of the mentioned cytokines.

Further, a positive, however insignificant secretion of IL-10 is presented in figure N.9. It is previously described that IL-10 acts inhibitory on IFN-γ, and as it is seen in figure N.15, there is no secretion of IFN-γ. In addition, IL-10 acts inhibitory on synthesis of pro-inflammatory cytokines IL-1, IL-6 and TNF-α. In possible synergetic activity with IL-4, IL-10 has the potential to block the production of several other cytokines as well, as described in chapter 1.3.8.

4.6 LPS dilution curves

Dilution curves for both IL-1β and TNF-α after stimulation with increasing concentrations of LPS for two and six hours, respectively, are presented in figures 3.16 to 3.19. The first figure (and table I.10) shows that the priming concentration of LPS (100 pg/mL) results in the secretion of 3.54 ± 0.04 pg/mL IL-1β after two hours. This value is below the base-line for negative control, which resulted in 25.50 ± 0.17 pg/mL IL-1β. Thus, the dilution curve implies that the priming concentration is too low to give any efficient secretion of IL-1β itself. After six hours of stimulation, however, the negative control is 100 times lower as for the priming concentration of LPS.

Figure 3.17 shows that the priming concentration results in an undetectably low secretion of TNF-α after two hours of stimulation. After six hours of stimulation, however, the value is detectable as presented in table I.11. The negative controls with monocytes are undetectable in either of the two TNF-α analyses.

The standard curves for LPS were prepared in order to establish whether the priming concentration of 100 pg/mL was high enough for the monocytes to secrete cytokines. It was in addition desirable to get an overview of the monocytes' dose-dependent secretion of IL-1β and TNF-α.

The priming is only performed to induce the synthesis of IL-1β in the cells prior to the inflammasome stimulation in monocytes, and not fully to stimulate the cells. It is, however, important to stress that these results are based on only one donor, and several donors may have resulted in other concentrations of secreted cytokine, especially for IL-1β.

4.7 Confocal microscopy

Confocal microscopy is not the optimal method for analysis and imaging of 100 nm particles. It was difficult to define the boundaries between the individual particles, as proven by figure 3.20. The lower detection limit with this Zeiss microscope at 63x magnitude is between 200-250 nm samples (Egeberg, 2012). It was therefore difficult to estimate the precise size of the smallest particles, which the manufacturer claimed to be 100 nm. It is however possible to see some smaller particles as well as larger fragments in figure 3.20. This is believed to be a mixture of individual particles as well as agglomerates of several 100 nm particles. These agglomerates are thought to be no larger than 1 µm in diameter, based on the scales on the image. By using PMT imaging, it was possible to see the particles' fluorescence, although they got photobleached very quickly. Hence, it was confirmed that the particles seen on the images were indeed particles and not contaminating microbial growth.

For the 1 µm particles, no PMT images are shown, but the DIC image in figure 3.21 shows a rather clear particle with a diameter of 0.734 µm. The definition of submicron particles is that these are smaller than 1 µm, thus, this measure is thought to be acceptable. Figure 3.22 shows in addition a larger section taken of the 1 µm particle sample where some agglomerates are seen to be 2 µm in size.

If these results are to be trusted, the smaller particles form agglomerates consisting of several particles per unit compared to the agglomerates formed by the 1 µm particles.

4.8 Further discussions

Human serum contains many factors that may influence the cultured cells and exert a batch-dependent effect. As mentioned in attachment E.2, the A+ serum batch used for culture of monocytes from donors C and D was different of that used for donors A and B. This can count as a non-comparable factor between the experimental parallels. The presence of growth factors in serum may also enable the survival and proliferation of any contaminating lymphoid cells. It is discussed in section 4.1 that the results may have been influenced by just that.

One of the benefits of using Bio-plex was that it was possible to achieve results for several cytokines from a small amount of sample volume. However, this method is more inaccurate, and causes the standard deviations and results to be much higher than with standard ELISA. However, it is a good indicative method for multi-analyses of cytokines from a small amount of sample.

It was considered whether to normalize the results. By doing this, unknown biological differences between the donors due to age and sex would have been eliminated. It was, however, decided not to do this, since the standard deviations became much larger than for the results that are presented here.

One of the purposes of these exposure studies was to examine size-dependent effects of two carboxyl coated submicron particles. All presented figures in chapter 3 suggest a general trend where the particles with a stated hydrodynamic diameter of 100 nm induce higher inflammatory responses than the particles with a diameter of 1 µm. As there is shown in mice that small particles to a higher degree than larger ones augment an allergic response, it is expected that the nanoparticles are able to induce a different immune response than micrometer sized particles. As described in chapter 1.5.3, characteristics of the particles such as the surface chemistry should also be considered together with the particles' surface areas when investigating potential biological effects. Figure 1.2 illustrates the slightly differences in composition and chemistry surface between the two types of particles. From this it is seen that the larger particles consist of silica particles in their outer matrix, whereas the smaller particles are coated with a polysaccharide matrix. It could be suggested that the silica coating of the 1 µm particles provide better bioavailability compared to the 100 nm particles. It is already proposed that the polysaccharide coating of the 100 nm particles may be recognized as the outer

cell wall of bacteria. This may be one reason for why inflammatory responses are induced in such amounts by the particles alone.

Chapter 1.6.3 describes one proposed model for NLRP3 inflammasome activation which includes ROS production in the cytoplasm. The submicron particles' cores consist of iron oxides with different oxidation states of the iron. It is expected that the higher oxidative state of iron in magnetite would affect the inflammasome to a higher degree than the less oxidative state in maghemite. Thus, the results in figure 3.1 correlate with theory. There is an additional theory describing that the coated SPIO particles may be degraded into iron ions within the lysosomes after being internalized by the cell. This could result in iron ions which could be able to diffuse passively through the lysosome membrane causing production of ROS and other radicals in the cytoplasm. This could in turn result in oxidative stress or even affect the iron metabolism in the body which may consequently activate the inflammasome (Singh et al., 2010, Gu et al., 2011). If iron ions really diffuse through the lysosome membrane, the transmembrane protein which regulates intracellular iron levels by exporting excess iron outside of the side, Ferroportin 1, may become saturated. Thus, the iron levels in cytoplasm increase above normal levels and could cause inflammatory responses.

Previous studies also discuss that magnetite is not very stable. Thus, it can undergo oxidation to form maghemite and iron ions (Fe^{2+}) (Haneda and Morrish, 1977, Singh et al., 2010). Magnetite and maghemite can therefore show different cellular responses due to their ability to undergo dissimilar reactions. Thus, these two submicron particles used in this project are not ideal for comparison of intracellular molecular mechanisms due to their structural differences. Their coatings are also dissimilar, and could be an important factor explaining the differences between the induced responses, although these differences are not always significant.

As discussed in chapter 1.5.3, it has been shown that particle concentrations below 100 µg/mL are considered non-toxic for magnetite nanoparticles coated with a bipolar surfactant. As for this project's particles, increasing toxicity is observed from 10 µg/mL and higher, suggesting that the carboxyl groups are more reactive and thus internalized by the cells at a lower concentration.

The cytokine production profile is descriptive of the sensitivity reactions that are caused by the stimulant. This is discussed in chapter 1.3.17. The four cytokines (IL-1β, IL-2, IL-6 and TNF-α) secreted after whole blood stimulations are produced by either Th1 or Th2 cells. Thus, the cytokine responses on the submicron particles are both involved in hypersensitivity reactions and in B cells' Ab production.

The different sizes of the particles (100 nm and 1 μm) did not result in different cytokine responses among the seventeen measured with Bio-plex. This could suggest that both particles were internalized by the monocytes by the same, or at least similar, uptake routes. In chapter 1.6.1, there are two different pathways described that are triggered by binding of LPS to TLR-4. The priming process could activate the MyD88-dependent pathway by LPS which has bound to its receptor at the monocyte membrane. As previously described, NF-κB is then believed to be activated and this would lead to early production of pro-inflammatory cytokines such as IL-1β and TNF-α. Since these cytokines are measured in the cell free supernatants, there is reason to believe that this has happened. However, it is further described that TLR-4 can be endocytosed by the cell. This is believed to initiate the MyD88-independent pathway from endosomal compartments, which finally would activate NF-κB at late times and still produce the same pro-inflammatory cytokines as the previous pathway. In addition, it is argued that the particles have been internalized and degraded by lysosomes. Sections 4.3 and 4.4 discuss that they could have been coated with C3b by complement and recognized by CR3. This receptor could be close to TLR-4 on the membrane, and it could therefore be possible that LPS and particles were endocytosed together by the leukocyte cells.

Per mass basis, it was expected that the nanoparticles would cause a greater inflammatory response due to their larger surface area compared to the 1 μm particles. If the particles formed any agglomerates, the surface area of the particles was also expected to decrease. It is discussed in chapter 4.7 that the 100 nm particles form agglomerates consisting of several particles, but these are still believed to be smaller than the agglomerates formed by the 1 μm particles.

The experimental methods in addition to stimulation periods may not have been ultimate for the performed analyses. The incubation periods could have been too short to achieve a full activation of the inflammasome complex. It is described that some cytokines are more late-acting than others, and especially concerning the cytokine

analyses of whole blood, the incubation period of six hours may be a crucial factor for the Bio-plex results.

It is speculated whether the achieved results of IL-1β are high enough to confirm that the submicron particles have activated the NLRP3 inflammasome. This may be due to the priming concentration of LPS not being high enough to achieve a successful pre-stimulation of the monocytes. An additional awareness arose after reading the catalog for the LPS where it is specified that "*stimulations of TLR-4 with E. coli LPS can be achieved with concentrations ranging from 10 ng to 10 µg/mL"*. The priming concentration which is used is 100 times lower than 10 ng, and this could be a major cause of the low amounts of IL-1β. However, the levels of secreted IL-6 and TNF-α illustrated in figures 3.2 and 3.5 show that both cytokines are secreted in nano-scale levels, and the pre-stimulation of monocytes with LPS is therefore thought to be adequate.

Other errors besides the low priming concentration with LPS may be the technique regarding the use of pipettes. In addition, the incubation times were not always precisely on time. This could be inflicting for instance the adherence of the monocytes to the plate's surface, as well as causing inaccuracies during the ELISA procedure. A significant systematic error worth mentioning is when two different individuals perform the same experimental procedures. This was sometimes the case during the isolation procedures of monocytes as well as the whole blood experiments.

4.9 Future perspectives

This study was designed for stimulation of monocytes and whole blood with SPIO submicron particles for up to six hours. As it is already described in chapter 1 that some cytokines are more late-acting than others, it would have been interesting to investigate whether a longer stimulation period would result in elevated cytokine responses. Further, it could be of interest to investigate the time-dependency of the immune responses. Periodical sampling during 24 hours, for instance, could give valuable information about the induction of long-term intracellular oxidative stress and responses of the mammalian immune system against these SPIO particles *in vitro*.

An electron microscope could also be used to track the internalization process of the particles in monocytes. This may also contribute to an increased understanding of the

processes involved in uptake and degradation of such submicron particles in the cells. Additionally, it would be of interest to test whether higher concentrations of particles would give further increasing cytokine secretions, or if internalization of 100 μg/mL is approaching a saturation point for the monocytes. More than three donors could also result in different and more reliable results.

Gravimetric analyses could also be of importance by considering whether the size or the amounts of particles influence the immune responses the most. It is assumed that there is a lot more of the 100 nm particles compared to the 1 μm particles per mass basis. It could therefore be interesting to compare the inflammatory responses to both particles by quantitative means and not only by size.

It is discussed that the inflammasome has been activated by the particles due to detected levels of active IL-1β in the cell-free supernatants. However, this is not a direct evidence of activation. Western blot could have been used to determine whether the pro-caspase-1 has been cleaved to generate two subunits, as described in chapter 1.6.3. This may have resulted in more reliable evidence on potential inflammasome activation by the SPIO submicron particles.

5 Conclusion

The purpose of this study was to investigate how particle size affects inflammatory response and what dose-response relationship these SPIO submicron particles generated. It was found that 100 nm particles induced a higher, although not significantly, inflammatory response compared to the 1 μm sized particles. These findings applied to CD11b up-regulation, complement activation and cytokine secretion. It was, however, interesting to find that the particles themselves activated the inflammasome without any priming of the monocytes in advance to particle stimulation. It has been discussed that the storage buffer of the particles may have been contaminated with LPS so that TLR-4 has been activated. It has also been proposed that the polysaccharide coating of the 100 nm particles has been recognized as bacterial component by some TLRs on the cell membrane.

Inflammasome activation may be explained by elevated ROS levels in cytoplasm. It is possible that the particles have been coated with C3b by the complement system and phagocytized by the monocytes through CD11b/CD18 receptor. This could be followed up by degradation of their carboxyl coating. This potential degradation could have resulted in iron ions which may have diffused passively through the lysosome membrane and generated elevated levels of ROS due to the imbalance in iron levels in the cytoplasm. The 100 nm particles consist of magnetite which is a more reactive state of iron than maghemite. This could be another reason for why the smaller particles exhibit a higher inflammatory response than the larger ones. Toxicity of the particles can be seen at 10 μg/mL, suggesting their potentially low biocompatibility above this concentration. However, silica coated 1 μm particles induce inflammation to a lower extent than the polysaccharide coated 100 nm particles.

References

ALLAVENA, P., BIANCHI, G., BONECCHI, R., CAMPBELL, E. & AL., E. 1999. *Chemokines*, Karger.

ANKAMWAR, B., LAI, T. C., HUANG, J. H., LIU, R. S., HSIAO, M., CHEN, C. H. & HWU, Y. K. 2010. Biocompatibility of Fe3O4 nanoparticles evaluated by in vitro cytotoxicity assays using normal, glia and breast cancer cells. *Nanotechnology,* 21**,** 075102/1-075102/9.

AXIS-SHIELD Lymphoprep, Isolation of human mononuclear cells.

BAUERNFEIND, F., ABLASSER, A., BARTOK, E., KIM, S., SCHMID-BURGK, J., CAVLAR, T. & HORNUNG, V. 2011. Inflammasomes: current understanding and open questions. *Cell. Mol. Life Sci.,* 68**,** 765-783.

BENNETT, S. & BREIT, S. N. 1994. Variables in the isolation and culture of human monocytes that are of particular relevance to studies of HIV. *J. Leukocyte Biol.,* 56**,** 236-40.

BONNEMAIN, B. 1998. Superparamagnetic agents in magnetic resonance imaging. Physicochemical characteristics and clinical applications. A review. *J. Drug Targeting,* 6**,** 167-174.

BORM, P. J. A. & DRISCOLL, K. 1996. Particles, inflammation and respiratory tract carcinogenesis. *Toxicol. Lett.,* 88**,** 109-113.

BOYUM, A. 1976. Isolation of lymphocytes, granulocytes and macrophages. *Scand J Immunol,* Suppl 5**,** 9-15.

BOYUM, A., BRINCKER FJERDINGSTAD, H., MARTINSEN, I., LEA, T. & LOVHAUG, D. 2002. Separation of human lymphocytes from citrated blood by density gradient (NycoPrep) centrifugation: monocyte depletion depending upon activation of membrane potassium channels. *Scand J Immunol,* 56**,** 76-84.

BREKKE, O.-L., CHRISTIANSEN, D., FURE, H., FUNG, M. & MOLLNES, T. E. 2007. The role of complement C3 opsonization, C5a receptor, and CD14 in E. coli-induced up-regulation of granulocyte and monocyte CD11b/CD18 (CR3), phagocytosis, and oxidative burst in human whole blood. *J. Leukocyte Biol.,* 81**,** 1404-1413.

CHAUDHURI, N., PAIVA, C., DONALDSON, K., DUFFIN, R., PARKER, L. C. & SABROE, I. 2010. Diesel exhaust particles override natural injury-limiting pathways in the lung. *Am. J. Physiol.,* 299**,** L263-L271.

CHEMICELL1μM. *screenMAG/B-Carboxyl* [Online]. Available: http://www.chemicell.com/products/fluorescent/docs/PI_screenMAG-Carboxyl_2102.pdf.

CHEMICELL100NM. *nano-screenMAG/B-ARA* [Online]. Available: http://www.chemicell.com/products/magneticfluorescent/docs/PI_nano-screenMAG-ARA_4415.pdf.

CHEN, G. & PEDRA, J. H. F. 2010. The inflammasome in host defense. *Sensors,* 10**,** 97-111.

COUNCIL_OF_EUROPE 2007. Guide to the Preparation, Use and Quality Assurance of Blood Components. 13th ed.

DUCHOW, J., MERCHANT, A., CRUSIAUX, A., HUSSON, C., ALONSO-VEGA, C., DE GROOTE, D., NEVE, P. & GOLDMAN, M. 1993. Impaired phagocyte responses to lipopolysaccharide in paroxysmal nocturnal hemoglobinuria. *Infect. Immun.,* 61**,** 4280-5.

EGEBERG, K. W. 2012. *RE: Lower detection limit for confocal microscopy.*

EISENBARTH STEPHANIE, C., COLEGIO OSCAR, R., O'CONNOR, W., SUTTERWALA FAYYAZ, S. & FLAVELL RICHARD, A. 2008. Crucial role for the Nalp3

inflammasome in the immunostimulatory properties of aluminium adjuvants. *Nature,* 453**,** 1122-6.
ESPEVIK, T., SØRENSEN, M. & VIK, R. 2010. Måling av TNF ved hjelp av ELISA.: NTNU.
FRANCHI, L., EIGENBROD, T., MUNOZ-PLANILLO, R. & NUNEZ, G. 2009. The inflammasome: a caspase-1-activation platform that regulates immune responses and disease pathogenesis. *Nat. Immunol.,* 10**,** 241-247.
GABAY, C. 2006. Interleukin-6 and chronic inflammation. *Arthritis Res. Ther.,* 8**,** No pp given.
GASQUE, P. 2004. Complement: a unique innate immune sensor for danger signals. *Mol. Immunol.,* 41**,** 1089-1098.
GRASSIAN, V. H., ADAMCAKOVA-DODD, A., PETTIBONE, J. M., O'SHAUGHNESSY, P. T. & THORNE, P. S. 2007. Inflammatory response of mice to manufactured titanium dioxide nanoparticles: comparison of size effects through different exposure routes. *Nanotoxicology,* 1**,** 211-226.
GROSS, O., THOMAS, C. J., GUARDA, G. & TSCHOPP, J. 2011. The inflammasome: an integrated view. *Immunol. Rev.,* 243**,** 136-151.
GU, J. L., XU, H. F., HAN, Y. H., DAI, W., HAO, W., WANG, C. Y., GU, N., XU, H. Y. & CAO, J. M. 2011. The internalization pathway, metabolic fate and biological effect of superparamagnetic iron oxide nanoparticles in the macrophage-like RAW264.7 cell. *Sci. China Life Sci.,* 54**,** 793-805.
GU, L., NI, Z., QIAN, J. & TOMINO, Y. 2007. Pravastatin Inhibits Carboxymethyllysine-Induced Monocyte Chemoattractant Protein 1 Expression in Podocytes via Prevention of Signalling Events. *Nephron,* 106**,** e1-e10.
GUPTA AJAY, K. & GUPTA, M. 2005. Synthesis and surface engineering of iron oxide nanoparticles for biomedical applications. *Biomaterials,* 26**,** 3995-4021.
HANEDA, K. & MORRISH, A. H. 1977. Magnetite to maghemite transformation in ultrafine particles. *J. Phys. (Paris), Colloq.***,** 321-3.
HUSEBYE, H., AUNE, M. H., STENVIK, J., SAMSTAD, E., SKJELDAL, F., HALAAS, O., NILSEN, N. J., STENMARK, H., LATZ, E., LIEN, E., MOLLNES, T. E., BAKKE, O. & ESPEVIK, T. 2010. The Rab11a GTPase Controls Toll-like Receptor 4-Induced Activation of Interferon Regulatory Factor-3 on Phagosomes. *Immunity,* 33**,** 583-596.
INVITROGEN 2011. HBSS - Hank's Balanced Salt Solution. *In:* TECHNOLOGIES, L. (ed.).
IWAMOTO, M. & NAGAI, Y. 1981. An easy quantitative cytotoxicity assay using a Coulter Counter. *Jpn J Exp Med,* 51**,** 109-15U.
JANEWAY, C. A., TRAVERS, P., WALPORT, M. & SCHLOMCHIK, M. J. 2001. *Immunobiology - The immune System in Health and Disease,* New York, Garland Science.
KAGAN, J. C., SU, T., HORNG, T., CHOW, A., AKIRA, S. & MEDZHITOV, R. 2008. TRAM couples endocytosis of Toll-like receptor 4 to the induction of interferon-β. *Nat. Immunol.,* 9**,** 361-368.
KINDT, T. J., GOLDSBY, R. A. & OSBORNE, B. A. 2007. *Kuby Immunology*, W. H. Freeman and Company.
LATZ, E. 2010. The inflammasomes: mechanisms of activation and function. *Curr. Opin. Immunol.,* 22**,** 28-33.
LUMINEX, C. 2011. *xMAP® Technology* [Online]. Available: http://www.luminexcorp.com/TechnologiesScience/xMAPTechnology/.
MADIGAN, M. T., MARTINKO, J. M., DUNLAP, P. V. & CLARK, D. P. 2009. *Brock Biology of Microorganisms*, Pearson Education, Inc.

MARTINON, F., BURNS, K. & TSCHOPP, J. 2002. The inflammasome: a molecular platform triggering activation of inflammatory caspases and processing of proIL-β. *Mol. Cell,* 10**,** 417-426.

MCGEEHAN, G. M., BECHERER, J. D., BAST, R. C., JR., BOYER, C. M., CHAMPION, B., CONNOLLY, K. M., CONWAY, J. G., FURDON, P., KARP, S., KIDAO, S. & ET AL. 1994. Regulation of tumour necrosis factor-alpha processing by a metalloproteinase inhibitor. *Nature,* 370**,** 558-61.

MEAGER, T. 1998. *The Molecular Biology of Cytokines*, John Wiley & Sons.

MOGENSEN, T. H. 2009. Pathogen recognition and inflammatory signaling in innate immune defenses. *Clin. Microbiol. Rev.,* 22**,** 240-273.

MOLLNES, T. E., BREKKE, O.-L., FUNG, M., FURE, H., CHRISTIANSEN, D., BERGSETH, G., VIDEM, V., LAPPEGARD, K. T., KOHL, J. & LAMBRIS, J. D. 2002a. Essential role of the C5a receptor in E. coli-induced oxidative burst and phagocytosis revealed by a novel lepirudin-based human whole blood model of inflammation. *Blood,* 100**,** 1869-1877.

MOLLNES, T. E., BREKKE, O.-L., FUNG, M., FURE, H., CHRISTIANSEN, D., BERGSETH, G., VIDEM, V., LAPPEGARD, K. T., KOHL, J. & LAMBRIS, J. D. 2002b. Essential role of the C5a receptor in E. coli-induced oxidative burst and phagocytosis revealed by a novel lepirudin-based human whole blood model of inflammation. [Erratum to document cited in CA137:200028]. *Blood,* 100**,** 2691.

MOLLNES, T. E. & LACHMANN, P. J. 1987. Activation of the third component of complement (C3) detected by a monoclonal anti-C3'g' neoantigen antibody in a one-step enzyme immunoassay. *J. Immunol. Methods,* 101**,** 201-7.

MOLLNES, T. E., REDL, H., HOEGAASEN, K., BENGTSSON, A., GARRED, P., SPEILBERG, L., LEA, T., OPPERMANN, M., GOETZE, O. & SCHLAG, G. 1993. Complement activation in septic baboons detected by neoepitope-specific assays for C3b/iC3b/C3c, C5a and the terminal C5b-9 complement complex (TCC). *Clin. Exp. Immunol.,* 91**,** 295-300.

MORGAN, B. P. 1989. Complement membrane attack on nucleated cells: resistance, recovery and non-lethal effects. *Biochem. J.,* 264**,** 1-14.

MORGAN, B. P. 1999. Regulation of the complement membrane attack pathway. *Crit. Rev. Immunol.,* 19**,** 173-198.

MORGAN, B. P. & GASQUE, P. 1997. Extrahepatic complement biosynthesis: where, when and why? *Clin. Exp. Immunol.,* 107**,** 1-7.

NEWTON, R. C., SOLOMON, K. A., COVINGTON, M. B., DECICCO, C. P., HALEY, P. J., FRIEDMAN, S. M. & VADDI, K. 2001. Biology of TACE inhibition. *Ann. Rheum. Dis.,* 60**,** iii25-iii32.

NILSEN, N. J. 7.10.2011 2011. *RE: IL-1β.*

NUESSLEIN, H. G. & SPIEGELBERG, H. L. 1990. Interleukin-4 induces both IgG4 and IgE secretion by peripheral blood B cells. *J. Clin. Lab. Anal.,* 4**,** 414-19.

PALSSON-MCDERMOTT, E. M. & O'NEILL, L. A. J. 2004. Signal transduction by the lipopolysaccharide receptor, Toll-like receptor-4. *Immunology,* 113**,** 153-162.

PARK, B. S., SONG, D. H., KIM, H. M., CHOI, B.-S., LEE, H. & LEE, J.-O. 2009. The structural basis of lipopolysaccharide recognition by the TLR4-MD-2 complex. *Nature (London, U. K.),* 458**,** 1191-1195.

PARRILLO, J. E. 1993. Pathogenetic mechanisms of septic shock. *N Engl J Med,* 328**,** 1471-7.

PELKA, K. & LATZ, E. 2011. Getting Closer to the Dirty Little Secret. *Immunity,* 34**,** 455-458.

QHOBOSHEANE, M., SANTRA, S., ZHANG, P. & TAN, W. 2001. Biochemically functionalized silica nanoparticles. *Analyst,* 126**,** 1274-8.
SCHALL, T. J., BACON, K., CAMP, R. D. R., HEBERT, C. A. & GOEDDEL, D. V. 1993. Human macrophage inflammatory protein α (MIP-1α) and MIP-1β chemokines attract distinct populations of lymphocytes. *J. Exp. Med.,* 177**,** 1821-5.
SCHINDLER, R., GELFAND, J. A. & DINARELLO, C. A. 1990. Recombinant C5a stimulates transcription rather than translation of interleukin-1 (IL-1) and tumor necrosis factor: translational signal provided by lipopolysaccharide or IL-1 itself. *Blood,* 76**,** 1631-8.
SIGMA-ALDRICH. 2011a. *RPMI Media* [Online]. Available: http://www.sigmaaldrich.com/life-science/cell-culture/classical-media-salts/rpmi-media.html.
SIGMA-ALDRICH 2011b. Tween-20.
SIGMA_ALDRICH. *Zymosan* [Online]. Available: http://www.sigmaaldrich.com/catalog/product/SIGMA/Z4250?lang=en&region=NO.
SIMMONS, D. L., TAN, S., TENEN, D. G., NICHOLSON-WELLER, A. & SEED, B. 1989. Monocyte antigen CD14 is a phospholipid anchored membrane protein. *Blood,* 73**,** 284-9.
SINGH, N., JENKINS, G. J. S., ASADI, R. & DOAK, S. H. 2010. Potential toxicity of superparamagnetic iron oxide nanoparticles (SPION). *Nano Rev.,* 1**,** No pp given.
SNAPPER, C. M. 1996. *Cytokine Regulation of Humoral Immunity*, John Wiley & Sons.
SPRONG, T., BRANDTZAEG, P., FUNG, M., PHARO, A. M., HOIBY, E. A., MICHAELSEN, T. E., AASE, A., VAN DER MEER, J. W. M., VAN DEUREN, M. & MOLLNES, T. E. 2003. Inhibition of C5a-induced inflammation with preserved C5b-9-mediated bactericidal activity in a human whole blood model of meningococcal sepsis. *Blood,* 102**,** 3702-3710.
STRAINIC, M. G., LIU, J., HUANG, D., AN, F., LALLI, P. N., MUQIM, N., SHAPIRO, V. S., DUBYAK, G. R., HEEGER, P. S. & MEDOF, M. E. 2008. Locally produced complement fragments C5a and C3a provide both costimulatory and survival signals to naive CD4+ T cells. *Immunity,* 28**,** 425-435.
SURETTE, M. E., PALMANTIER, R., GOSSELIN, J. & BORGEAT, P. 1993. Lipopolysaccharides prime whole human blood and isolated neutrophils for the increased synthesis of 5-lipoxygenase products by enhancing arachidonic acid availability: Involvement of the CD14 antigen. *J. Exp. Med.,* 178**,** 1347-55.
TAKEUCHI, O. & AKIRA, S. 2010. Pattern recognition receptors and inflammation. *Cell (Cambridge, MA, U. S.),* 140**,** 805-820.
THÈZE, J. 1999. *The Cytokine Network and Immune Functions*, Oxford.
THOMSON, A. W. & LOTZE, M. T. 2003. *The Cytokine Handbook*, Academic Press.
TSCHOPP, J. & SCHRODER, K. 2010. NLRP3 inflammasome activation: the convergence of multiple signaling pathways on ROS production? *Nat. Rev. Immunol.,* 10**,** 210-215.
UEMATSU, S. & AKIRA, S. 2006. Toll-like receptors and innate immunity. *J. Mol. Med. (Heidelberg, Ger.),* 84**,** 712-725.
WANG, X. & QUINN, P. J. 2010. Endotoxins: lipopolysaccharides of gram-negative bacteria. *Subcell. Biochem.,* 53**,** 3-25.
WARD, P. A. 2004. The dark side of C5A in sepsis. *Nat. Rev. Immunol.,* 4**,** 133-142.
WIKIPEDIA. 2011. *Polysorbate 20* [Online]. Available: http://en.wikipedia.org/wiki/Polysorbate_20 [Accessed 11.10.2011.

YAMAMOTO, M., SATO, S., HEMMI, H., UEMATSU, S., HOSHINO, K., KAISHO, T., TAKEUCHI, O., TAKEDA, K. & AKIRA, S. 2003. TRAM is specifically involved in the Toll-like receptor 4-mediated MyD88-independent signaling pathway. *Nat. Immunol.,* 4**,** 1144-1150.

YAZDI AMIR, S., GUARDA, G., RITEAU, N., DREXLER STEFAN, K., TARDIVEL, A., COUILLIN, I. & TSCHOPP, J. 2010. Nanoparticles activate the NLR pyrin domain containing 3 (Nlrp3) inflammasome and cause pulmonary inflammation through release of IL-1α and IL-1β. *Proc Natl Acad Sci U S A,* 107**,** 19449-54.

ZANONI, I., OSTUNI, R., MAREK, L. R., BARRESI, S., BARBALAT, R., BARTON, G. M., GRANUCCI, F. & KAGAN, J. C. 2011. CD14 Controls the LPS-Induced Endocytosis of Toll-like Receptor 4. *Cell (Cambridge, MA, U. S.),* 147**,** 868-880.

ZHOU, W., MARSH, J. E. & SACKS, S. H. 2001. Intrarenal synthesis of complement. *Kidney Int.,* 59**,** 1227-1235.

ZIEGLER, S. F., TOUGH, T. W., FRANKLIN, T. L., ARMITAGE, R. J. & ALDERSON, M. R. 1991. Induction of macrophage inflammatory protein-1β gene expression in human monocytes by lipopolysaccharide and IL-7. *J. Immunol.,* 147**,** 2234-9.

Table of contents- Attachments

Attachment A

A.1 List of reagents

Reagents/ components	Specifications	Product/ Cat. nr.	Manufacturer/ Brand	Origin of manufacturer
A+ serum	Heat inact./active. Pooled from 4 donors at the Blood bank, St. Olavs.	-	Blood bank at St. Olav's Hospital	Norway
Antibody: CD11b	Human reactivity	333142	BD Biosciences	USA
Antibody: CD14	Human reactivity	345784	BD Biosciences	USA
Antibody: Anti-TCC	Anti-Complement component C5b-9 (human). Mouse monoclonal antibody	DIA 011-01	AntibodyShop	Denmark
Antibody: Streptavidin-HRP	Mouse monoclonal antibody	405210	BioLegend	USA
Antibody: TCC	Biotinylated Monoclonal Anti-Human SC5b-9	A711	Quidel	USA
ATP	Bacterial source min. 99%. Mm=551.14 g/mol	A7699	Sigma-Aldrich	USA
Bio-Plex Pro™ Assay	Bio-Plex Pro Human Cytokine 17-Plex Panel	M50-00031YV	BioRad	USA
BSA	10% Albumine from bovine serum	A7030	Sigma-Aldrich	USA
Buffy coat (PBMC)	Consentually donated A+ blood from healthy individuals	-	Blood bank at St. Olav's Hospital	Norway
EDTA		300410		
Cell stain: LDS-751		L7595	Invitrogen	USA
Color agent A and B	A: Hydrogen Peroxide B: Tetramethylbenzi-dine (TMB)		BioLegend	USA
FBS	Heat-inactivated Fetal Bovine Serum	10270-106	Gibco	USA
Gentamicin	0.5%		Gibco Life Tech	Germany
Hanks' Balanced Salt Solution		H9269	Sigma-Aldrich	USA

IL-1β ELISA kit	Human IL-1β ELISA Set II BD OptEIA™	557953	BD Biosciences	USA
Isotone	Coulter Isotone II Diluent	8448011	Beckman Coulter	USA
LPS	Ultra-pure LPS from *Escherichia coli* 0111-B4 strain – TLR4 ligand	tlrl-3pelps	Invivogen	USA
Lymphoprep	ρ=1.077 g/mL	LYS 3773	Axis-Shield	UK
Particles 100 nm 1 µm	nano-screenMAG-ARA screenMAG-Carboxyl	4415-1 2102-1	Chemicell	Germany
PBS	Dulbecco's PBS, liquid	D8537	Sigma-Aldrich	USA
PBS	Tablets	BR0014G	Oxoid	England
PFA		P6148	Sigma-Aldrich	USA
Refludan	Lepirudin	PZN-2480375	Celgene	USA
RPMI-1640	With L-glutamine and $NaHCO_3$	R8758	Sigma-Aldrich	USA
Sulfuric acid	1 M H_2SO_4		Merck	Germany
TCC standard	Zymosan-activated serum	-	As described by (Mollnes and Lachmann, 1987)	Norway
TNF-α ELISA kit	Human TNF-α DuoSet	DY210	R&D Systems	USA
Tween-20		P1379	Sigma-Aldrich	USA
Water	Distilled		Braun	Germany
Water: Milli-Q	From Advantage A10 Ultra-pure Water Purification System with 0.22 µm Millipak filter	0169	Merck Millipore	USA
Whole blood	Consentually donated blood from healthy individuals	-	-	Norway
Zap-oglobin	Lysing agent of erythrocytes		Beckman Counter	USA
Zymosan	Prepared from Saccharomyces cerevisiae	Z4250	Sigma-Aldrich	USA

A.2 List of instruments

Type of instrument	Manufacturer	Model	Origin of manufacturer
Centrifuge	Kubota	8700	Japan
Cell counter	Beckman Counter	Nerliens Meszansky Z_2	USA
Confocal microscope	Zeiss	LSM 510 Meta	Germany
Flow cytometer	Beckman Coulter	Epics XL-MCL	USA
Incubator	Thermo Scientific	Forma Steri-Cycle	USA
Microplate absorbance reader	BioRad	iMark	USA
Microplate detection system	BioRad	Dual-laser flow-based microplate detection system	USA
Plate shaker	Heidolph	Vibramax 100	Germany
Plate washer (Bio-plex)	BioRad	Bio-Plex Pro Wash Station	USA
Plate washer (ELISA)	Thermo Labsystems	Ultrawash	USA

A.3 List of equipment

Type of equipment	Manufacturer	Model	Origin of manufacturer
Blood collection tube: (4 ml)	BD Biosciences	BD Vacutainer	USA
Bio-Plex plates (96 wells)	BioRad	Bio-Plex Pro flat bottom plates for magnetic based washing	USA
Cannula (0.5 x 16 mm)	Nipro	HN 2516 ET	Belgium
Cell culture plates (24 wells)	Sigma-Aldrich	Corning Costar 3527	USA
Cell culture plates (96 wells)	Sigma-Aldrich	Corning Costar 3599	USA
CryoTubes: Conical (1.0 ml) Round (1.8 ml) Round (4.5 ml)	Nunc	 Cat. Nr.: 375353 Cat. Nr.: 375418 Cat. Nr.: 337516	Denmark
ELISA plates	Nunc	Immuno 96 MicroWell Solid Plates, flat bottom	Denmark
ELISA plate seal	Sigma-Aldrich	T9571	USA
PCR plates	BD Biosciences	Falcon	USA
Syringe (20 ml)	Braun	Omnifix	Germany
Syringe filter	Sarstedt	0.20 µm Filtropur Syringe Filter	Germany

A.4 References

MOLLNES, T. E. & LACHMANN, P. J. 1987. Activation of the third component of complement (C3) detected by a monoclonal anti-C3'g' neoantigen antibody in a one-step enzyme immunoassay. *J. Immunol. Methods,* 101**,** 201-7.

Attachment B –Experimental procedures and analyses

B.1 Isolation of PBMC and stimulation of monocytes

The experimental procedures outlined in chapter 2.1 are described in more details in this chapter.

B.1.1 Calculation of the amount of cells in the cell suspension and needed experimental volumes for the stimulation of monocytes

The concentration of peripheral blood mononuclear cells (PBMC) in the isolated cell suspension was counted by an electrical counter. The average concentration from three counting parallels was multiplied with the total volume of cell suspension of 25 mL. All final concentrations are shown for each donor in table B.1.

Table B.1 Average concentrations from three counting parallels for each PBMC donor A-F.

Donor	Cell count [$\cdot 10^6$ cells/mL]
A	802
B	709
C	319
D	514
E	385
F	546

Each of these cell pellets was thereafter resuspended in 10 mL RPMI-1640. The cell concentration in the sample wells had to be $c_2=4\cdot10^6$ cells/mL for adhesion. The volume, V_2, with the given concentration c_2 was 0.5 mL per well. The volume, V_1, needed from each of these cell suspensions was calculated by equation B.1.

$$c_1 V_1 = c_2 V_2 \qquad \text{(B.1)}$$

The cell suspensions were diluted in RPMI-1640 medium with 5% active A+ serum for the adhesion to the wells.

B.1.2 Calculations for LPS, ATP and submicron particles

Particles with hydrodynamic volumes of 100 nm and 1 µm were used for stimulation of monocytes. The concentrations of each of their stock standards were $c_{100\ nm}$=25 mg/mL and $c_{1\ \mu m}$=50 mg/mL, respectively. Serial dilutions for both particles were done in filtered Milli-Q water.

The concentrations presented in table B.2 were the final concentration of both sizes of particles.

Table B.2 Overview of the final concentrations of particles in each sample parallel.

Dilution	Final concentration in well
A	100 µg/mL
B	10 µg/mL
C	1 µg/mL
D	0.1 µg/mL
E	0.01 µg/mL

There were three sample parallels for each concentration given in table B.2. The total volume in each well was 500 µL. The monocytes from donors A-D were stimulated with the same stimuli in both active and heat inactivated 5% A+ serum in RPMI-1640 medium, whereas the monocytes from donors E and F were stimulated in active 5% A+ serum only.

Some test wells contained neither monocytes nor stimuli (presented as M-MO). These were included as negative controls to whether there was a secretion of cytokines when no monocytes were present. Another negative control was medium with only monocytes without any stimuli (presented as M+MO). This sample was included to control whether the monocytes alone were capable of inducing secretion of cytokines.

Positive control with 27 ng/mL LPS functioned as positive control confirming that the monocytes were capable of secreting cytokines after stimulation with higher concentrations of a microbial component. ATP, on the other hand, was a positive control on the activation of the inflammasome. The concentration of ATP in the control wells was 3 mM.

The priming concentration of LPS was decided to be 100 pg/mL. Listed in table 2.1 in chapter 2 are the respective volumes of medium, LPS, ATP and particles added to each of the sample wells.

B.2 IL-1β ELISA

Stimulated monocytes from donors A-F were all analyzed with traditional IL-1β ELISA, as described in chapter 2.3.1. In the following sections B.2.1-B.2.4, calculations of the volumes needed for the ELISA procedure are shown. The results for each donor are given in attachments C-H, respectively.

B.2.1 Needed volumes for the coating procedure

Capture Antibody was diluted 1:250 in PBS. The coating volume was reduced to 50 µL/well from the recommended 100 µL/well.

B.2.2 Standard preparation and dilutions

Sample dilutions and standards were prepared in Assay Diluent prepared from 5% heat inactivated Fetal Bovine Serum in PBS.

The standard preparations were made by serial 1:2 dilutions within the plate from concentrations ranging from 250 pg/mL to 3.9 pg/mL. The highest concentration was prepared from a lyophilized stock standard reconstituted in sterile and filtered Milli-Q water. The standard's stock concentration was c_{stock}=34 ng/mL.

B.2.3 Dilutions of the samples

All samples from particle stimulation were diluted 1:5 and 1:10, whereas the positive controls with respectively 27 ng/mL LPS and 3 mM ATP were in addition diluted 1:25.

B.2.4 The rest of the reagents used during ELISA

Detection Antibody was diluted 1:500 in Assay Diluent, while Enzyme Reagent was diluted 1:250 in Assay Diluent. Further, Substrate Solution was mixed in a 1:1 relation between the reagents A and B. Finally, 50 µl/well Stop Solution (H_2SO_4) was added.

B.3 TNF-α ELISA

Stimulated monocytes from donors D-F were all analyzed with traditional TNF-α ELISA, as described in chapter 2.3.2. In the following sections B.3.1-B.3.4, calculations of the volumes needed for the ELISA procedure are shown. The results for each donor are given in attachments F-H.

B.3.1 Needed volumes for the coating procedure

Capture Antibody was diluted to a working concentration of 4 µg/mL in PBS. The coating volume was reduced to 50 µL/well from the recommended 100 µL/well.

B.3.2 Standard preparation and dilutions

Sample dilutions and standards were prepared in Reagent Diluent prepared with 1% heat inactivated Bovine Serum Albumine in PBS.

The standard preparations were made by serial 1:2 dilutions within the plate from concentrations ranging from 8 ng/mL to 0.125 ng/mL. The standard's stock concentration was c_{stock}=340 ng/mL.

B.3.3 Dilutions of the samples

All samples from particle stimulation were diluted 1:5 and 1:10, whereas the positive controls with respectively 27 ng/mL LPS and 3 mM ATP were in addition diluted 1:25.

B.3.4 The rest of the reagents used during ELISA

Detection Antibody was diluted to a working concentration of 250 ng/mL in Reagent Diluent, while Enzyme Reagent was diluted 1:200. Further, Substrate Solution was mixed in a 1:1 relation between the reagents A and B. Finally, 50 µl/well Stop Solution (H_2SO_4) was added.

B.4 TCC ELISA

Samples from whole blood donors G-I were analyzed with TCC ELISA. The procedure is outlined in chapter 2.3.3.

The coating antibody Anti-C5b-9 was diluted 1:1000 in BPS. The TCC-standard was diluted 1:100 to yield 10 AU/mL. Serial 1:2 dilutions from 10 AU/mL to 0.156 AU/mL were performed within the plate. The detection antibody was diluted to 1:500, and the Streptavidin-HRP 1:1000. The substrate solution and stop solution were used as previously described in section B.2.4.

Attachment C – Donor A

C.1 Results

Tables C.1a) and b) present the raw data from the ELISA analysis performed on the monocytes stimulated with 100 nm and 1 µm particles, in both active and heat inactivated A+ serum, respectively.

Table C.1 Concentrations of secreted IL-1β [pg/mL] from monocytes isolated from blood donor A. These cells have adhered in active A+ serum, and have thereafter been primed with LPS and exposed to different stimuli of particles in active and inactivated A+ serum, respectively. A mark (*) indicates an undetectably low value.

a) 100 nm particles.

Stimuli concentrations	Active A+ serum, cytokine conc. ± SD [pg/mL]	Heat inactivated A+ serum, cytokine conc. ± SD [pg/mL]
Particle: 0.01 µg/mL	6.535 ± 0.006	6.431 ± 0.006
Particle: 0.1 µg/mL	7.586 ± 0.005	3.686 ± 0.004
Particle: 1.0 µg/m	10.017 ± 0.017	2.998 ± 0.006
Particle: 10 µg/mL	223.884 ± 0.064	6.095 ± 0.001
Particle: 100 µg/mL	318.790 ± 0.005	386.105 ± 0.047
ATP: 3 mM	372.570 ± 0.022	100.995 ± 0.019
M+MO	0.500 ± 0.002	-
M ÷ MO	*	2.893 ± 0.043

b) 1 µm particles.

Stimuli concentrations	Active A+ serum, cytokine conc. ± SD [pg/mL]	Heat inactivated A+ serum, cytokine conc. ± SD [pg/mL]
Particle: 0.01 µg/mL	5.565 ± 0.015	2.026 ± 0.003
Particle: 0.1 µg/mL	4.865 ± 0.007	2.734 ± 0.008
Particle: 1.0 µg/m	4.545 ± 0.010	1.167 ± 0.002
Particle: 10 µg/mL	8.173 ± 0.012	2.212 ± 0.002
Particle: 100 µg/mL	277.093 ± 0.110	71.052 ± 0.047
LPS: 27 ng/mL	-	-
M+MO	0.695 ± 0.012	0.908 ± 0.008
M ÷ MO	*	*

Figure C.1 illustrates the results from donor A which are presented in tables C.1a) and b) graphically. All results in this attachment have first been processed in Microplate Manager 6, before being plotted in Excel to give the following graph. There are uncertainties whether there is a correlation between the points, therefore are all results treated as separate values.

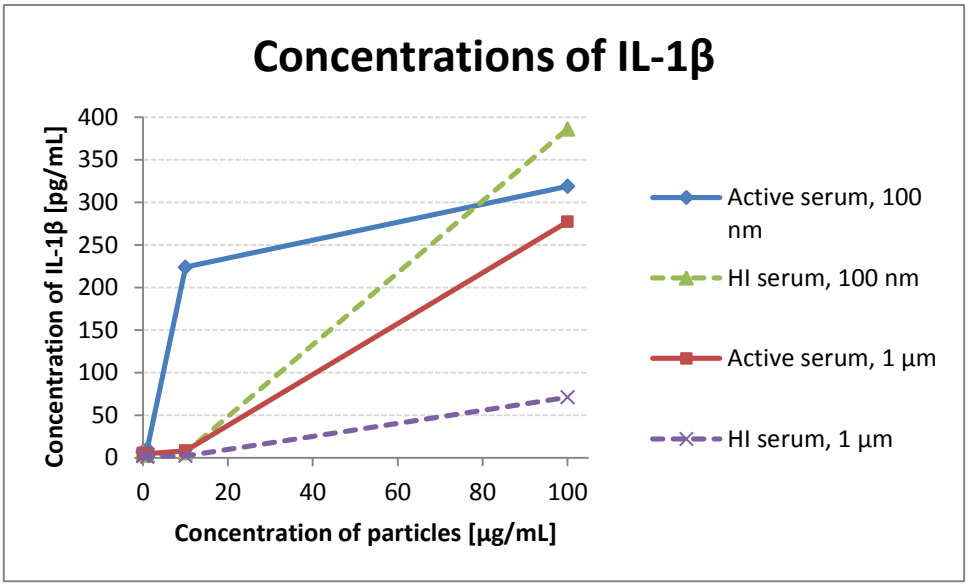

Figure C.1 Concentrations of secreted cytokine IL-1β from monocytes isolated from donor A. All data points are presented in table C.1. The ATP control in active A+ serum is 372.57 ± 0.02 pg/mL, and 101.00 ± 0.02 pg/mL in heat inactivated A+ serum.

C.2 Sources of errors in this experiment

Following the priming period of two hours, the A+ medium in the ATP sample wells was replaced with fresh medium before the ATP stimuli. This was the case only for the samples with ATP control, causing the other samples to have been treated in a different manner than these. This may have caused the monocytes to secrete higher volumes of IL-1β because of the freshly added nutrient-filled medium which was not added to the other samples.

The positive control with 27 ng/mL LPS has not been primed prior to stimulation. These samples are therefore not treated on equal terms as the other ones, but they are still valid in showing that the monocytes are able to secrete IL-1β.

All incubation periods are ± 2 minutes.

Attachment D – Donor B

D.1 Results

Tables D.1a) and b) present the values for the experimental ELISA analysis performed on the monocytes stimulated with both particles, in active as well as in heat inactivated A+ serum, respectively.

Table D.1 Concentrations of secreted IL-1β [pg/mL] from monocytes isolated from blood donor B. These cells have adhered in active A+ serum, and have thereafter been primed with LPS and exposed to different stimuli of particles in active and inactivated A+ serum, respectively. A mark (*) indicates an undetectably low value.

a) 100 nm particles.

Stimuli concentrations	Active A+ serum, cytokine conc. ± SD [pg/mL]	Heat inactivated A+ serum, cytokine conc. ± SD [pg/mL]
Particle: 0.01 µg/mL	17.095 ± 0.015	20.531 ± 0.002
Particle: 0.1 µg/mL	18.235 ± 0.004	19.798 ± 0.019
Particle: 1.0 µg/m	21.528 ± 0.020	17.259 ± 0.012
Particle: 10 µg/mL	394.309 ± 0.017	31.304 ± 0.054
Particle: 100 µg/mL	367.166 ± 0.040	390.544 ± 0.078
ATP: 3 mM	404.533 ± 0.110	415.680 ± 0.051
M+MO	19.568 ± 0.054	31.821 ± 0.009
M ÷ MO	*	*

b) 1 µm particles.

Stimuli concentrations	Active A+ serum, cytokine conc. ± SD [pg/mL]	Heat inactivated A+ serum, cytokine conc. ± SD [pg/mL]
Particle: 0.01 µg/mL	40.502 ± 0.017	28.369 ± 0.017
Particle: 0.1 µg/mL	51.905 ± 0.024	29.369 ± 0.040
Particle: 1.0 µg/m	38.373 ± 0.117	30.601 ± 0.031
Particle: 10 µg/mL	42.377 ± 0.046	40.528 ± 0.040
Particle: 100 µg/mL	275.108 ± 0.004	94.397 ± 0.079
LPS: 27 ng/mL	344.871 ± 0.004	353.123 ± 0.108
M+MO	45.819 ± 0.027	48.916 ± 0.052
M ÷ MO	*	*

Figure D.1 illustrates the results from donor B which are presented in tables D.1a) and b) graphically.

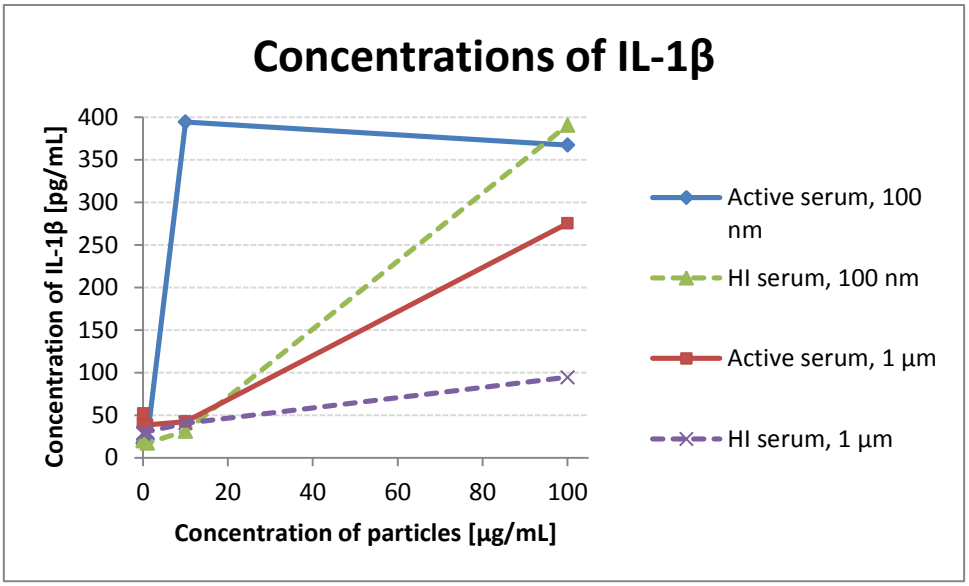

Figure D.1 Concentrations of secreted cytokine IL-1β from monocytes isolated from donor B. All data points are presented in table D.1. The ATP control in active A+ serum is 404.53 ± 0.11 pg/mL, and 415.68 ± 0.05 pg/mL in heat inactivated A+ serum.

D.2 Calculation example

A calculation example for one of the values that are obtained by Microplate Manager 6 is showed in this section. By using standard data set from current experiment, the standard curve shown in figure D.2 is obtained.

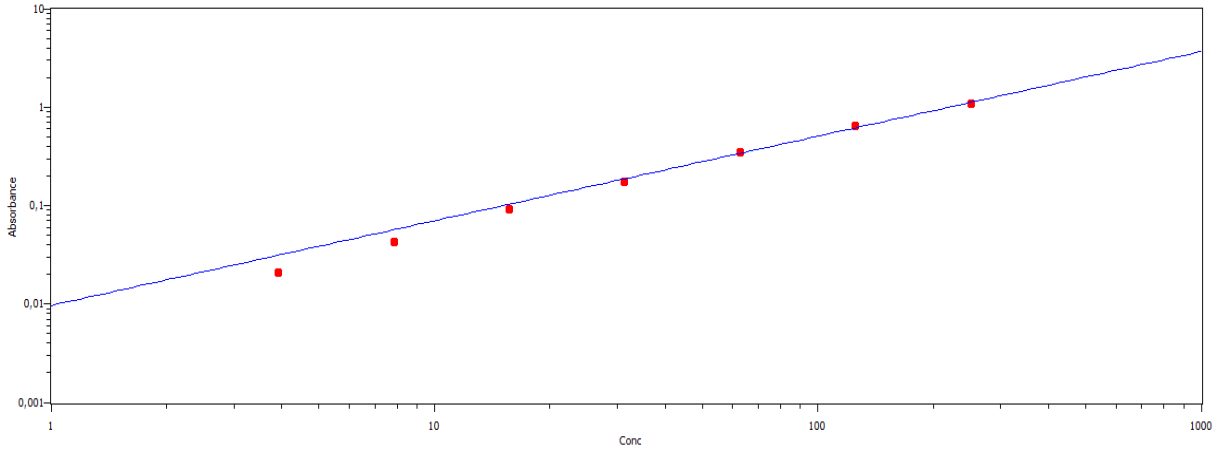

Figure D.2 Standard curve obtained by Microplate Manager 6 based on the ELISA results from monocytes from donor B which were stimulated with 100 nm particles in active A+ serum. A log-log curve fit is used, and the best-fit for the trend line is r^2=0.993.

A log-log curve provides the best straight line for these measurements. The data consist of the logarithm of the response OD and the logarithm of the concentration. The equation of the standard curve for the log-log method is presented in equation D.1:

$$\log_{10}(y) = \text{intercept} + \text{slope} \cdot \log_{10}(x) \qquad \text{(D.1)}$$

Here, y is the concentration of IL-1β in each sample.

Microplate Manager gives the following data with their respective uncertainties for the intercept and the slope:

Intercept: -2.014 ± 0.038

Slope: 0.860 ± 0.016

The OD measurements describing the amount of cytokine in the samples were done at both 450 nm and 570 nm. By subtracting the OD values measured at 570 nm from those measured at 450 nm, the following raw data were achieved. These values describe the optical densities for the sample triplets stimulated with 1.0 µg/mL of 100 nm particles in active A+ serum.

Triplet 1: 0.157
Triplet 2: 0.117
Triplet 3: 0.131

The average concentration is calculated as shown:

$$\frac{0.157+0.117+0.131}{3}=0.135$$

This value is then applied for y in equation D.1, and the equation will eventually turn out as the following by using all the given values for the intercept, slope and y:

$$\log(0.135)=-2.014+0.860\cdot\log(x)$$
$$\Rightarrow \log(x)=\frac{\log(0.135)+2.014}{0.860}\approx 1.3306$$
$$\Rightarrow y=10^{1,3306}\approx \underline{21.410}$$

The calculated IL-1β concentration of 21.410 pg/mL is in close compliance with the value presented in table D.1a). All presented results are based on the undiluted samples. Next, the uncertainty in this measurement is calculated by equation D.2.

$$SD=\sqrt{\frac{\sum_{i=1}^{n}(x_i-\bar{x})^2}{(n-1)}} \qquad (D.2)$$

$$SD = \sqrt{\frac{(0,157-0,135)^2+(0,117-0,135)^2+(0,131-0,135)^2}{(3-1)}} \approx \underline{0,020}$$

The standard deviation 0.020 pg/mL is in compliance with the value presented in table D.1a). The resulting IL-1β concentration in the respective sample is 21.410 ± 0.020 pg/mL (conc. ± SD).

D.3 Sources of errors in this experiment

In section B.2.2, the IL-1β standard curve was prepared as if the stock standard was 53 ng/mL. This may have caused higher measured values of secreted IL-1β than what would be right. However, the serial dilutions are performed correctly.

All incubation periods are ± 2 minutes.

Attachment E – Donor C

E.1 Results

Tables E.1a) and b) present the values for the IL-1β analysis performed on the monocytes isolated from donor C. These were stimulated with both particle sizes, in both active and heat inactivated A+ serum, respectively.

Table E.1 Concentrations of secreted IL-1β [pg/mL] from monocytes isolated from blood donor C. These cells have adhered in active A+ serum, and have thereafter been primed with LPS and exposed to different stimuli of particles in active and inactivated A+ serum, respectively. A mark (*) indicates an undetectably low value.

a) 100 nm particles.

Stimuli concentrations	Active A+ serum, cytokine conc. ± SD [pg/mL]	Heat inactivated A+ serum, cytokine conc. ± SD [pg/mL]
Particle: 0.01 µg/mL	53.440 ± 0.058	14.807 ± 0.006
Particle: 0.1 µg/mL	59.883 ± 0.059	11.443 ± 0.035
Particle: 1.0 µg/m	87.896 ± 0.119	23.803 ± 0.105
Particle: 10 µg/mL	245.543 ± 0.027	63.068 ± 0.064
Particle: 100 µg/mL	196.067 ± 0.012	227.169 ± 0.088
ATP: 3 mM	231.306 ± 0.016	258.646 ± 0.031
M+MO	19.886 ± 0.181	0.036 ± 0.002
M ÷ MO	*	*

b) 1 µm particles.

Stimuli concentrations	Active A+ serum, cytokine conc. ± SD [pg/mL]	Heat inactivated A+ serum, cytokine conc. ± SD [pg/mL]
Particle: 0.01 µg/mL	48.028 ± 0.066	13.067 ± 0.053
Particle: 0.1 µg/mL	64.323 ± 0.193	16.987 ± 0.086
Particle: 1.0 µg/m	82.104 ± 0.239	10.585 ± 0.004
Particle: 10 µg/mL	62.699 ± 0.063	14.815 ± 0.062
Particle: 100 µg/mL	211.193 ± 0.019	169.822 ± 0.056
LPS: 27 ng/mL	205.569 ± 0.112	201.853 ± 0.024
M+MO	*	25.791 ± 0.069
M ÷ MO	*	0.099 ± 0.001

Figure E.1 illustrates the results from donor C which are presented in tables E.1a) and b) graphically.

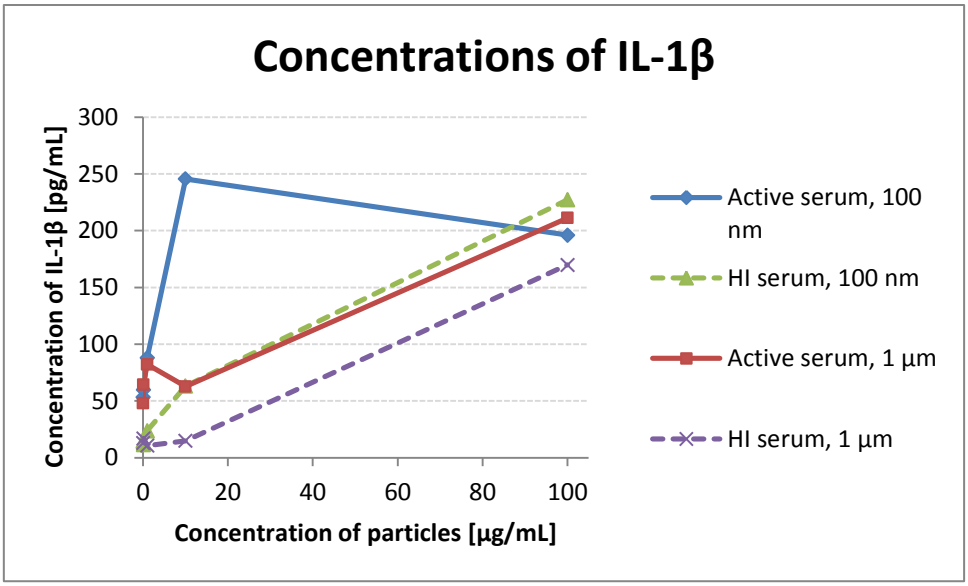

Figure E.1 Concentrations of secreted cytokine IL-1β from monocytes isolated from donor C. All data points are presented in table E.1. The ATP control in active serum is 231.31 ± 0.02 pg/mL in active A+ serum, and 258.65 ± 0.03 pg/mL in heat inactivated A+ serum.

E.2 Sources of errors in this experiment

The A+ serum used for the culture and stimulation of this donor's monocytes was a different batch than for the previous two donors (A and B).

All incubation periods are ± 2 minutes.

Attachment F – Donor D

F.1 Active versus heat inactivated A+ serum

F.1.1 Results

Tables F.1a) and b) present the values for the experimental IL-1β analysis performed on the monocytes isolated from donor D. These cells were stimulated with 100 nm and 1 µm particles, respectively, in both active and heat inactivated A+ serum.

Table F.1 Concentrations of secreted IL-1β [pg/mL] from monocytes isolated from blood donor D. These cells have adhered in active A+ serum, and have thereafter been primed with LPS and exposed to different stimuli of particles in active and inactivated A+ serum, respectively. A mark (*) indicates an undetectably low value.
a) 100 nm particles.

Stimuli concentrations	Active A+ serum, cytokine conc. ± SD [pg/mL]	Heat inactivated A+ serum, cytokine conc. ± SD [pg/mL]
Particle: 0.01 µg/mL	33.967 ± 0.022	22.807 ± 0.009
Particle: 0.1 µg/mL	34.581 ± 0.030	46.505 ± 0.100
Particle: 1.0 µg/m	55.624 ± 0.051	24.802 ± 0.032
Particle: 10 µg/mL	253.624 ± 0.032	56.221 ± 0.079
Particle: 100 µg/mL	244.964 ± 0.024	266.168 ± 0.064
ATP: 3 mM	251.868 ± 0.080	270.999 ± 0.046
M+MO	21.019 ± 0.016	27.459 ± 0.028
M ÷ MO	0.031 ± 0.001	*

b) 1 µm particles.

Stimuli concentrations	Active A+ serum, cytokine conc. ± SD [pg/mL]	Heat inactivated A+ serum, cytokine conc. ± SD [pg/mL]
Particle: 0.01 µg/mL	47.940 ± 0.084	35.498 ± 0.045
Particle: 0.1 µg/mL	42.048 ± 0.036	48.904 ± 0.035
Particle: 1.0 µg/m	51.067 ± 0.017	28.322 ± 0.052
Particle: 10 µg/mL	72.005 ± 0.069	62.153 ± 0.053
Particle: 100 µg/mL	229.231 ± 0.078	111.642 ± 0.077
LPS: 27 ng/mL	173.645 ± 0.078	87.665 ± 0.132
M+MO	27.403 ± 0.050	39.801 ± 0.103
M ÷ MO	*	1.763 ± 0.010

Figure F.1 illustrates the results from donor D which are presented in tables F.1a) and b) graphically.

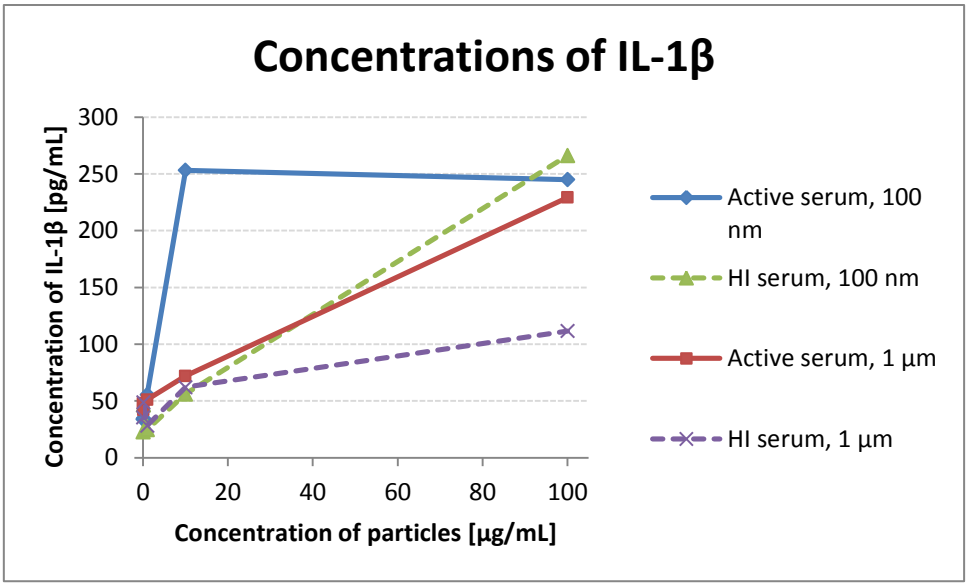

Figure F.1 Concentrations of secreted cytokine IL-1β from monocytes isolated from donor D. All data points are presented in tables F.1. The ATP control in active serum is 251.87 ± 0.08 pg/mL in active A+ serum and 271.00 ± 0.05 pg/mL in heat inactivated A+ serum.

F.1.2 Sources of errors in this experiment

All incubation periods are ± 2 minutes.

F.2 Priming versus non-priming

Donor D has already been presented in section F.1. The results given show the differences of cytokine secretion in two types of A+ serum, active and heat inactivated. In the following chapters, all experimental data are from active A+ serum only.

F.2.1 Results for IL-1β with standard ELISA

This section compares secretion of cytokine IL-1β from primed versus unprimed monocytes.

Tables F.2a) and b) present the values for the experimental IL-1β analysis performed on the monocytes isolated from donor D. One part of the cells has been primed prior to stimulation with 100 nm and 1 µm particles, whereas the other part of the cells has not been primed in advance. The unprimed analyses have been performed as a negative control of the particles, to observe whether the priming procedure is influencing the amount of secreted cytokines or not.

Table F.2 Concentrations of secreted IL-1β [pg/mL] from monocytes isolated from blood donor D. These cells have adhered in active A+ serum, and one part has thereafter been primed with LPS prior to exposure to different stimuli of particles in active A+ serum, whereas the other part has not been primed. A mark (*) indicates an undetectably low value.

a) 100 nm particles.

Stimuli concentrations	Primed, IL-1β conc. ± SD [pg/mL]	Unprimed, IL-1β conc. ± SD [pg/mL]
Particle: 0.01 µg/mL	33.967 ± 0.022	42.803 ± 0.058
Particle: 0.1 µg/mL	34.581 ± 0.030	-
Particle: 1.0 µg/m	55.624 ± 0.051	-
Particle: 10 µg/mL	253.215 ± 0.032	-
Particle: 100 µg/mL	244.964 ± 0.024	251.685 ± 0.018
ATP: 3 mM	251.868 ± 0.080	-
M+MO	21.019 ± 0.016	-
M ÷ MO	0.031 ± 0.001	-

b) 1 µm particles.

Stimuli concentrations	Primed, IL-1β conc. ± SD [pg/mL]	Unprimed, IL-1β conc. ± SD [pg/mL]
Particle: 0.01 µg/mL	47.940 ± 0.084	47.792 ± 0.020
Particle: 0.1 µg/mL	42.048 ± 0.036	-
Particle: 1.0 µg/m	51.067 ± 0.017	-
Particle: 10 µg/mL	72.005 ± 0.069	-
Particle: 100 µg/mL	229.231 ± 0.078	141.277 ± 0.009
LPS: 27 ng/mL	173.645 ± 0.078	-
M+MO	27.403 ± 0.050	-
M ÷ MO	*	-

Figure F.2 illustrates the results from donor D which are presented in tables F.2a) and b) graphically.

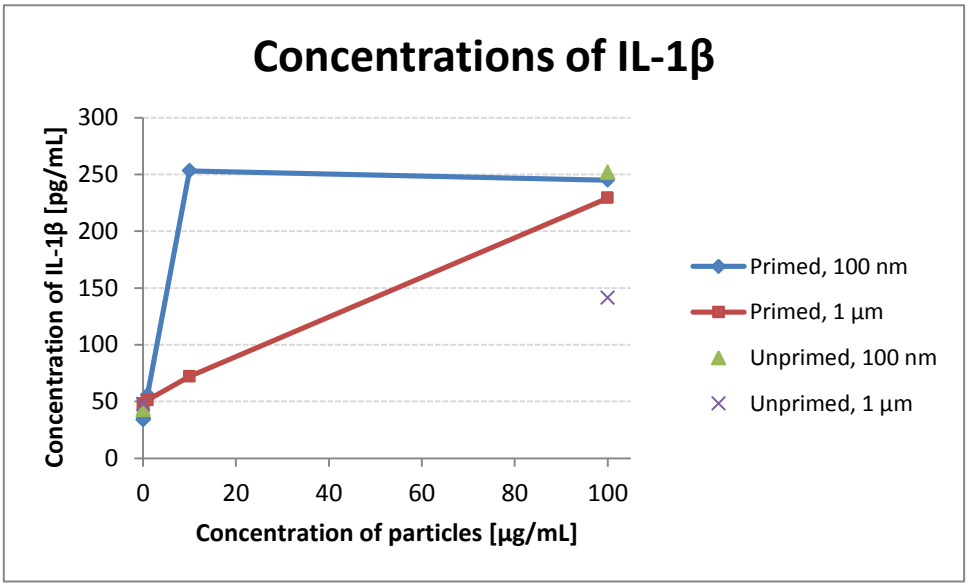

Figure F.2 Concentrations of secreted cytokine IL-1β from monocytes isolated from donor D. All data points are presented in table F.2. The ATP control is 251.87 ± 0.08 pg/mL for the primed monocytes.

F.2.1.1 Sources of errors in this experiment

There are no samples for unprimed monocytes with concentrations 0.1-10 µg/mL for neither particle sizes. The results for the unprimed data points are therefore given as single values in the graphical presentation in figure B.2.

All incubation periods are ± 2 minutes.

F.2.2 Results for TNF-α with standard ELISA

This section compares secretion of cytokine TNF-α after both priming and non-priming of the monocytes. Tables F.3a) and b) present the values for the experimental TNF-α analysis performed on the same samples as those presented in section F.2.1.

Table F.3 Concentrations of secreted TNF-α [pg/mL] from monocytes isolated from blood donor D. A mark (*) indicates an undetectably low value.
a) 100 nm particles.

Stimuli concentrations	**Primed, TNF-α conc. ± SD [pg/mL]**	**Unprimed, TNF-α conc. ± SD [pg/mL]**
Particle: 0.01 µg/mL	*	*
Particle: 0.1 µg/mL	98 ± 50	-
Particle: 1.0 µg/m	205 ± 112	-
Particle: 10 µg/mL	3 265 ± 52	-
Particle: 100 µg/mL	5 066 ± 143	3 422 ± 44
ATP: 3 mM	53 ± 30	*
M+MO	*	*
M ÷ MO	*	*

b) 1 µm particles.

Stimuli concentrations	**Primed, TNF-α conc. ± SD [pg/mL]**	**Unprimed, TNF-α conc. ± SD [pg/mL]**
Particle: 0.01 µg/mL	*	*
Particle: 0.1 µg/mL	*	-
Particle: 1.0 µg/m	*	-
Particle: 10 µg/mL	42 ± 15	-
Particle: 100 µg/mL	1 281 ± 25	199 ± 4
LPS: 27 ng/mL	1 172 ± 142	-
M+MO	*	-
M ÷ MO	*	-

Figure F.3 illustrates the results from donor D which are presented in tables F.3a) and b) graphically.

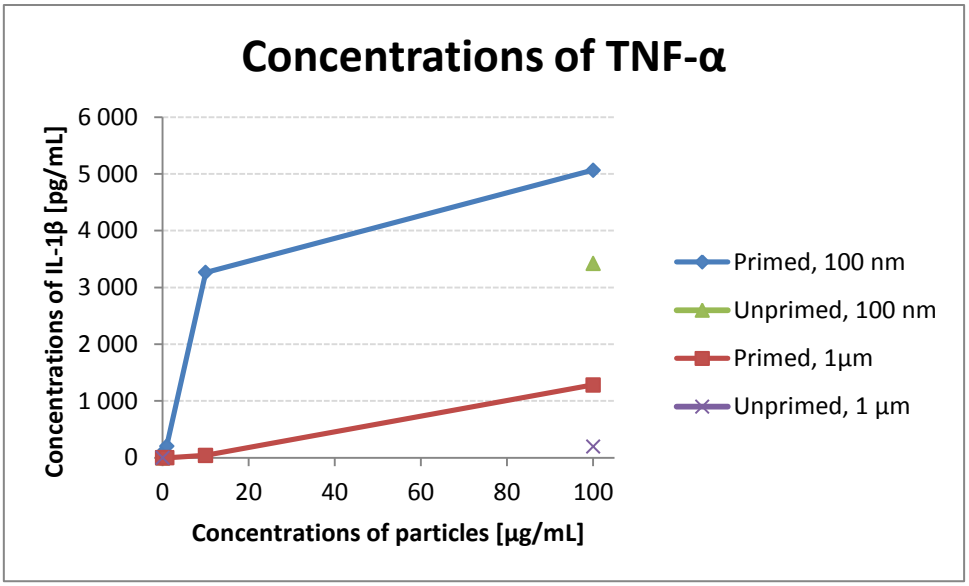

Figure F.3 Concentrations of secreted cytokine TNF-α from monocytes isolated from donor D. All data points are presented in tables F.3.

F.2.2.1 Sources of errors in this experiment

The same errors are present for the TNF-α analysis as the ones described for IL-1β in section F.2.1.1. In addition, the cytokine samples used for the analysis of TNF-α have been thawed once already before being thawed additionally for these analyses. This may have caused some lower protein activity because of denaturation, though this has previously been shown to have negligible influence on the results (Mihaylova, 2011).

F.2.3 Results from Bio-plex

The results from bio-plex are based on the experimental procedure described in chapter 2.4.

Four cytokines have shown significant results from the analysis of the primed versus non-primed monocytes from donor D with the 17-plex. These are IL-2, IL-6, GM-CSF and IFN-γ. The graphical results for each cytokine are presented in figures F.4-F.7, whereas the values are not given.

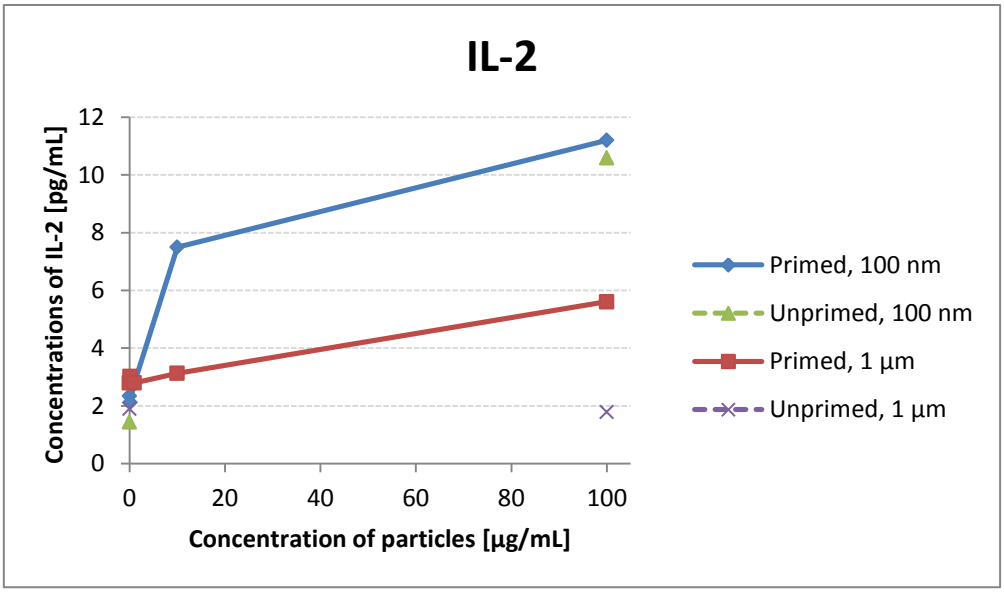

Figure F.4 Concentrations of secreted cytokine IL-2 from monocytes isolated from donor D. The samples have been analyzed with Bio-17-plex.

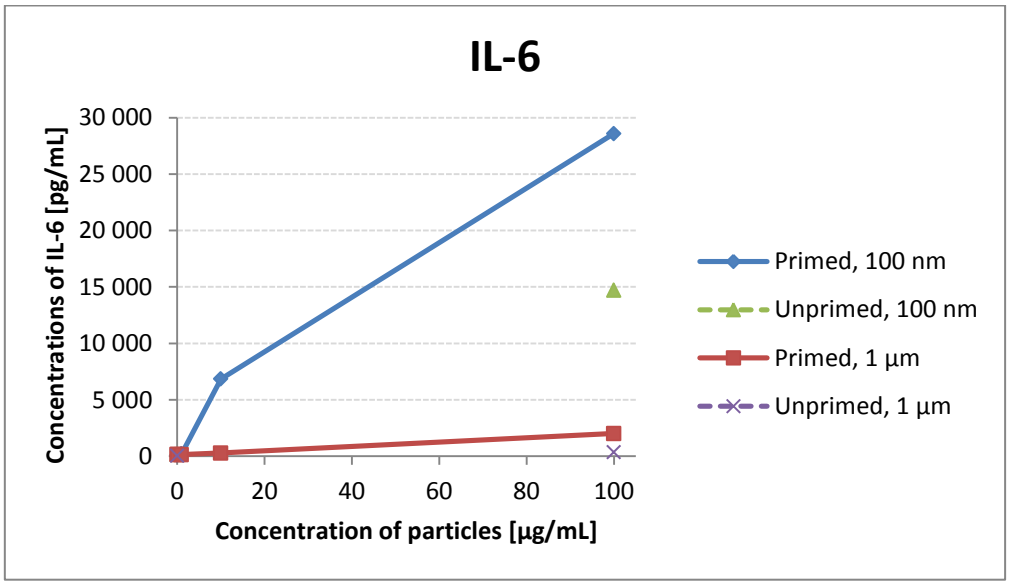

Figure F.5 Concentrations of secreted cytokine IL-6 from monocytes isolated from donor D. The samples have been analyzed with Bio-17-plex.

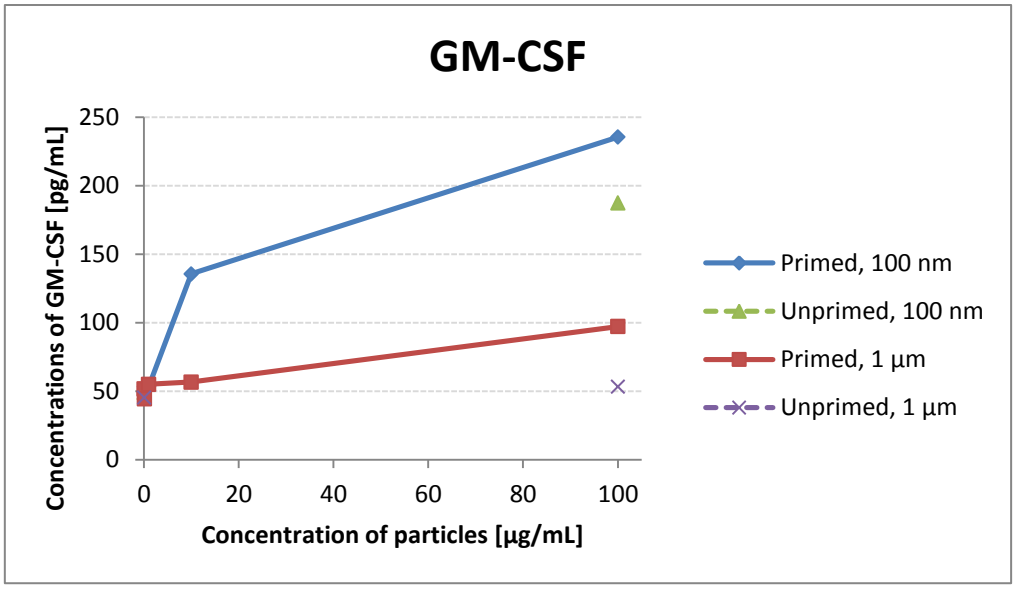

Figure F.6 Concentrations of secreted cytokine GM-CSF from monocytes isolated from donor D. The samples have been analyzed with Bio-17-plex.

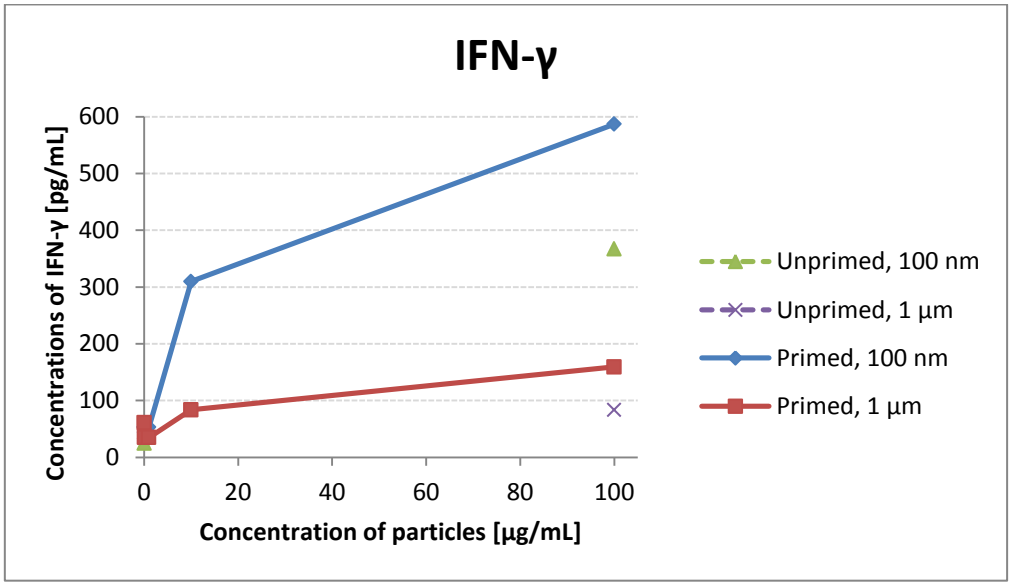

Figure F.7 Concentrations of secreted cytokine IFN-γ from monocytes isolated from donor D. The samples have been analyzed with Bio-17-plex.

F.3 References

MIHAYLOVA, D. 2011. Submicron Particles and Inflammation. NTNU.

Attachment G – Donor E

G.1 Priming versus non-priming

G.1.1 Results

Tables G.1a) and b) present the values for the experimental IL-1β analysis performed on the monocytes isolated from donor E. One part of the cells has been primed prior to stimulation with 100 nm and 1 µm particles, whereas the other part of the cells has not been primed in advance.

Table G.1 Concentrations of secreted IL-1β [pg/mL] from monocytes isolated from blood donor E. These cells have adhered in active A+ serum, and one part has thereafter been primed with LPS prior to exposure to different stimuli of particles in active A+ serum, whereas the other part has not been primed. A mark (*) indicates an undetectably low value.
a) 100 nm particles. (¤) Unprimed ATP control.

Stimuli concentrations	Primed, IL-1β conc. ± SD [pg/mL]	Unprimed, IL-1β conc. ± SD [pg/mL]
Particle: 0.01 µg/mL	0.683 ± 0.010	3.231 ± 0.117
Particle: 0.1 µg/mL	0.960 ± 0.047	4.136 ± 0.108
Particle: 1.0 µg/m	0.994 ± 0.024	18.494 ± 0.166
Particle: 10 µg/mL	78.962 ± 0.034	25.990 ± 0
Particle: 100 µg/mL	355.065 ± 0.161	359.729 ± 0.044
ATP: 3 mM	323.195 ± 0.013	95.862 ± 0.060 ¤
M+MO	0.539 ± 0.010	1.297 ± 0.021
M ÷ MO	*	*

b) 1 µm particles.

Stimuli concentrations	Primed, IL-1β conc. ± SD [pg/mL]	Unprimed, IL-1β conc. ± SD [pg/mL]
Particle: 0.01 µg/mL	0.932 ± 0.017	3.007 ± 0.025
Particle: 0.1 µg/mL	1.178 ± 0.028	4.429 ± 0.040
Particle: 1.0 µg/m	1.075 ± 0.029	4.205 ± 0.017
Particle: 10 µg/mL	3.640 ± 0.040	4.301 ± 0.026
Particle: 100 µg/mL	58.829 ± 0.143	12.669 ± 0.049
LPS: 27 ng/mL	10.412 ± 0.064	-
M+MO	22.798 ± 0.149	-
M ÷ MO	23.629 ± 0.129	-

Figure G.1 illustrates the results from donor E which are presented in tables G.1a) and b) graphically.

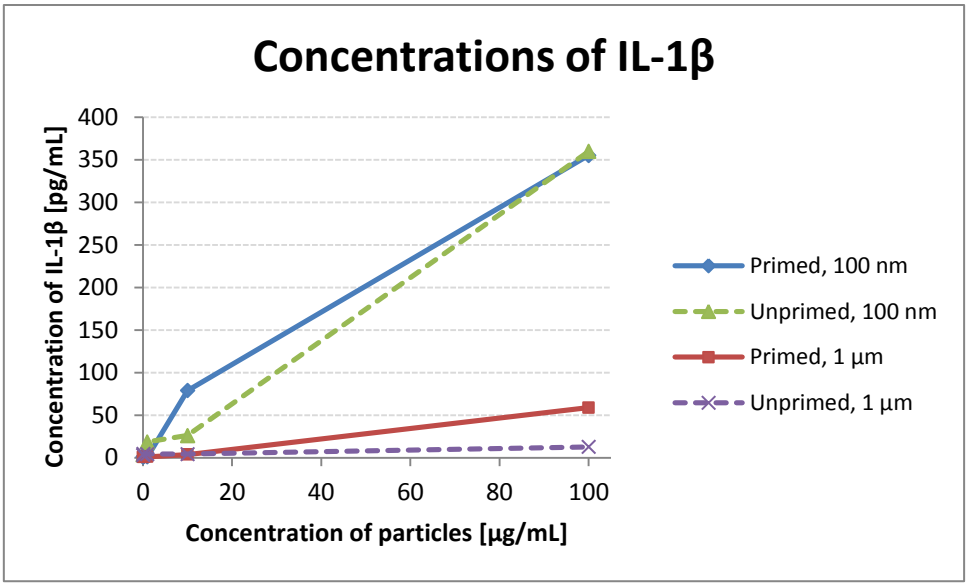

Figure G.1 Concentrations of secreted IL-1β from monocytes isolated from donor E. All data points are presented in table G.1. Primed ATP control is 323.20 ± 0.01 pg/mL (mean ± SD), whereas unprimed ATP control is 95.86 ± 0.06 pg/mL

G.1.1.1 Sources of errors in this experiment

All incubation periods are ± 2 minutes.

G.1.2 Results for TNF-α with standard ELISA

This section compares secretion of cytokine TNF-α after both priming and non-priming of the monocytes. Tables G.2a) and b) present the values for the experimental TNF-α analysis performed on the same samples as those in section G.1.1.

Table G.2 Concentrations of secreted TNF-α [pg/mL] from monocytes isolated from blood donor E. A mark (*) indicates an undetectably low value.
a) 100 nm particles.

Stimuli concentrations	**Primed, TNF-α conc. ± SD [pg/mL]**	**Unprimed, TNF-α conc. ± SD [pg/mL]**
Particle: 0.01 µg/mL	*	*
Particle: 0.1 µg/mL	*	*
Particle: 1.0 µg/m	*	*
Particle: 10 µg/mL	942 ± 71	536 ± 157
Particle: 100 µg/mL	3 908 ± 38	4 011 ± 12
ATP: 3 mM	*	*
M+MO	*	*
M ÷ MO	*	*

b) 1 µm particles.

Stimuli concentrations	Primed, TNF-α conc. ± SD [pg/mL]	Unprimed, TNF-α conc. ± SD [pg/mL]
Particle: 0.01 µg/mL	*	*
Particle: 0.1 µg/mL	*	*
Particle: 1.0 µg/m	*	*
Particle: 10 µg/mL	18 ± 77	65 ± 115
Particle: 100 µg/mL	271 ± 33	13 ± 22
LPS: 27 ng/mL	173 ± 23	-
M+MO	*	-
M ÷ MO	*	-

Figure G.2 illustrates the results from donor E which are presented in tables G.2a) and b) graphically.

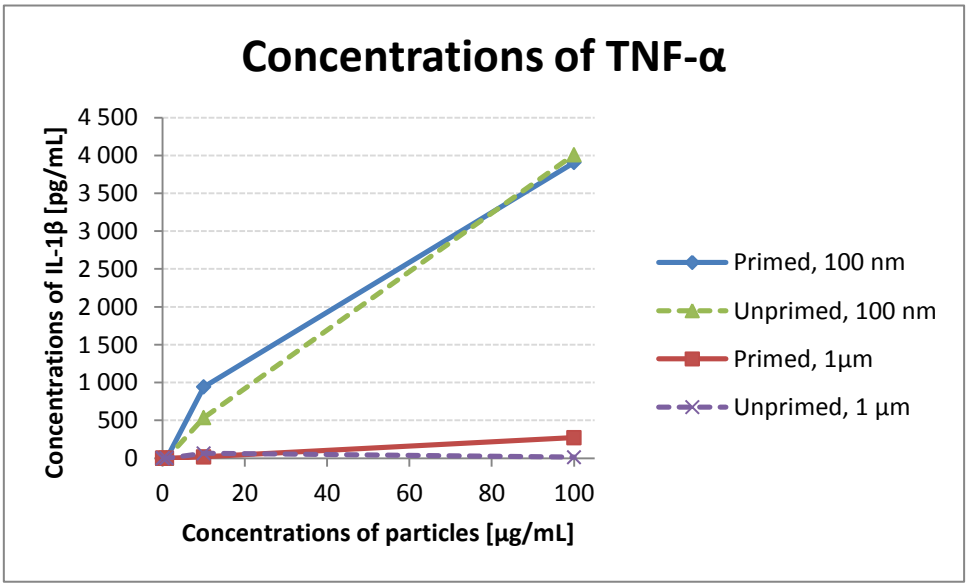

Figure G.2 Concentrations of secreted cytokine TNF-α from monocytes isolated from donor E. All data points are presented in table G.2.

G.1.2.1 Sources of errors in this experiment

The samples have been thawed once already. This may have resulted in lower levels of cytokine, but, as explained in attachment F.2.2.1, it is believed that this has not influenced significantly upon the results.

G.1.3 Results from Bio-plex

The same cytokines have shown significant results as for donor D in attachment F.2.3. Graphical presentations for each cytokine follow in figures G.3-G.6.

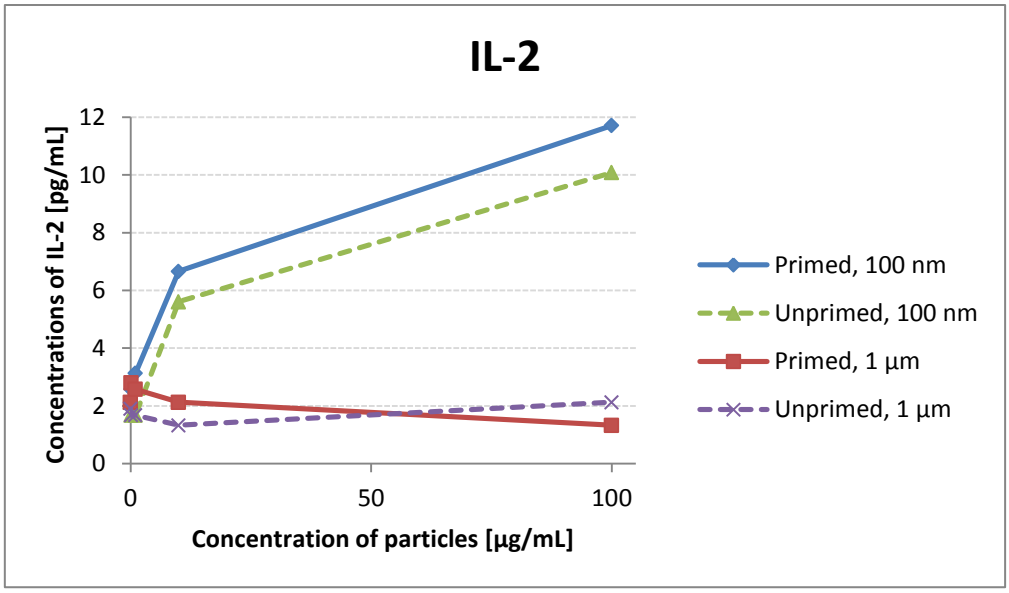

Figure G.3 Concentrations of secreted cytokine IL-2 from monocytes isolated from donor E. The samples have been analyzed with Bio-17-plex.

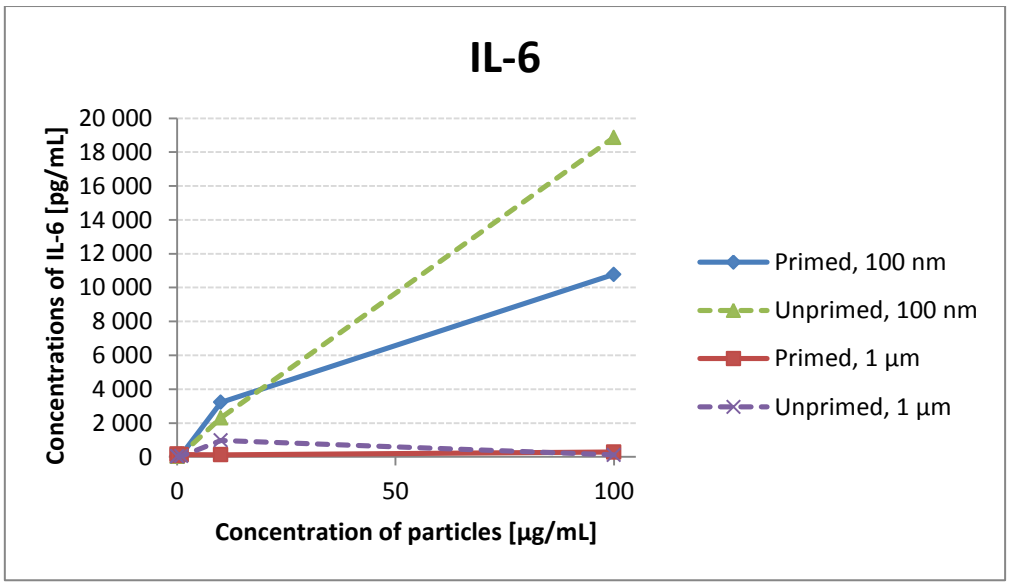

Figure G.4 Concentrations of secreted cytokine IL-6 from monocytes isolated from donor E. The samples have been analyzed with Bio-17-plex.

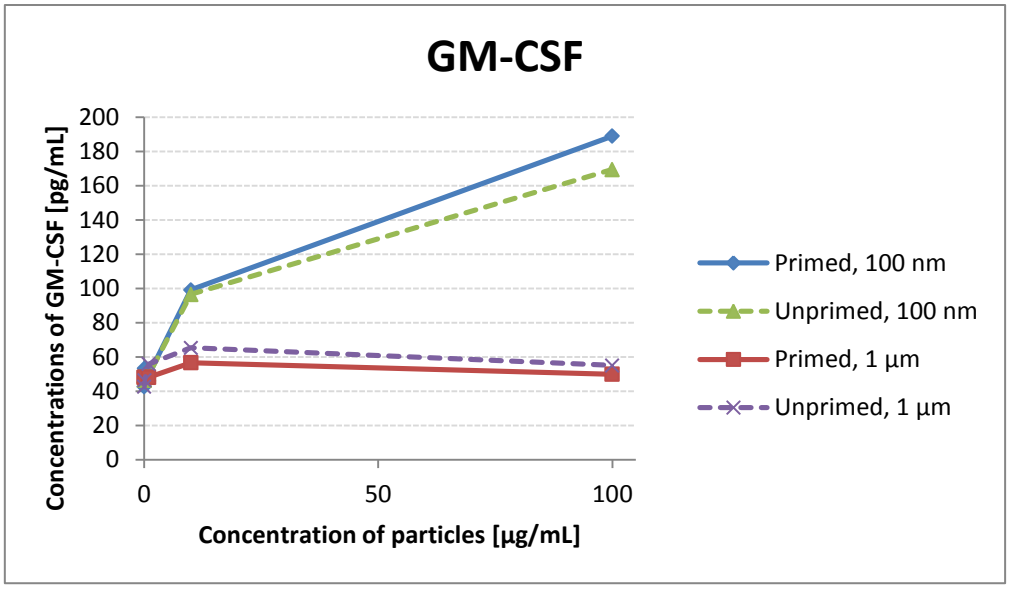

Figure G.5 Concentrations of secreted cytokine GM-CSF from monocytes isolated from donor E. The samples have been analyzed with Bio-17-plex.

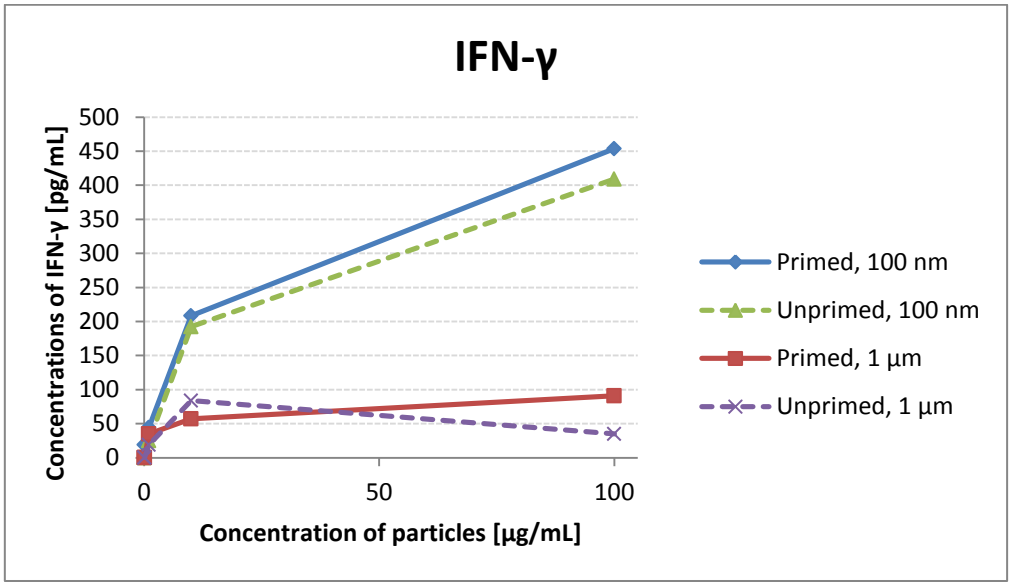

Figure G.6 Concentrations of secreted cytokine IFN-γ from monocytes isolated from donor E. The samples have been analyzed with Bio-17-plex.

Attachment H – Donor F

H.1 Priming versus non-priming

H.1.1 Results

Tables H.1a) and b) present the values for the experimental IL-1β analysis performed on the monocytes isolated from donor F. One part of the cells has been primed prior to stimulation with 100 nm and 1 µm particles, whereas the other part of the cells has not been primed in advance.

Table H.1 Concentrations of secreted IL-1β [pg/mL] from monocytes isolated from PBMC donor F. These cells have adhered in active A+ serum, and one part has thereafter been primed with LPS prior to exposure to different stimuli of particles in active A+ serum, whereas the other part has not been primed. A mark (*) indicates an undetectably low value.
a) 100 nm particles. (¤) Unprimed ATP control.

Stimuli concentrations	Primed, IL-1β conc. ± SD [pg/mL]	Unprimed, IL-1β conc. ± SD [pg/mL]
Particle: 0.01 µg/mL	4.724 ± 0.023	0.018 ± 0.012
Particle: 0.1 µg/mL	10.869 ± 0.114	0.185 ± 0.037
Particle: 1.0 µg/m	18.036 ± 0.116	0.250 ± 0.045
Particle: 10 µg/mL	301.585 ± 0.039	125.157 ± 0.188
Particle: 100 µg/mL	306.800 ± 0.038	383.507 ± 0.036
ATP: 3 mM	333.732 ± 0.012	276.568 ± 0.086 ¤
M+MO	0.184 ± 0.014	0.699 ± 0.128
M ÷ MO	*	*

b) 1 µm particles.

Stimuli concentrations	Primed, IL-1β conc. ± SD [pg/mL]	Unprimed, IL-1β conc. ± SD [pg/mL]
Particle: 0.01 µg/mL	10.869 ± 0.084	0.070 ± 0.039
Particle: 0.1 µg/mL	8.688 ± 0.102	0.108 ± 0.021
Particle: 1.0 µg/m	16.662 ± 0.112	0.969 ± 0.172
Particle: 10 µg/mL	11.999 ± 0.097	0.080 ± 0.015
Particle: 100 µg/mL	173.351 ± 0.083	8.762 ± 0.055
LPS: 27 ng/mL	50.308 ± 0.202	-
M+MO	0.998 ± 0.041	-
M ÷ MO	0.046 ± 0.025	-

Figure H.1 illustrates the results from donor F which are presented in tables H.1a) and b) graphically.

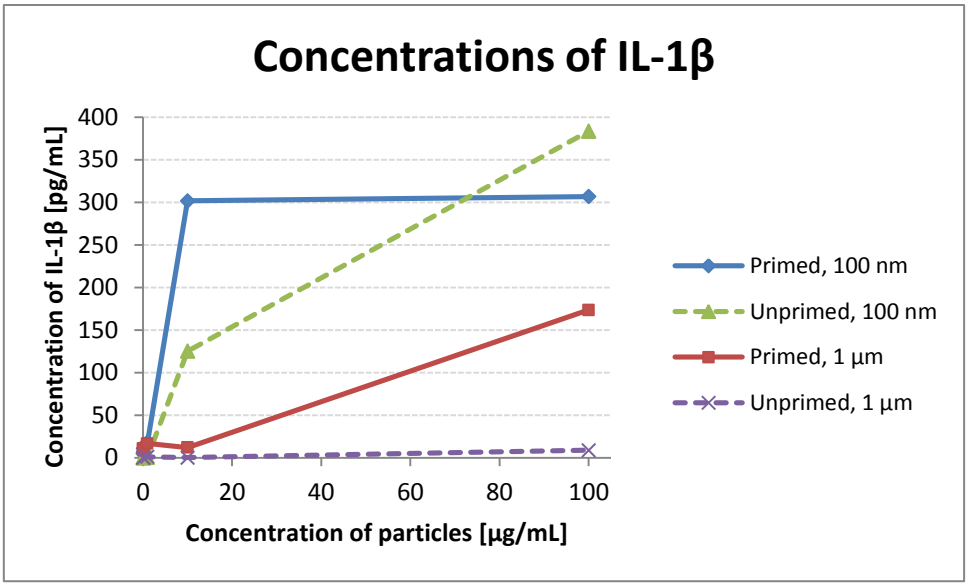

Figure H.1 Concentrations of secreted cytokine IL-1β from monocytes isolated from donor F. All data points are presented in tables H.1. Primed ATP control is 333.73 ±0.01 pg/mL (mean ± SD), whereas unprimed ATP control is 276.57 ± 0.09 pg/mL.

H.1.1.1 Sources of errors in this experiment

All incubation periods are ± 2 minutes.

H.1.2 Results for TNF-α with standard ELISA

This section compares secretion of cytokine TNF-α after both priming and non-priming of the monocytes. Tables H.2a) and b) present the values for the experimental TNF-α analysis performed on the same samples as those in section H.1.1.

Table H.2 Concentrations of secreted TNF-α [pg/mL] from monocytes isolated from blood donor F. A mark (*) indicates an undetectably low value.
a) 100 nm particles.

Stimuli concentrations	**Primed, TNF-α conc. ± SD [pg/mL]**	**Unprimed, TNF-α conc. ± SD [pg/mL]**
Particle: 0.01 µg/mL	*	*
Particle: 0.1 µg/mL	72 ± 60	*
Particle: 1.0 µg/m	98 ± 30	*
Particle: 10 µg/mL	2 526 ± 184	1 304 ± 106
Particle: 100 µg/mL	5 362 ± 101	4 938 ± 52
ATP: 3 mM	*	*
M+MO	*	*
M ÷ MO	*	*

b) 1 µm particles.

Stimuli concentrations	Primed, TNF-α conc. ± SD [pg/mL]	Unprimed, TNF-α conc. ± SD [pg/mL]
Particle: 0.01 µg/mL	*	*
Particle: 0.1 µg/mL	*	*
Particle: 1.0 µg/m	*	*
Particle: 10 µg/mL	*	*
Particle: 100 µg/mL	685 ± 74	106 ± 31
LPS: 27 ng/mL	840 ± 178	-
M+MO	*	-
M ÷ MO	*	-

Figure H.2 illustrates the results from donor F which are presented in tables H.2a) and b) graphically.

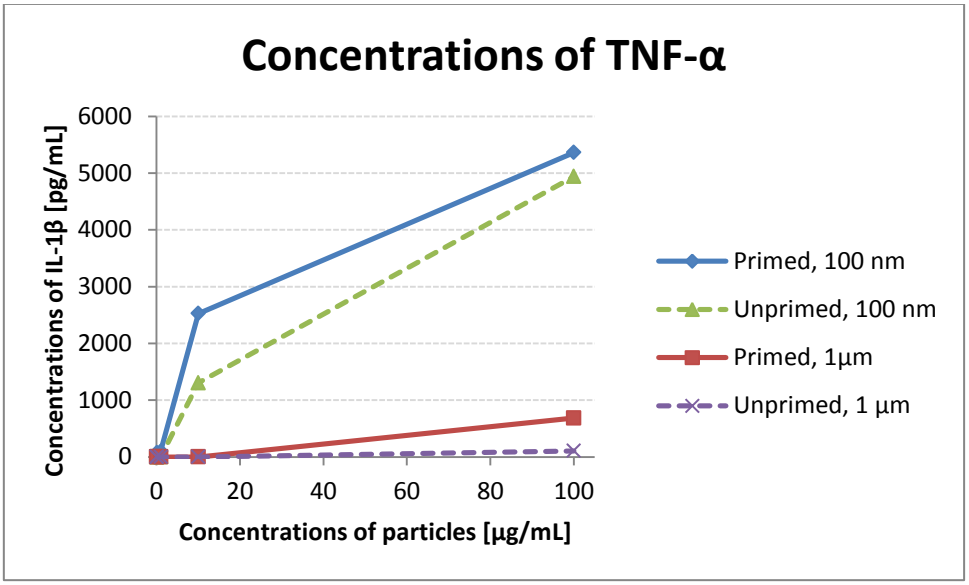

Figure H.2 Concentrations of secreted cytokine TNF-α from monocytes isolated from donor F. All data points are presented in tables H.2.

H.1.2.1 Sources of errors in this experiment

Potential errors may be similar to those mentioned in attachment F.2.2.1.

H.1.3 Results from Bio-plex

The same cytokines have shown significant results as for donor D and E in attachments F.2.3 and G.1.3. Graphical presentations for each cytokine follow in figures H.3-H.6.

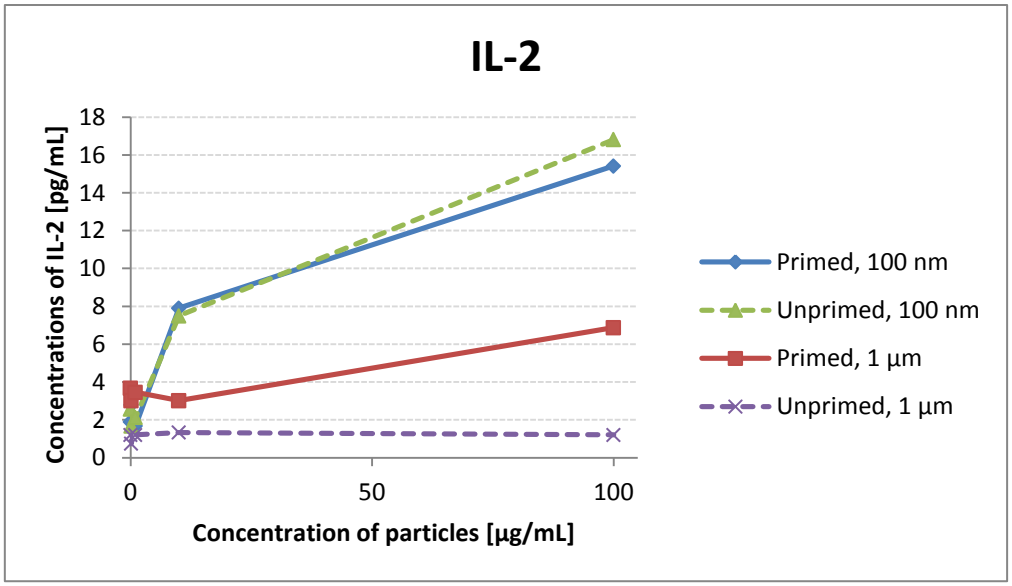

Figure H.3 Concentrations of secreted cytokine IL-2 from monocytes isolated from donor F. The samples have been analyzed with Bio-17-plex.

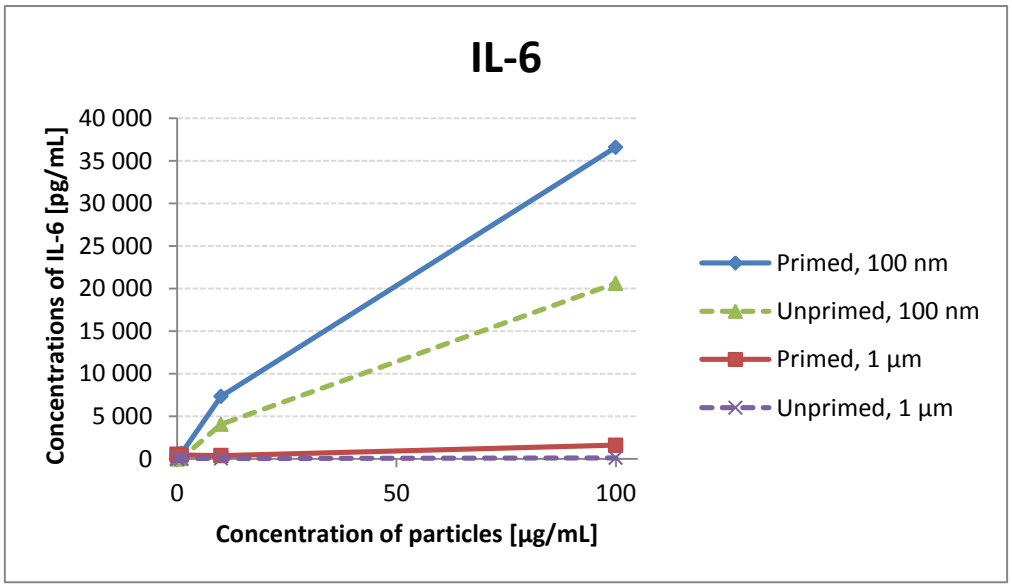

Figure H.4 Concentrations of secreted cytokine IL-6 from monocytes isolated from donor F. The samples have been analyzed with Bio-17-plex.

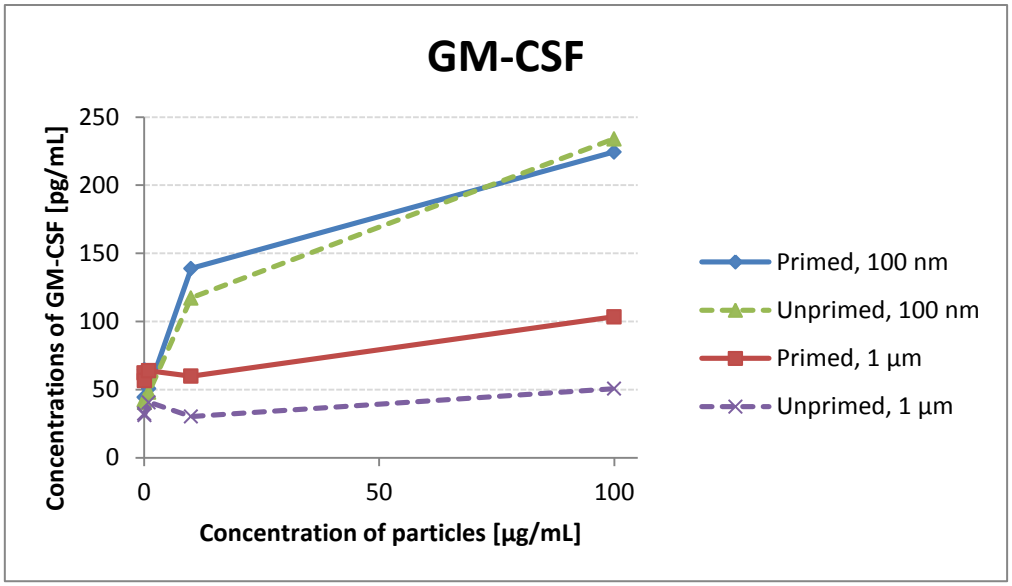

Figure H.5 Concentrations of secreted cytokine GM-CSF from monocytes isolated from donor F. The samples have been analyzed with Bio-17-plex.

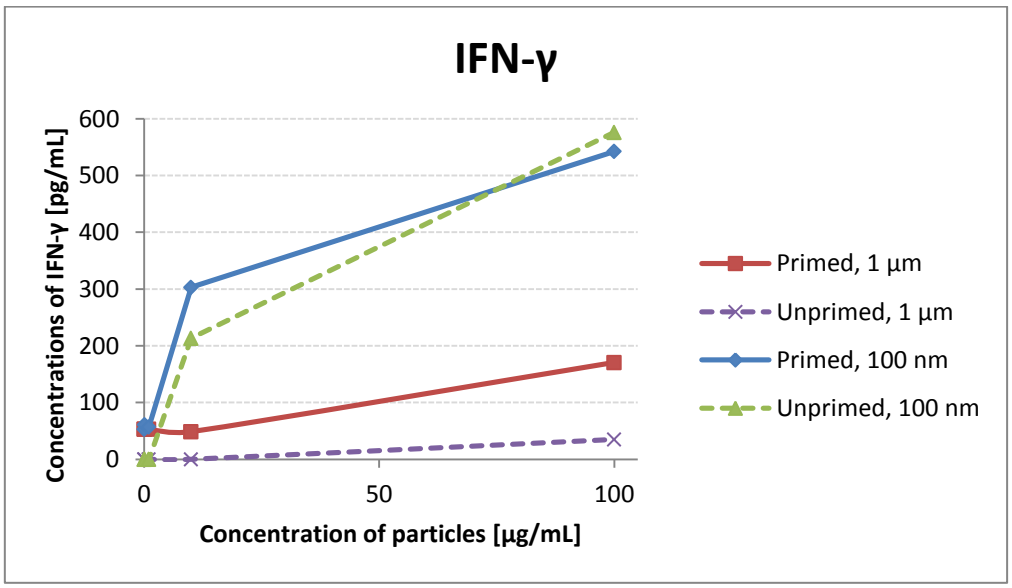

Figure H.6 Concentrations of secreted cytokine IFN-γ from monocytes isolated from donor F. The samples have been analyzed with Bio-17-plex.

Attachment I – Average results from isolated monocytes

I.1 Average results for donors A-D

The average result from the four individual donors A-D (attachments C-F) is presented in tables I.1a) and b), in addition to a graphical presentation in figure 3.8, chapter 3.

Table I.1 Average concentrations (n=4) of secreted IL-1β [pg/mL]. A mark (*) indicates an undetectably low value.
a) 100 nm particles.

Stimuli concentrations	Active A+ serum, IL-1β conc. ± SD [pg/mL]	Heat inactivated A+ serum, IL-1β conc. ± SD [pg/mL]
Particle: 0.01 µg/mL	27.759 ± 20.512	16.144 ± 7.298
Particle: 0.1 µg/mL	30.071 ± 22.765	20.358 ± 18.632
Particle: 1.0 µg/m	43.766 ± 35.221	17.216 ± 10.051
Particle: 10 µg/mL	279.238 ± 77.713	39.172 ± 25.934
Particle: 100 µg/mL	281.747 ± 76.076	317.497 ± 83.340
ATP: 3 mM	315.069 ± 86.257	261.580 ± 128.623
M+MO	15.243 ± 9.849	15.056 ± 17.230
M ÷ MO	*	*

b) 1 µm particles.

Stimuli concentrations	Active A+ serum, IL-1β conc. ± SD [pg/mL]	Heat inactivated A+ serum, IL-1β conc. ± SD [pg/mL]
Particle: 0.01 µg/mL	35.509 ± 20.272	19.740 ± 15.068
Particle: 0.1 µg/mL	40.785 ± 25.622	24.499 ± 19.574
Particle: 1.0 µg/m	44.022 ± 32.095	17.669 ± 14.180
Particle: 10 µg/mL	46.314 ± 28.277	29.927 ± 26.754
Particle: 100 µg/mL	248.156 ± 33.107	111.728 ± 42.150
LPS: 27 ng/mL	241.362 ± 91.052	214.214 ± 133.160
M+MO	18.479 ± 22.689	28.854 ± 20.918
M ÷ MO	*	*

I.2 Average IL-1β results for donors D-F

The average IL-1β result from the three donors D-F (attachments F-H) is presented in tables I.2a) and b), in addition to a graphical presentation in figure 3.1, chapter 3.

Table I.2 Average concentrations (n=3) of secreted IL-1β [pg/mL] from monocytes. A mark (*) indicates an undetectably low value. (¤) Values are based on only two donors (E-F)
a) 100 nm particles.

Stimuli concentrations	Primed, IL-1β conc. ± SD [pg/mL]	Unprimed, IL-1β conc. ± SD [pg/mL]
Particle: 0.01 µg/mL	13.125 ± 18.163	15.351 ± 23.829
Particle: 0.1 µg/mL	15.470 ± 17.276	2.161 ± 2.794 ¤
Particle: 1.0 µg/m	24.885 ± 27.952	9.372 ± 12.900 ¤
Particle: 10 µg/mL	211.254 ± 117.093	75.574 ± 70.122 ¤
Particle: 100 µg/mL	302.276 ± 55.190	331.640 ± 70.257
ATP: 3 mM	302.932 ± 44.535	186.215 ± 127.778 ¤
M+MO	7.247 ± 11.928	0.998 ± 0.423 ¤
M ÷ MO	*	*

b) 1 µm particles.

Stimuli concentrations	Primed, IL-1β conc. ± SD [pg/mL]	Unprimed, IL-1β conc. ± SD [pg/mL]
Particle: 0.01 µg/mL	19.914 ± 24.775	16.956 ± 26.745
Particle: 0.1 µg/mL	17.305 ± 21.755	2.269 ± 3.055 ¤
Particle: 1.0 µg/m	22.935 ± 25.579	2.587 ± 2.288 ¤
Particle: 10 µg/mL	29.215 ± 37.292	2.191 ± 2.985 ¤
Particle: 100 µg/mL	153.804 ± 86.866	54.236 ± 75.405
LPS: 27 ng/mL	78.122 ± 85.097	-
M+MO	17.066 ± 14.105	-
M ÷ MO	7.892 ± 16.676	-

I.3 Average TNF-α results for donors D-F

The average TNF-α result (n=3) is presented in tables I.3a) and b), in addition to a graphical presentation in figure 3.2, chapter 3.

Table I.3 Average concentrations of secreted TNF-α [pg/mL] from monocytes (n=3). A mark (*) indicates an undetectably low value. (¤) Values are based on only two donors (E-F)
a) 100 nm particles.

Stimuli concentrations	Primed, TNF-α conc. ± SD [pg/mL]	Unprimed, TNF-α conc. ± SD [pg/mL]
Particle: 0.01 µg/mL	*	*
Particle: 0.1 µg/mL	57 ± 51	*
Particle: 1.0 µg/m	101 ± 103	*
Particle: 10 µg/mL	2 244 ± 1187	920 ± 655 ¤
Particle: 100 µg/mL	4 779 ± 768	4 124 ± 764
ATP: 3 mM	18 ± 31	*
M+MO	*	*
M ÷ MO	*	*

b) 1 µm particles.

Stimuli concentrations	Primed, TNF-α conc. ± SD [pg/mL]	Unprimed, TNF-α conc. ± SD [pg/mL]
Particle: 0.01 µg/mL	*	*
Particle: 0.1 µg/mL	*	*
Particle: 1.0 µg/m	*	*
Particle: 10 µg/mL	20 ± 21	33 ± 38 ¤
Particle: 100 µg/mL	746 ± 508	106 ± 93
LPS: 27 ng/mL	728 ± 509	-
M+MO	*	-
M ÷ MO	*	-

I.4 Average Bio-plex results for donors D-F

The average Bio-plex results from three donors (D-F) are presented in tables I.4-I.8, in addition to respective graphical presentations in figures 3.3-3.7 in chapter 3. In addition, TNF-α results are listed in table I.9, but these are not presented in chapter 3 due to "out of range" values.

Table I.4 Average concentrations of secreted IL-1β [pg/mL] from monocytes (n=3). A mark (*) indicates an undetectably low value. (¤) Values are based on only two donors (E-F). (+) Non-primed ATP control.

a) 100 nm particles.

Stimuli concentrations	Primed, IL-1β conc. ± SD [pg/mL]	Unprimed, IL-1β conc. ± SD [pg/mL]
Particle: 0.01 µg/mL	8.190 ± 3.454	11.523 ± 14.758
Particle: 0.1 µg/mL	8.450 ± 3.809	2.630 ± 1.188 ¤
Particle: 1.0 µg/m	10.680 ± 4.409	4.280 ± 2.333 ¤
Particle: 10 µg/mL	117.413 ± 73.151	43.995 ± 11.363 ¤
Particle: 100 µg/mL	1 081.843 ± 657.911	852.597 ± 508.911
ATP: 3 mM	337.063 ± 188.321	92.415 ± 62.897 ¤+
M+MO	1.493 ± 0	3.655 ± 0.049 ¤
M ÷ MO	0.040 ± 0	*

b) 1 µm particles.

Stimuli concentrations	Primed, IL-1β conc. ± SD [pg/mL]	Unprimed, IL-1β conc. ± SD [pg/mL]
Particle: 0.01 µg/mL	10.180 ± 4.910	8.450 ± 9.751
Particle: 0.1 µg/mL	8.623 ± 3.735	3.295 ± 2.821 ¤
Particle: 1.0 µg/m	9.753 ± 6.288	3.105 ± 2.722 ¤
Particle: 10 µg/mL	13.193 ± 10.286	7.700 ± 7.905 ¤
Particle: 100 µg/mL	70.743 ± 44.311	22.950 ± 23.085
LPS: 27 ng/mL	43.637 ± 28.903	-
M+MO	3.170 ± 0	-
M ÷ MO	*	-

Table I.5 Average concentrations of secreted IL-2 [pg/mL] from monocytes (n=3). A mark (*) indicates an undetectably low value. (¤) Values are based on only two donors (E-F). (+) Non-primed ATP control.

a) 100 nm particles.

Stimuli concentrations	Primed, IL-2 conc. ± SD [pg/mL]	Unprimed, IL-2 conc. ± SD [pg/mL]
Particle: 0.01 µg/mL	2.127 ± 0.225	2.053 ± 0.569
Particle: 0.1 µg/mL	2.503 ± 0.342	1.680 ± 0 ¤
Particle: 1.0 µg/m	2.537 ± 0.760	1.905 ± 0.318 ¤
Particle: 10 µg/mL	7.357 ± 0.637	6.555 ± 1.336 ¤
Particle: 100 µg/mL	12.777 ± 2.303	12.493 ± 3.747
ATP: 3 mM	4.140 ± 1.256	2.015 ± 0.474 ¤+
M+MO	1.450 ± 0.483	0.855 ± 0.502 ¤
M ÷ MO	*	*

b) 1 µm particles.

Stimuli concentrations	Primed, IL-2 conc. ± SD [pg/mL]	Unprimed, IL-2 conc. ± SD [pg/mL]
Particle: 0.01 µg/mL	2.870 ± 0.777	1.670 ± 0.398
Particle: 0.1 µg/mL	2.947 ± 0.127	1.210 ± 0.665
Particle: 1.0 µg/m	2.947 ± 0.458	1.445 ± 0.332
Particle: 10 µg/mL	2.760 ± 0.548	1.330 ± 0
Particle: 100 µg/mL	4.603 ± 2.904	1.710 ± 0.465
LPS: 27 ng/mL	6.233 ± 1.481	-
M+MO	1.900 ± 0.633	-
M ÷ MO	*	-

Table I.6 Average concentrations of secreted IL-6 [pg/mL] from monocytes (n=3). A mark (*) indicates an undetectably low value. (¤) Values are based on only two donors (E-F). (+) Non-primed ATP control.

a) 100 nm particles.

Stimuli concentrations	Primed, IL-6 conc. ± SD [pg/mL]	Unprimed, IL-6 conc. ± SD [pg/mL]
Particle: 0.01 µg/mL	198.297 ± 181.561	72.657 ± 80.507
Particle: 0.1 µg/mL	258.620 ± 291.957	22.635 ± 9.907 ¤
Particle: 1.0 µg/m	333.300 ± 283.324	104.140 ± 84.669 ¤
Particle: 10 µg/mL	5 801.347 ± 2 240.452	3 181.010 ± 1 241.722 ¤
Particle: 100 µg/mL	25 319.957 ± 13 212.177	18 068.680 ± 3 038.853
ATP: 3 mM	147.057 ± 113.785	7.630 ± 6.520 ¤+
M+MO	*	27.875 ± 2.765 ¤
M ÷ MO	*	*

b) 1 µm particles.

Stimuli concentrations	Primed, IL-6 conc. ± SD [pg/mL]	Unprimed, IL-6 conc. ± SD [pg/mL]
Particle: 0.01 µg/mL	283.423 ± 201.362	27.163 ± 13.378
Particle: 0.1 µg/mL	212.477 ± 176.604	24.885 ± 21.432 ¤
Particle: 1.0 µg/m	238.927 ± 177.035	27.590 ± 23.405 ¤
Particle: 10 µg/mL	256.507 ± 125.944	502.615 ± 660.940 ¤
Particle: 100 µg/mL	1 292.790 ± 899.543	190.170 ± 137.362
LPS: 27 ng/mL	1 778.333 ± 993.369	-
M+MO	38.160 ± 12.720	-
M ÷ MO	*	-

Table I.7 Average concentrations of secreted GM-CSF [pg/mL] from monocytes (n=3). A mark (*) indicates an undetectably low value. (¤) Values are based on only two donors (E-F). (+) Non-primed ATP control.

a) 100 nm particles.

Stimuli concentrations	Primed, GM-CSF conc. ± SD [pg/mL]	Unprimed, GM-CSF conc. ± SD [pg/mL]
Particle: 0.01 µg/mL	45.663 ± 3.779	46.877 ± 3.695
Particle: 0.1 µg/mL	57.087 ± 6.507	43.505 ± 3.981 ¤
Particle: 1.0 µg/m	51.327 ± 1.789	49.005 ± 1.252 ¤
Particle: 10 µg/mL	124.533 ± 22.079	106.955 ± 14.701 ¤
Particle: 100 µg/mL	216.277 ± 24.328	197.000 ± 33.354
ATP: 3 mM	71.413 ± 9.293	49.330 ± 6.845 ¤+
M+MO	52.480 ± 17.493	43.505 ± 3.981 ¤
M ÷ MO	42.61 ± 14.203	*

b) 1 µm particles.

Stimuli concentrations	Primed, GM-CSF conc. ± SD [pg/mL]	Unprimed, GM-CSF conc. ± SD [pg/mL]
Particle: 0.01 µg/mL	54.003 ± 7.370	40.157 ± 6.819
Particle: 0.1 µg/mL	49.757 ± 6.248	38.835 ± 10.585 ¤
Particle: 1.0 µg/m	55.653 ± 7.875	48.265 ± 10.713 ¤
Particle: 10 µg/mL	57.740 ± 1.871	47.795 ± 24.855 ¤
Particle: 100 µg/mL	83.523 ± 29.296	53.033 ± 2.410
LPS: 27 ng/mL	92.390 ± 7.223	-
M+MO	57.244 ± 12.907	-
M ÷ MO	*	-

Table I.8 Average concentrations of secreted IFN-γ [pg/mL] from monocytes (n=3). A mark (*) indicates an undetectably low value. (¤) Values are based on only two donors (E-F). (+) Non-primed ATP control.
a) 100 nm particles.

Stimuli concentrations	Primed, IFN-γ conc. ± SD [pg/mL]	Unprimed, IFN-γ conc. ± SD [pg/mL]
Particle: 0.01 µg/mL	41.597 ± 19.595	*
Particle: 0.1 µg/mL	52.665 ± 11.901 ¤	*
Particle: 1.0 µg/m	51.403 ± 6.532	*
Particle: 10 µg/mL	273.693 ± 56.753	202.960 ± 14.863 ¤
Particle: 100 µg/mL	527.700 ± 67.842	450.693 ± 110.466
ATP: 3 mM	111.553 ± 18.637	*
M+MO	*	*
M ÷ MO	*	*

b) 1 µm particles.

Stimuli concentrations	Primed, IFN-γ conc. ± SD [pg/mL]	Unprimed, IFN-γ conc. ± SD [pg/mL]
Particle: 0.01 µg/mL	56.995 ± 5.777	*
Particle: 0.1 µg/mL	43.935 ± 12.693	*
Particle: 1.0 µg/m	40.943 ± 10.363	*
Particle: 10 µg/mL	63.127 ± 18.289	*
Particle: 100 µg/mL	140.217 ± 43.228	51.200 ± 28.129
LPS: 27 ng/mL	163.863 ± 40.266	-
M+MO	*	-
M ÷ MO	*	-

Table I.9 Average concentrations of secreted TNF-α [pg/mL] from monocytes (n=3). A mark (*) indicates an undetectably low value. (#) indicates an "out of range" value above standard curve. (¤) Values are based on only two donors (E-F). (+) Non-primed ATP control. **a)** 100 nm particles.

Stimuli concentrations	Primed, TNF-α conc. ± SD [pg/mL]	Unprimed, TNF-α conc. ± SD [pg/mL]
Particle: 0.01 µg/mL	46.597 ± 30.591	8.267 ± 2.934
Particle: 0.1 µg/mL	88.380 ± 79.110	8.460 ± 1.754 ¤
Particle: 1.0 µg/m	77.510 ± 35.335	21.955 ± 15.563 ¤
Particle: 10 µg/mL	2 541.620 ± 1 643.723	981.670 ± 698.664 ¤
Particle: 100 µg/mL	#	#
ATP: 3 mM	73.160 ± 18.926	12.525 ± 1.336 ¤+
M+MO	*	12.550 ± 4.907
M ÷ MO	*	*

b) 1 µm particles.

Stimuli concentrations	Primed, TNF-α conc. ± SD [pg/mL]	Unprimed, TNF-α conc. ± SD [pg/mL]
Particle: 0.01 µg/mL	64.490 ± 36.904	7.057 ± 4.210
Particle: 0.1 µg/mL	51.223 ± 45.967	8.770 ± 2.192 ¤
Particle: 1.0 µg/m	59.643 ± 37.904	9.880 ± 4.186 ¤
Particle: 10 µg/mL	69.777 ± 46.409	48.430 ± 40.390 ¤
Particle: 100 µg/mL	489.003 ± 351.192	44.370 ± 41.266
LPS: 27 ng/mL	850.420 ± 474.682	-
M+MO	*	-
M ÷ MO	*	-

I.5 LPS dilution curve

A LPS dilution curve was prepared from one donor and analyzed for both IL-1β and TNF-α, as described in attachments B.2 and B.3. The results are given in sections I.5.1-I.5.2. Dilution curves are prepared for two different exposure periods, namely two and six hours.

I.5.1 IL-1β results

The IL-1β results are presented in table I.10 as well as graphically illustrated in figures 3.16 and 3.18 in chapter 3.

Table I.10 LPS dilution curve (n=1) based on amounts of secreted IL-1β [pg/mL]. A mark (*) indicates an undetectably low value.

LPS concentrations [pg/mL]	2 hours IL-1β conc. ± SD [pg/mL]	6 hours IL-1β conc. ± SD [pg/mL]
25	6.437 ± 0.058	5.081 ± 0.086
50	2.405 ± 0.007	28.680 ± 0.100
100	3.543 ± 0.035	208.842 ± 0.164
250	19.715 ± 0.049	264.561 ± 0.061
500	60.720 ± 0.088	263.443 ± 0.160
2 500	111.382 ± 0.093	256.002 ± 0.017
5 000	111.603 ± 0.103	256.477 ± 0.015
25 000	126.107 ± 0.106	249.487 ± 0.055
M+MO	25.497 ± 0.167	2.320 ± 0.007
M ÷ MO	*	*

I.5.2 TNF-α results

The TNF-α results are presented in table I.11 as well as graphically illustrated in figures 3.17 and 3.19 in chapter 3.

Table I.11 LPS dilution curve (n=1) based on amounts of secreted TNF-α [pg/mL]. A mark (*) indicates an undetectably low value.

LPS concentrations [pg/mL]	2 hours IL-1β conc. ± SD [pg/mL]	6 hours IL-1β conc. ± SD [pg/mL]
25	*	*
50	*	17 ± 29
100	*	1 038 ± 387
250	349 ± 69	2 895 ± 179
500	836 ± 87	3 558 ± 112
2 500	1 732 ± 88	3 365 ± 134
5 000	1 611 ± 89	3 277 ± 60
25 000	2 003 ± 72	3 706 ± 116
M+MO	*	*
M ÷ MO	*	*

Attachment J – Donor G

Donor G was the first one out of three whole blood donors. Whole blood was used for TCC, cytokine and flow cytometric analyses, and all results for this donor are presented in sections J.1-J.3.

J.1 Flow cytometry

J.1.1 Results

Whole blood was sampled out for flow cytometric analysis after 15 minutes (T15) incubation with stimulants. After gating for CD14+ monocytes, up-regulation of CD11b was measured by flow cytometry for both monocytes and granulocytes. Data analysis was performed using a FACScan program on samples of 5000 events. The results are listed in table J.1, and shown in figures J.1 and J.2.

Table J.1 CD11b monocytes and granulocytes from donor G, together with absolute zero time line (T_0), and positive and negative controls.

		Cell fluorescent intensity distribution	
Particle size	**Concentration of particles [µg/mL]**	**CD11b monocytes**	**CD11b granulocytes**
100 nm	**0.1**	47.8	35.9
	1.0	80.6	137.0
	10	182.7	336.8
	100	339.8	406.8
1 µm	**0.1**	60.4	38.5
	1.0	55.7	40.0
	10	56.7	45.7
	100	69.8	83.5
T_0		51.9	34.3
ATP		155.4	126.3
Zymosan		299.6	491.4
LPS		235.0	50.0
PBS		56.2	40.3

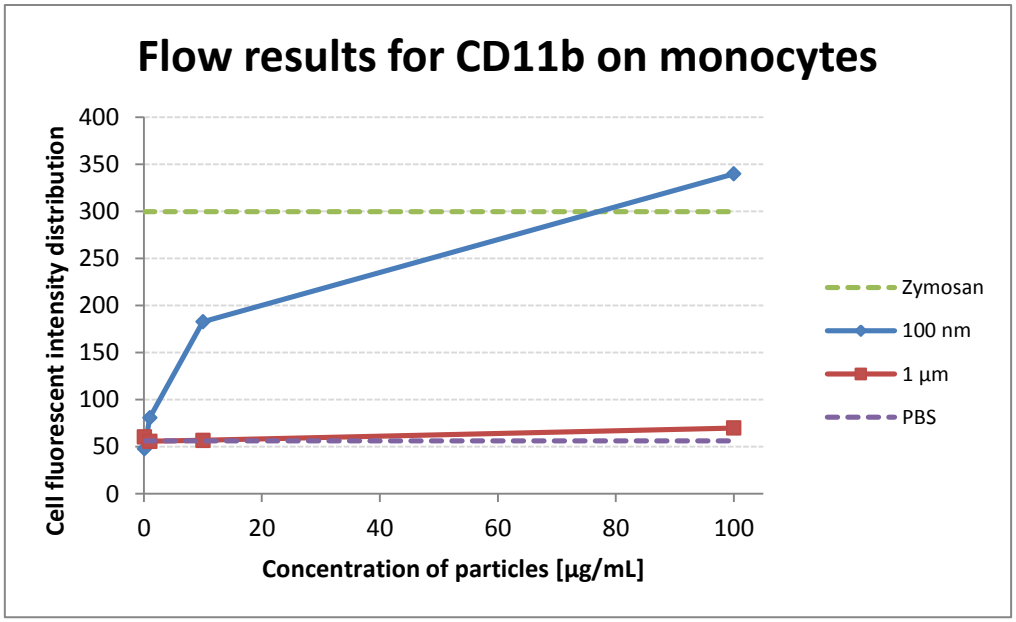

Figure J.1 CD11b monocytes with positive (Zymosan) and negative (PBS) controls, after gating for CD14+ cells.

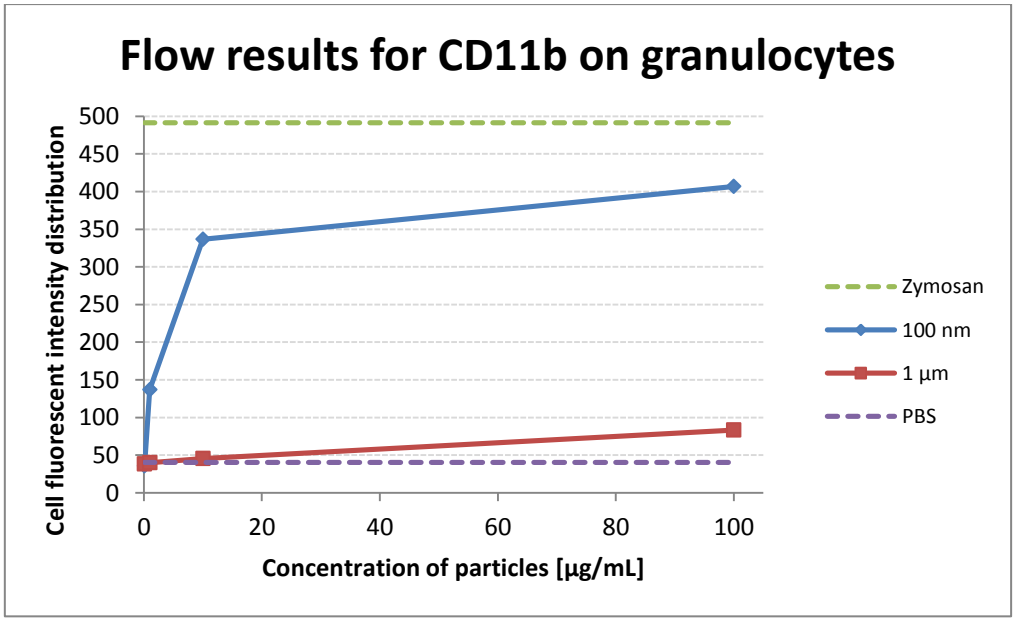

Figure J.2 CD11b granulocytes, with positive (Zymosan) and negative (PBS) controls.

J.1.2 Sources of errors in this experiment

The expiration date of the LDS-751 die was year 2010. However, it was believed that this die still gave reliable results.

J.2 TCC

Whole blood was sampled out for TCC analysis after a 60 minutes (T60) long incubation period. The results are listed in table J.2, and shown in figure J.3.

Table J.2 TCC analysis of whole blood donor G after stimulation with particles, positive and negative controls, in addition to absolute zero time line (T_0).

Particle size	Concentration of particles [µg/mL]	Concentrations of TCC [AU/mL]
100 nm	**0.1**	1.712
	1.0	4.534
	10	7.678
	100	7.938
1 µm	**0.1**	2.451
	1.0	2.050
	10	2.503
	100	7.419
T_0		0.908
ATP		1.121
Zymosan		11.758
LPS		1.712
PBS		0.628

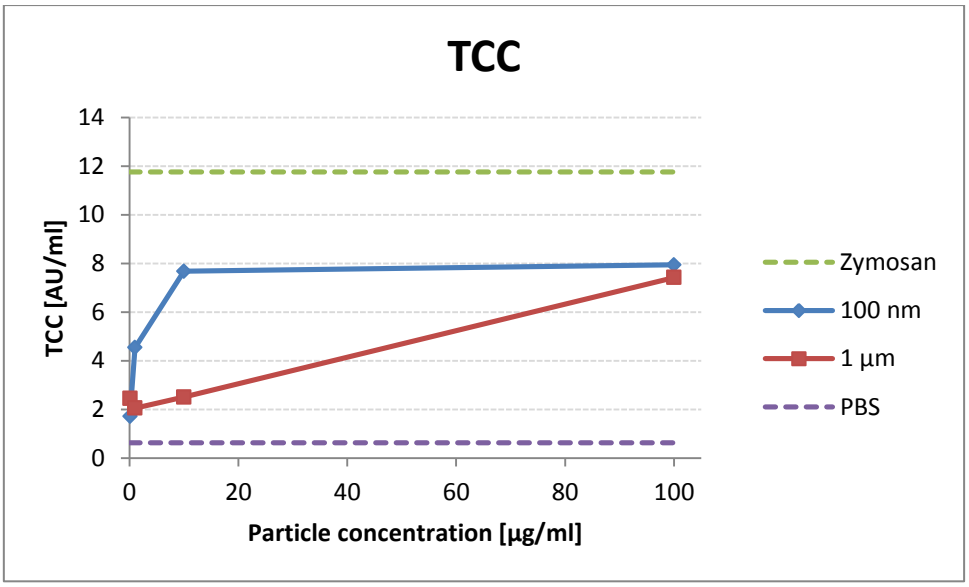

Figure J.3 TCC results [AU/mL] for donor G, with positive (Zymosan) and negative (PBS) controls.

J.3 Cytokine analysis

Whole blood was sampled out for cytokine analysis after being incubated for 6 hours (T360).

J.3.1 IL-1β ELISA

The results for IL-1β from ELISA analysis are listed in table J.3, and shown in figure J.4.

Table J.3 IL-1β analysis of whole blood with ELISA, after stimulation with particles, positive and negative controls, in addition to absolute zero time line (T_0).

Particle size	Concentration of particles [µg/mL]	Concentrations of IL-1β [pg/mL]
100 nm	**0.1**	62.186
	1.0	30.762
	10	37.591
	100	103.536
1 µm	**0.1**	50.461
	1.0	45.640
	10	26.804
	100	8.436
T_0		*
ATP		1.192
Zymosan		217.069
LPS		262.429
PBS		31.470

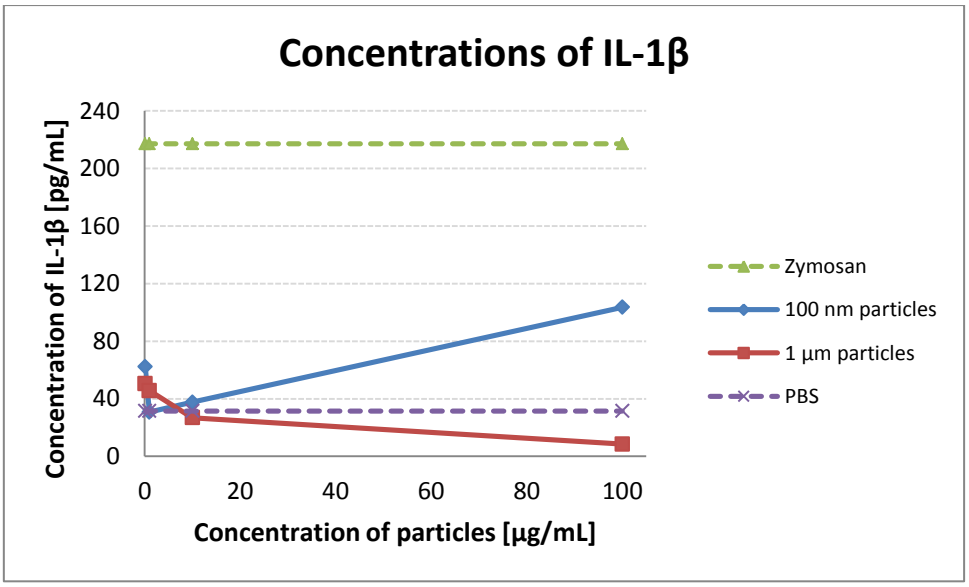

Figure J.4 Concentrations of IL-1β [pg/mL] from T360 whole blood donor G, analyzed with ELISA.

J.3.2 Bio-plex

In addition to IL-1β, three other cytokines gave significant results when analyzed with 17-plex. The data points are not given, but the results are illustrated in figures J.5-J.8. The samples were diluted 1:4.

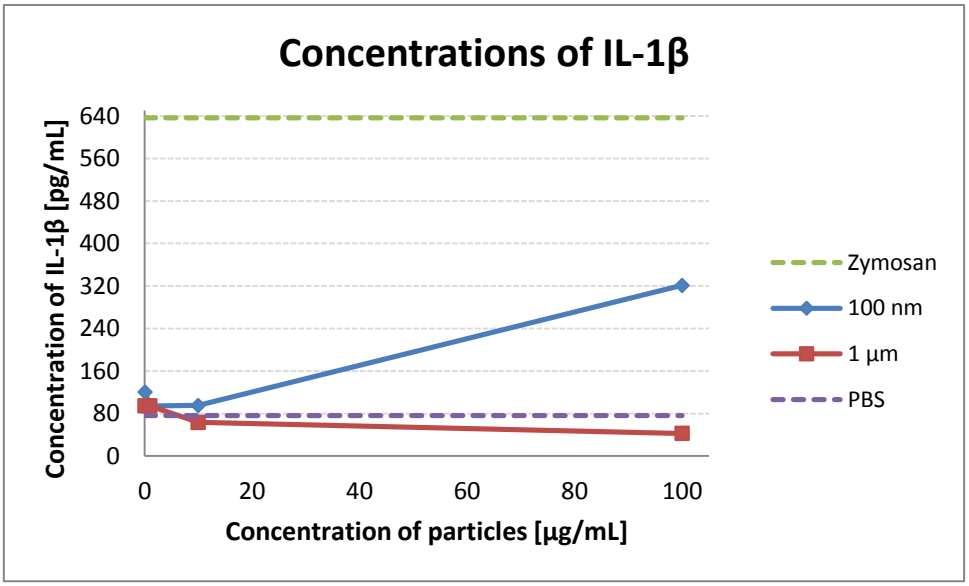

Figure J.5 Concentrations of IL-1β [pg/mL] from T360 whole blood, analyzed with Bio-plex.

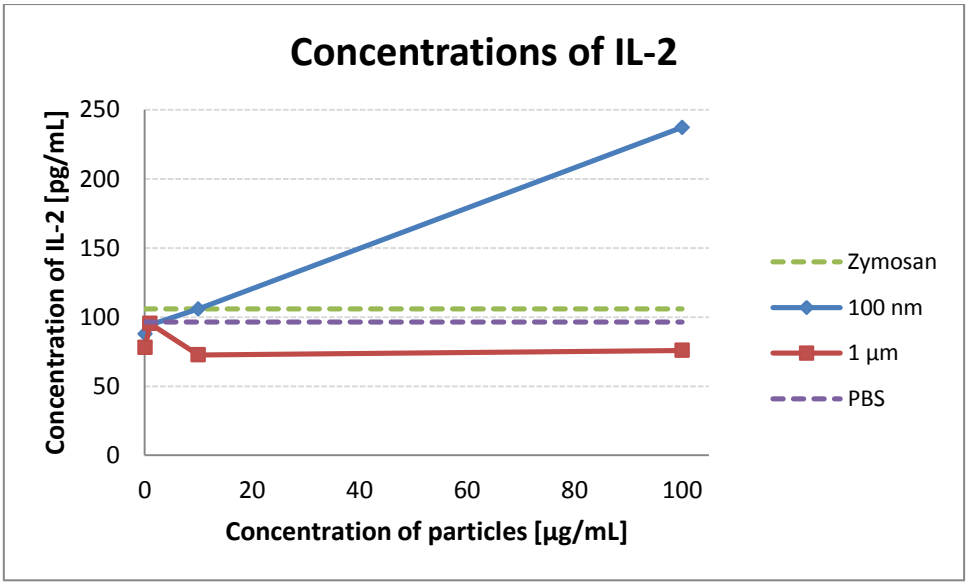

Figure J.6 Concentrations of IL-2 [pg/mL] from T360 whole blood, analyzed with Bio-plex.

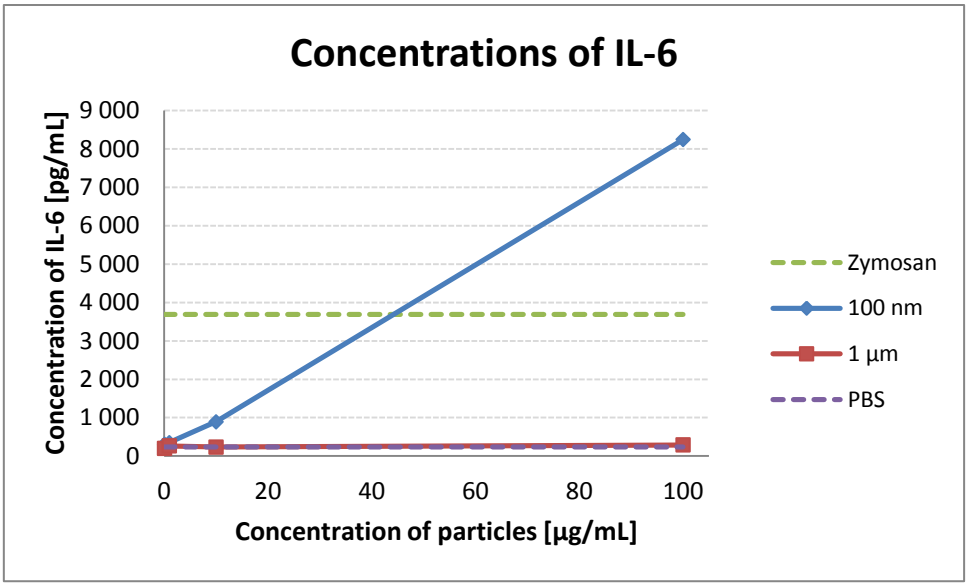

Figure J.7 Concentrations of IL-6 [pg/mL] from T360 whole blood, analyzed with Bio-plex.

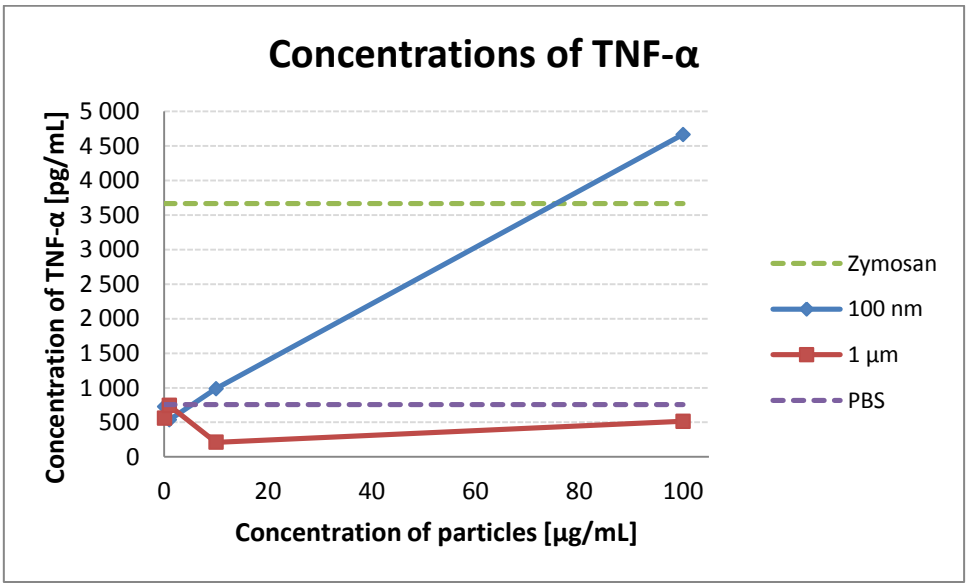

Figure J.8 Concentrations of TNF-α [pg/mL] from T360 whole blood, analyzed with Bio-plex.

Attachment K – Donor H

K.1 Flow cytometry

K.1.1 Results

As for donor G (attachment J), whole blood from donor H was sampled out for flow cytometric analysis at T15. The results are listed in table K.1, and shown in figures K.1 and K.2.

Table K.1 CD11b monocytes and granulocytes from donor H, together with absolute zero time line (T_0), and positive and negative controls.

		Cell fluorescent intensity distribution	
Particle size	**Concentration of particles [µg/mL]**	**CD11b monocytes**	**CD11b granulocytes**
100 nm	**0.1**	51.4	40.0
	1.0	53.3	41.4
	10	57.3	47.0
	100	174.7	192.8
1 µm	**0.1**	65.5	42.9
	1.0	69.8	47.8
	10	70.4	55.7
	100	73.7	151.2
T_0		53.8	41.0
ATP		346.0	181.1
Zymosan		235.0	509.4
LPS		125.2	47.8
PBS		50.5	43.3

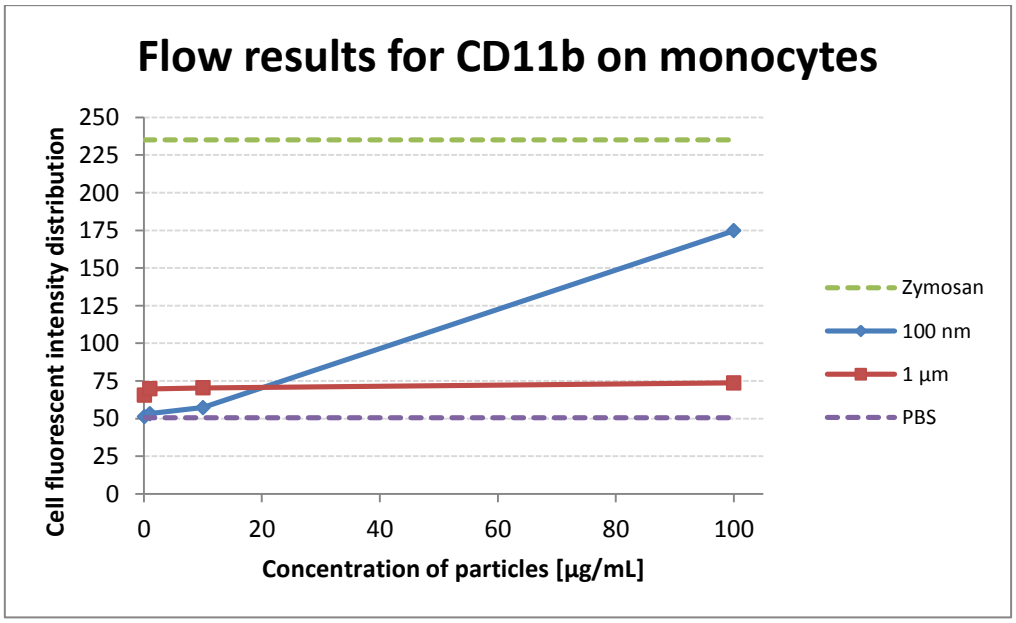

Figure K.1 CD11b monocytes with positive (Zymosan) and negative (PBS) controls, after gating for CD14+ cells.

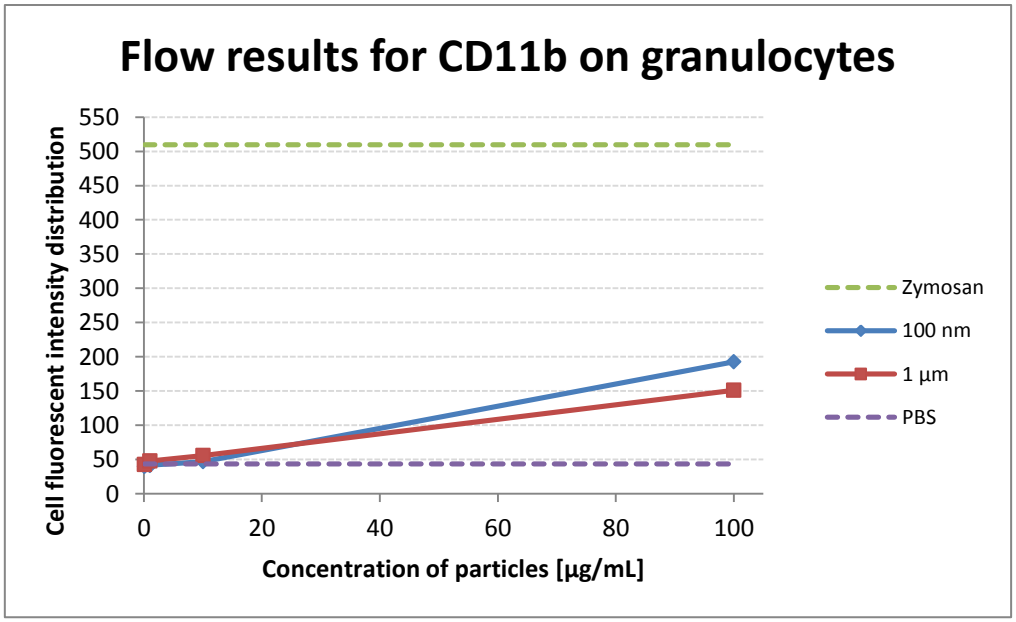

Figure K.2 CD11b granulocytes, with positive (Zymosan) and negative (PBS) controls.

K.1.2 Sources of errors in this experiment

The errors are the same as described in attachment J.1.2.

K.2 TCC

Whole blood was sampled out for TCC analysis at T60. The results are listed in table K.2, and shown in figure K.3.

Table K.2 TCC analysis of whole blood from donor H after stimulation with particles, positive and negative controls, in addition to absolute zero time line (T_0).

Particle size	Concentration of particles [µg/mL]	Concentrations of TCC [AU/mL]
100 nm	**0.1**	0.590
	1.0	2.199
	10	5.063
	100	9.673
1 µm	**0.1**	0.908
	1.0	1.387
	10	2.973
	100	8.135
T_0		0.071
ATP		0.479
Zymosan		12.114
LPS		2.149
PBS		1.478

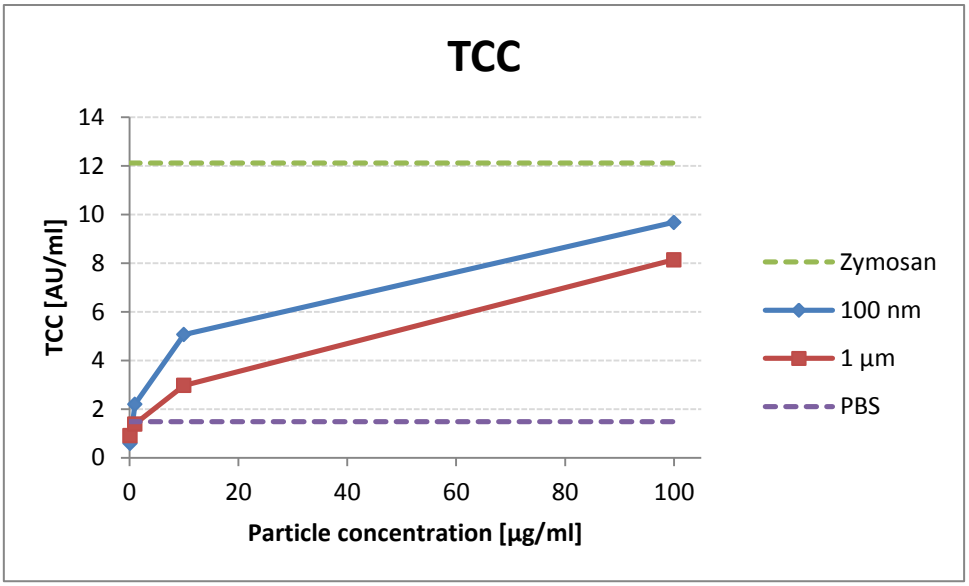

Figure K.3 TCC results [AU/mL] for donor H, with positive (Zymosan) and negative (PBS) controls.

K.3 Cytokine analysis

Whole blood was sampled out for cytokine analysis at T360.

K.3.1 IL-1β ELISA

The results for IL-1β from ELISA analysis are listed in table K.3, and shown in figure K.4.

Table K.3 IL-1β analysis of whole blood with ELISA, after stimulation with particles, positive and negative controls, in addition to absolute zero time line (T_0).

Particle size	Concentration of particles [µg/mL]	Concentrations of IL-1β [pg/mL]
100 nm	**0.1**	52.782
	1.0	58.528
	10	131.137
	100	264.131
1 µm	**0.1**	61.241
	1.0	90.721
	10	34.499
	100	23.012
T_0		*
ATP		0.593
Zymosan		226.177
LPS		283.694
PBS		32.613

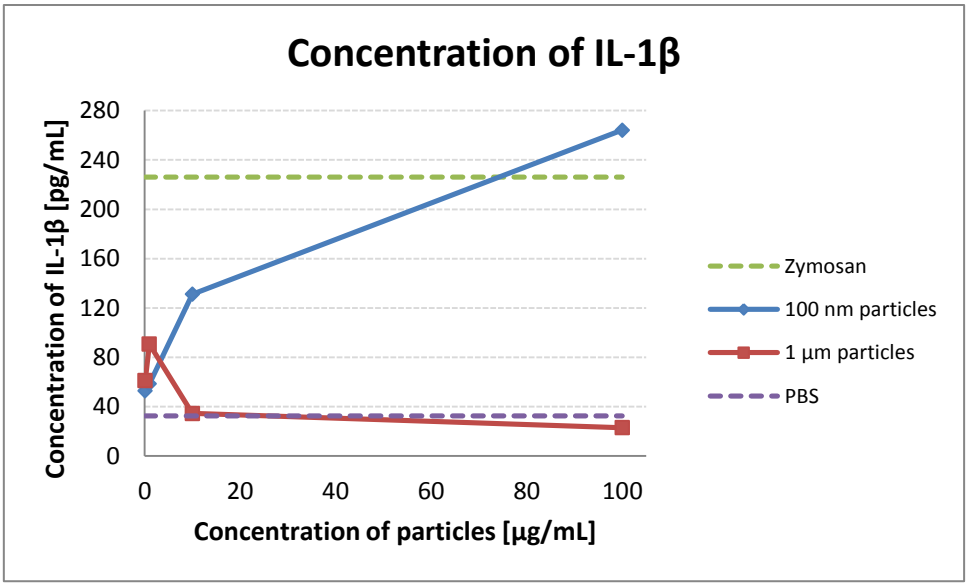

Figure K.4 Concentrations of IL-1β [pg/mL] from T360 whole blood.

K.3.2 Bio-plex

In addition to IL-1β, three other cytokines gave significant results when analyzed with 17-plex. The data points are not given, but the results are illustrated in figures K.5-K.8.

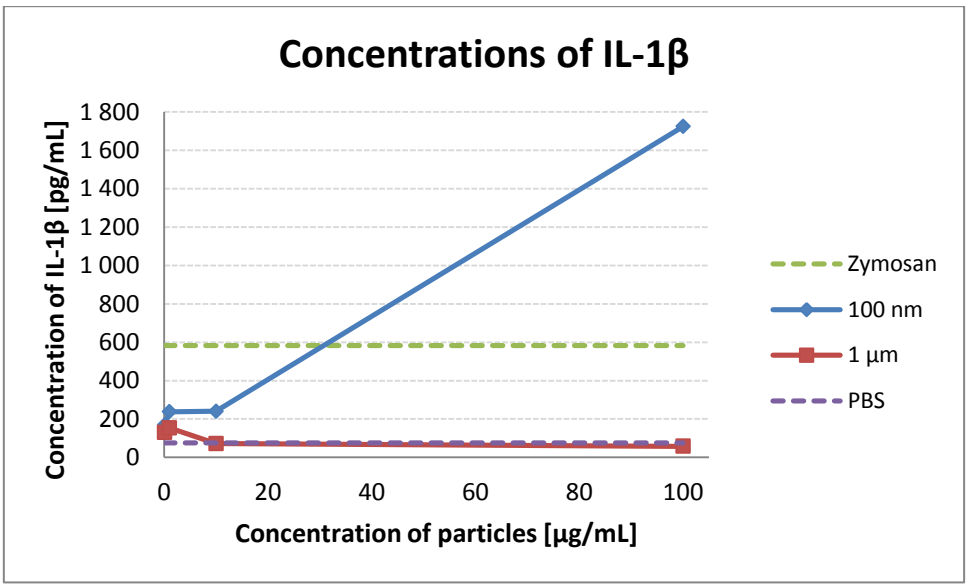

Figure K.5 Concentrations of IL-1β [pg/mL] from T360 whole blood, analyzed with Bio-plex.

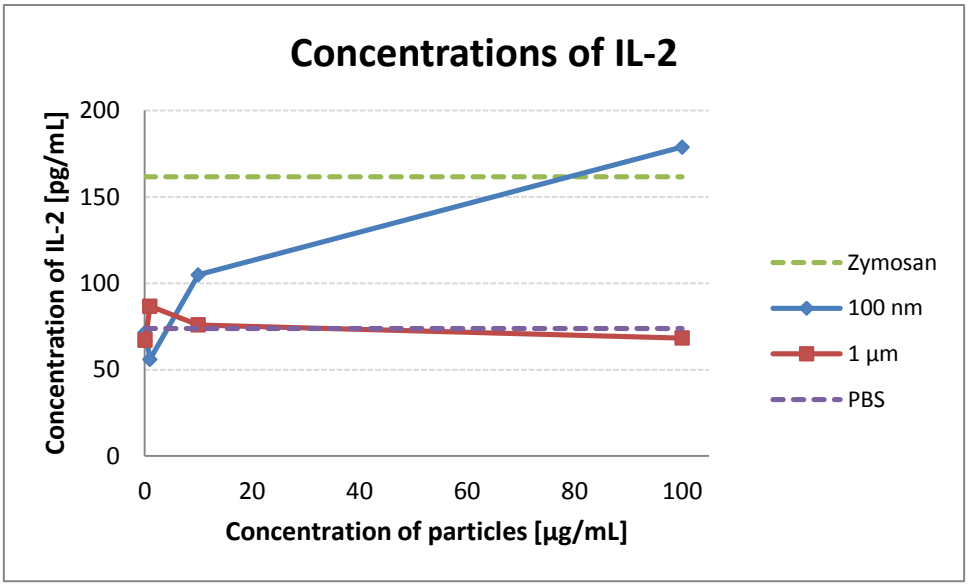

Figure K.6 Concentrations of IL-2 [pg/mL] from T360 whole blood, analyzed with Bio-plex.

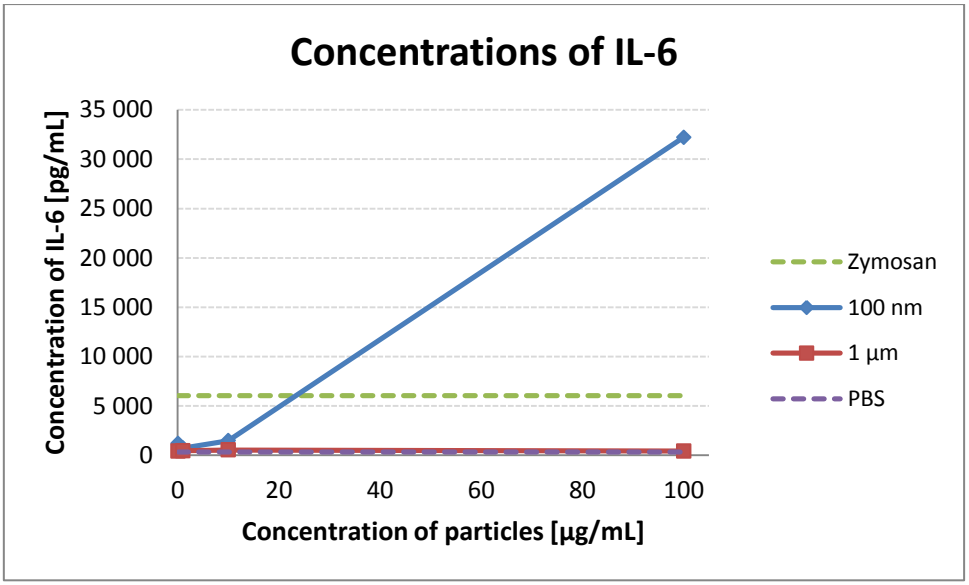

Figure K.7 Concentrations of IL-6 [pg/mL] from T360 whole blood, analyzed with Bio-plex.

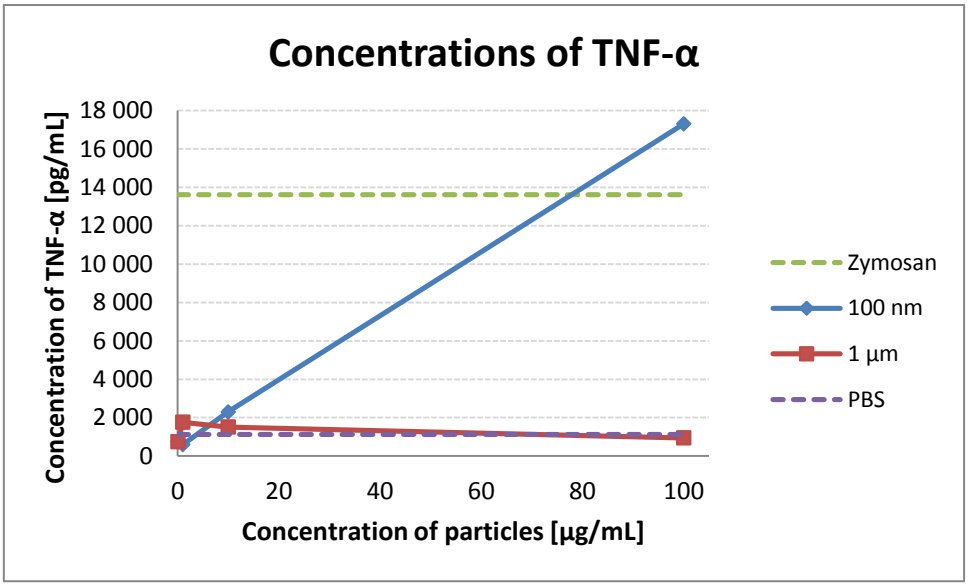

Figure K.8 Concentrations of TNF-α [pg/mL] from T360 whole blood, analyzed with Bio-plex.

Attachment L – Donor I

L.1 Flow cytometry

L.1.1 Results

As for donors G and H (attachments J and K), whole blood from donor I was sampled out for flow cytometric analysis at T15. The results are listed in table L.1, and shown in figures L.1 and L.2.

Table L.1 CD11b monocytes and granulocytes from donor I, together with absolute zero time line (T_0), and positive and negative controls.

		Cell fluorescent intensity distribution	
Particle size	**Concentration of particles [µg/mL]**	**CD11b monocytes**	**CD11b granulocytes**
100 nm	**0.1**	93.1	61.5
	1.0	116.5	131.0
	10	235.0	339.8
	100	310.6	378.6
1 µm	**0.1**	104.6	66.7
	1.0	123.0	79.9
	10	142.0	145.9
	100	226.7	291.6
T_0		54.7	128.6
ATP		218.7	143.3
Zymosan		248.0	429.4
LPS		174.7	81.3
PBS		115.5	96.5

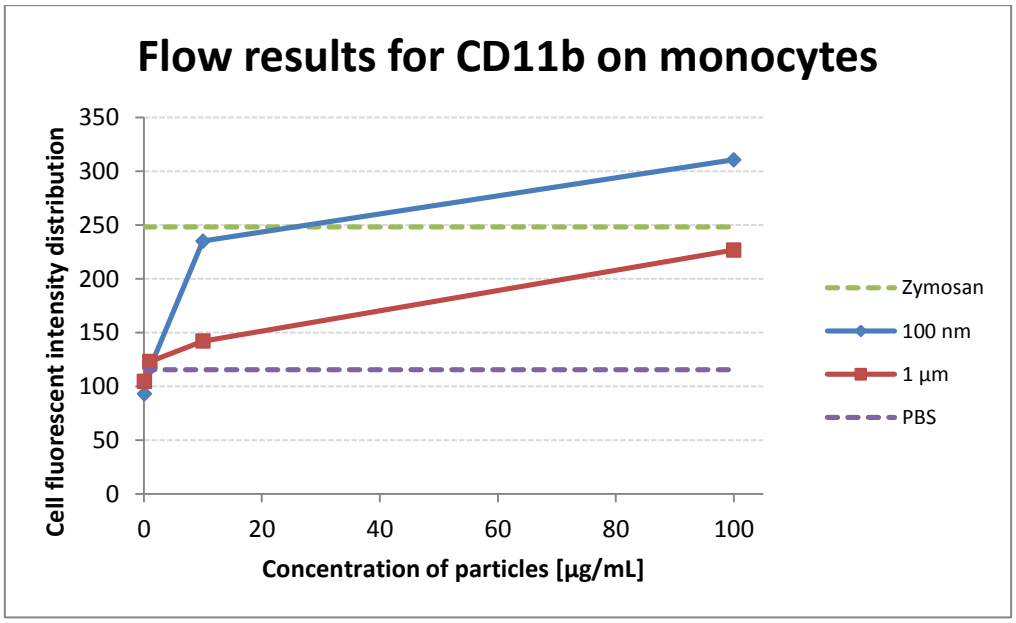

Figure L.1 CD11b monocytes with positive (Zymosan) and negative (PBS) controls, after gating for CD14+ cells.

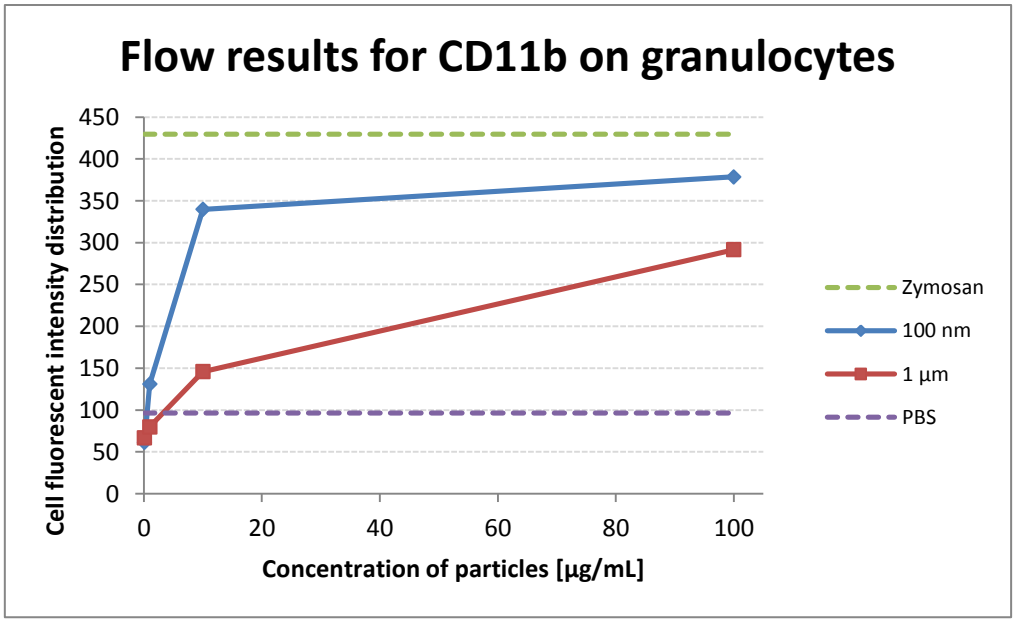

Figure L.2 CD11b granulocytes, with positive (Zymosan) and negative (PBS) controls.

L.1.2 Sources of errors in this experiment

The errors are the same as described in attachment J.1.2.

L.2 TCC

Whole blood was sampled out for TCC analysis at T60. The results are listed in table L.2, and shown in figure L.3.

Table L.2 TCC analysis of whole blood from donor I after stimulation with particles, positive and negative controls, in addition to absolute zero time line (T_0).

Particle size	Concentration of particles [µg/mL]	Concentrations of TCC [AU/mL]
100 nm	**0.1**	4.131
	1.0	6.032
	10	9.741
	100	8.796
1 µm	**0.1**	2.920
	1.0	3.241
	10	5.725
	100	9.741
T_0		2.657
ATP		2.920
Zymosan		9.741
LPS		2.249
PBS		2.350

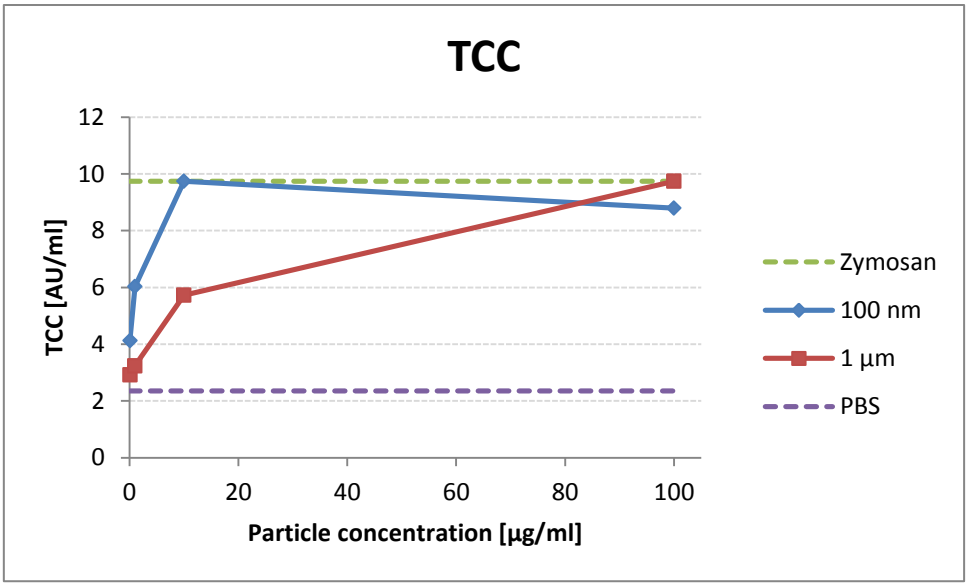

Figure L.3 TCC results [AU/mL] for donor I, with positive (Zymosan) and negative (PBS) controls.

L.3 Cytokine analysis

Whole blood was sampled out for cytokine analysis at T360.

L.3.1 IL-1β ELISA

The results for IL-1β from ELISA analysis are listed in table L.3 and shown in figure L.4.

Table L.3 IL-1β analysis of whole blood with ELISA, after stimulation with particles, positive and negative controls, in addition to absolute zero time line (T_0).

Particle size	Concentration of particles [µg/mL]	Concentrations of IL-1β [pg/mL]
100 nm	**0.1**	38.064
	1.0	73.643
	10	66.921
	100	182.888
1 µm	**0.1**	37.728
	1.0	51.133
	10	59.472
	100	16.219
T_0		0.579
ATP		0.438
Zymosan		274.748
LPS		265.268
PBS		83.238

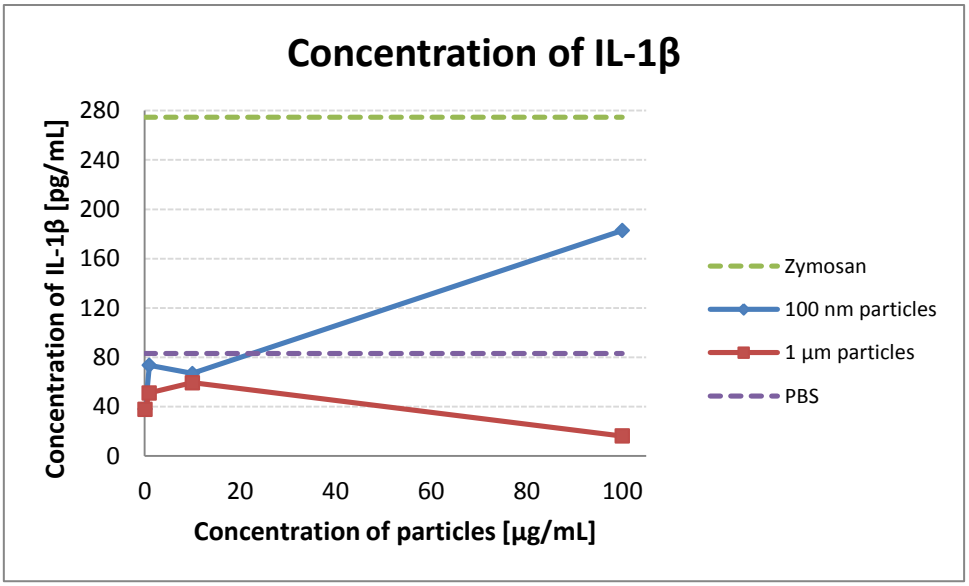

Figure L.4 Concentrations of IL-1β [pg/mL] from T360 whole blood.

L.3.2 Bio-plex

In addition to IL-1β, three other cytokines gave significant results when analyzed with 17-plex. The data points are not given, but the results are illustrated in figures L.5-L.8.

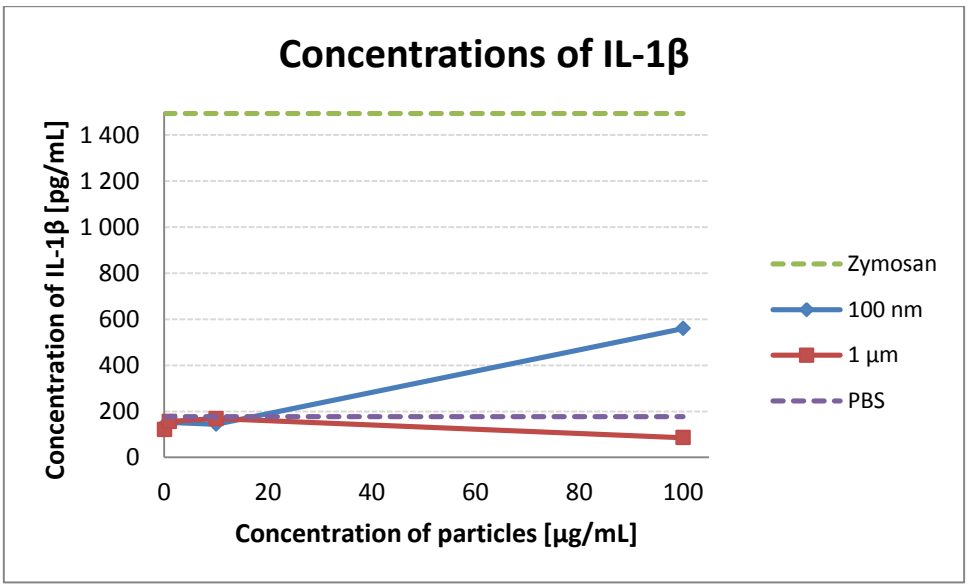

Figure L.5 Concentrations of IL-1β [pg/mL] from T360 whole blood, analyzed with Bio-plex.

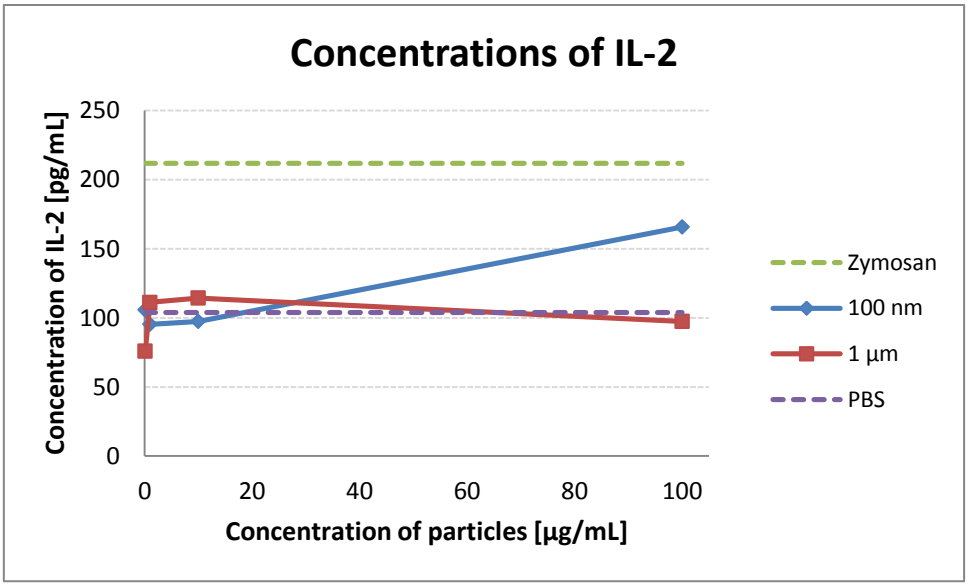

Figure L.6 Concentrations of IL-2 [pg/mL] from T360 whole blood, analyzed with Bio-plex.

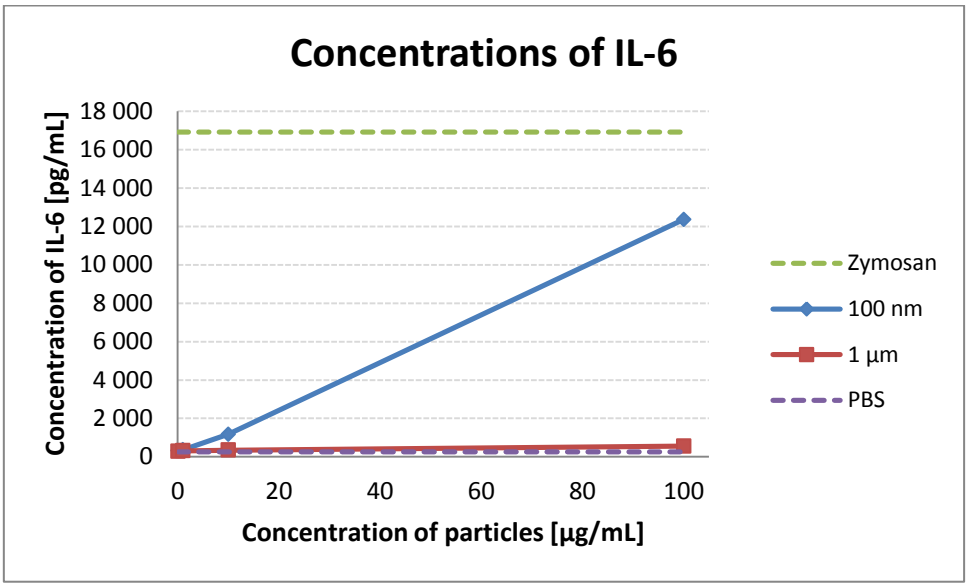

Figure L.7 Concentrations of IL-6 [pg/mL] from T360 whole blood, analyzed with Bio-plex.

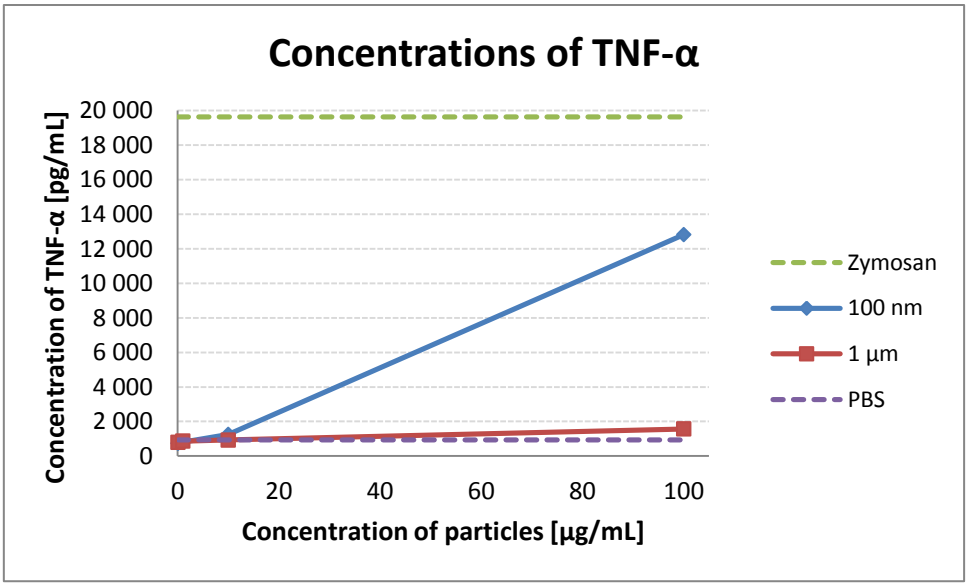

Figure L.8 Concentrations of TNF-α [pg/mL] from T360 whole blood, analyzed with Bio-plex.

Attachment M – Average results from whole blood experiments

Whole blood was used for flow cytometric, TCC and cytokine analyses. The average results for donors G-I are shown for each analysis in sections M.1-M.3, with their respective graphical illustrations in chapter 3.

M.1 Flow cytometry

M.1.1 Results

The average results for up-regulation of CD11b monocytes and granulocytes are listed in table M.1, and shown in figures 3.9a) and b) in chapter 3. Data analysis was performed using a FACScan program on samples of 5000 events, and it was gated for CD14+ monocytes.

Table M.1 Average values for CD11b monocytes and granulocytes (n=3), together with absolute zero time line (T_0), and positive and negative controls.

		Cell fluorescent intensity distribution	
Particle size	**Concentration of particles [µg/mL]**	**CD11b monocytes**	**CD11b granulocytes**
100 nm	**0.1**	64.100 ± 25.179	45.800 ± 13.750
	1.0	83.467 ± 31.697	103.133 ± 53.547
	10	158.333 ± 91.322	241.200 ± 168.189
	100	275.033 ± 88.109	326.067 ± 116.270
1 µm	**0.1**	76.833 ± 24.181	49.367 ± 15.171
	1.0	82.833 ± 35.493	55.900 ± 21.147
	10	89.700 ± 45.808	82.433 ± 55.191
	100	123.400 ± 89.482	175.433 ± 106.145
T_0		53.467 ± 1.429	67.967 ± 52.617
ATP		240.033 ± 97.074	150.233 ± 28.050
Zymosan		260.867 ± 34.168	476.733 ± 41.968
LPS		178.300 ± 54.988	59.700 ± 18.738
PBS		74.067 ± 35.995	60.033 ± 31.617

M.2 TCC

The average TCC results from T60 are listed in table M.2, and shown in figure 3.10.

Table M.2 TCC analysis (n=3) after stimulation with particles, positive and negative controls, in addition to absolute zero time line (T_0).

Particle size	Concentration of particles [µg/mL]	Concentrations of TCC [AU/mL]
100 nm	**0.1**	2.144 ± 1.810
	1.0	4.255 ± 1.932
	10	7.494 ± 2.344
	100	8.802 ± 0.868
1 µm	**0.1**	2.093 ± 1.053
	1.0	2.226 ± 0.939
	10	3.734 ± 1.740
	100	8.432 ± 1.189
T_0		1.212 ± 1.320
ATP		1.507 ± 1.265
Zymosan		11.204 ± 1.280
LPS		2.037 ± 0.286
PBS		1.485 ± 0.861

M.3 Cytokine analysis

M.3.1 IL-1β ELISA

The IL-1β results from T360 analyzed with regular ELISA are listed in table M.3, and shown in figure 3.11.

Table M.3 Average IL-1β analysis of three whole blood donors with ELISA, after stimulation with particles, positive and negative controls, in addition to absolute zero time line (T_0). A mark (*) indicates an undetectably low value.

Particle size	Concentration of particles [µg/mL]	Concentrations of IL-1β [pg/mL]
100 nm	**0.1**	51.011 ± 12.160
	1.0	54.311 ± 21.750
	10	78.550 ± 47.840
	100	183.518 ± 80.300
1 µm	**0.1**	49.810 ± 11.770
	1.0	62.498 ± 24.600
	10	40.258 ± 17.080
	100	15.889 ± 7.290
T_0		*
ATP		0.741 ± 0.400
Zymosan		239.331 ± 31.010
LPS		270.464 ± 11.550
PBS		49.107 ± 29.560

M.3.2 Bio-plex

The results from T360 of three independent whole blood donors analyzed with 17-plex are listed in tables M.4-M-7. Their respective graphical presentations are given in figures 3.12-3.15 in chapter 3.

Table M.4 Average IL-1β results of three whole blood donors analyzed with Bio-plex. A mark (*) indicates an undetectably low value.

Particle size	Concentration of particles [µg/mL]	Concentrations of IL-1β [pg/mL]
100 nm	**0.1**	142.57 ± 23.70
	1.0	161.47 ± 72.28
	10	159.84 ± 73.92
	100	868.41 ± 750.73
1 µm	**0.1**	115.21 ± 18.61
	1.0	134.73 ± 34.98
	10	101.28 ± 58.55
	100	61.81 ± 21.92
T_0		*
ATP		20.85 ± 14.79
Zymosan		904.67 ± 511.09
LPS		3 390.40 ± 1 107.56
PBS		109.75 ± 58.66

Table M.5 Average IL-2 results of three whole blood donors analyzed with Bio-plex. A mark (*) indicates an undetectably low value.

Particle size	Concentration of particles [µg/mL]	Concentrations of IL-2 [pg/mL]
100 nm	**0.1**	88.45 ± 17.21
	1.0	81.89 ± 22.40
	10	102.79 ± 4.63
	100	193.99 ± 38.06
1 µm	**0.1**	73.73 ± 5.80
	1.0	97.79 ± 12.42
	10	87.64 ± 23.20
	100	80.56 ± 15.14
T_0		*
ATP		33.33 ± 31.21
Zymosan		159.83 ± 52.93
LPS		224.36 ± 89.60
PBS		91.33 ± 15.67

Table M.6 Average IL-6 results of three whole blood donors analyzed with Bio-plex. A mark (*) indicates an undetectably low value.

Particle size	Concentration of particles [µg/mL]	Concentrations of IL-6 [pg/mL]
100 nm	**0.1**	604.53 ± 509.63
	1.0	482.40 ± 216.35
	10	1 179.13 ± 292.79
	100	17 608.65 ± 12 816.70
1 µm	**0.1**	301.95 ± 115.67
	1.0	342.20 ± 98.30
	10	375.61 ± 159.55
	100	420.83 ± 131.48
T_0		*
ATP		43.15 ± 41.87
Zymosan		8 883.21 ± 7 054.87
LPS		24 354.27 ± 12 121.21
PBS		284.45 ± 58.84

Table M.7 Average TNF-α results of three whole blood donors analyzed with Bio-plex. A mark (*) indicates an undetectably low value.

Particle size	Concentration of particles [µg/mL]	Concentrations of TNF-α [pg/mL]
100 nm	**0.1**	745.60 ± 22.03
	1.0	646.63 ± 141.76
	10	1 515.22 ± 698.49
	100	11 598.44 ± 6 407.69
1 µm	**0.1**	705.51 ± 127.42
	1.0	1 123.49 ± 553.36
	10	885.91 ± 652.88
	100	1 009.77 ± 530.12
T_0		*
ATP		200.17 ± 198.42
Zymosan		12 309.47 ± 8 068.84
LPS		20 288.00 ± 13 301.19
PBS		936.57 ± 183.43

Attachment N – Remaining cytokine results from Bio-plex

This attachment is supplementary to chapter 3. The purpose of it is to show the remaining of the seventeen cytokines analyzed with Bio-plex that yielded a dose-dependent, but non-significant response. All results in this attachment will only be illustrated graphically and shortly described in chapter 3 and 4. None of the results are normalized, and all uncertainties are shown as SD.

N.1 Results from samples with stimulated monocytes

There were in total nine cytokines that gave any positive responses from monocyte stimulation samples when analyzed with Bio-17-plex. These were IL-1β, IL-2, IL-6, IL-8, G-CSF, GM-CSF, IFN-γ, MCP-1 and TNF-α. Among these, IL-2, IL-6, GM-CSF, IFN-γ and TNF-α are presented in chapter 3 and attachment I. Results from the remaining four cytokines are presented here.

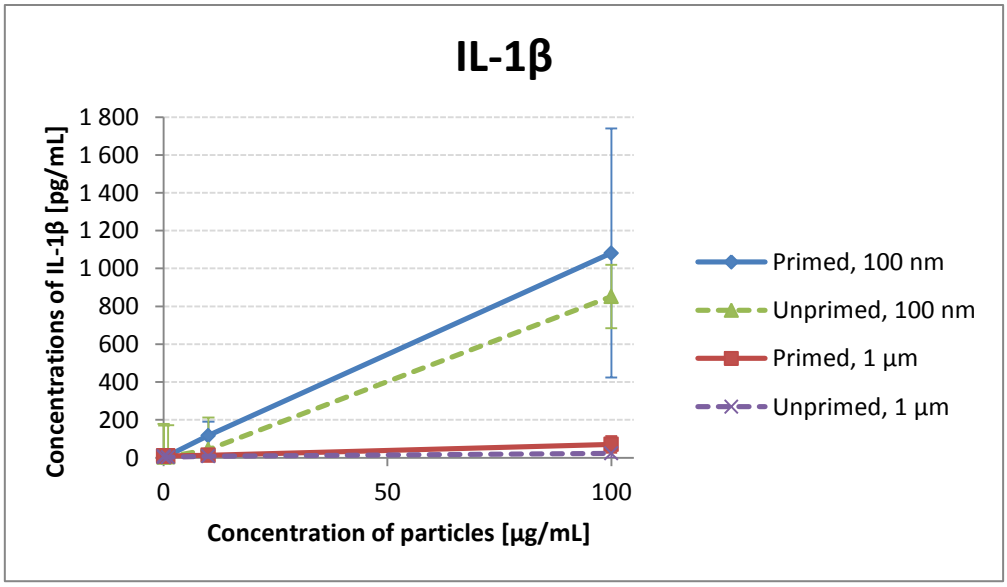

Figure N.1 Secretion of IL-1β from monocytes, analyzed with Bio-plex (n=3).

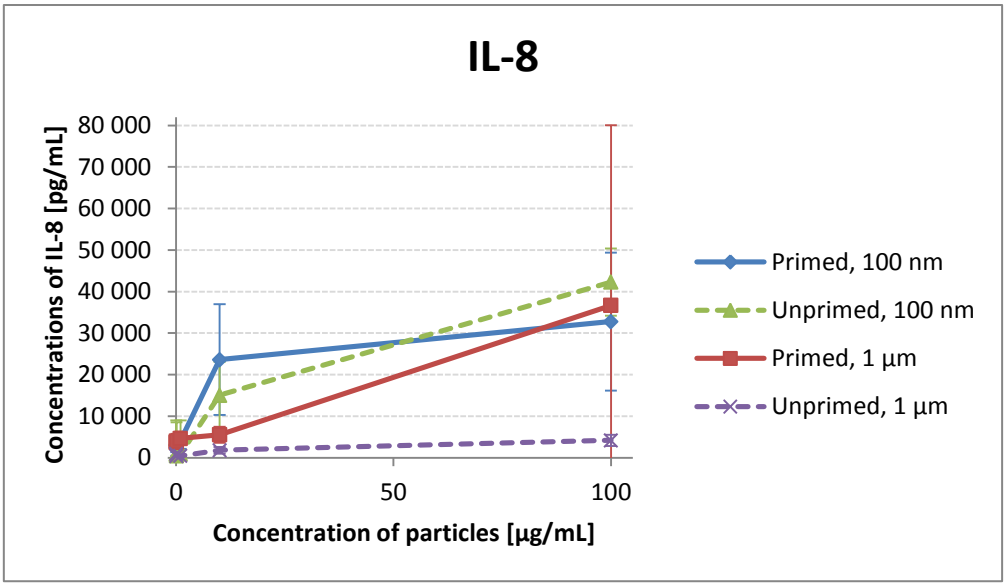

Figure N.2 Secretion of IL-8 from monocytes, analyzed with Bio-plex (n=3).

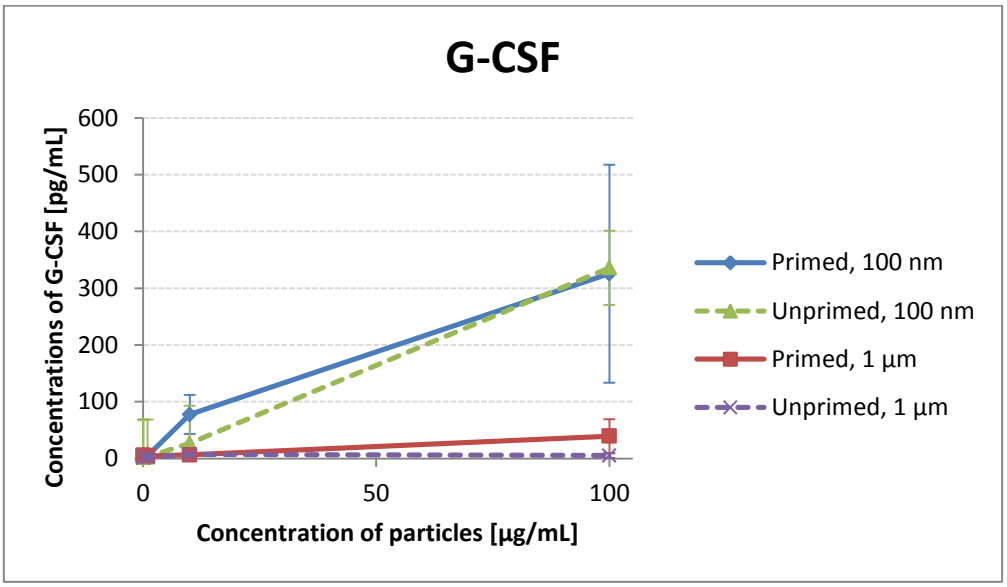

Figure N.3 Secretion of G-CSF from monocytes, analyzed with Bio-plex (n=3).

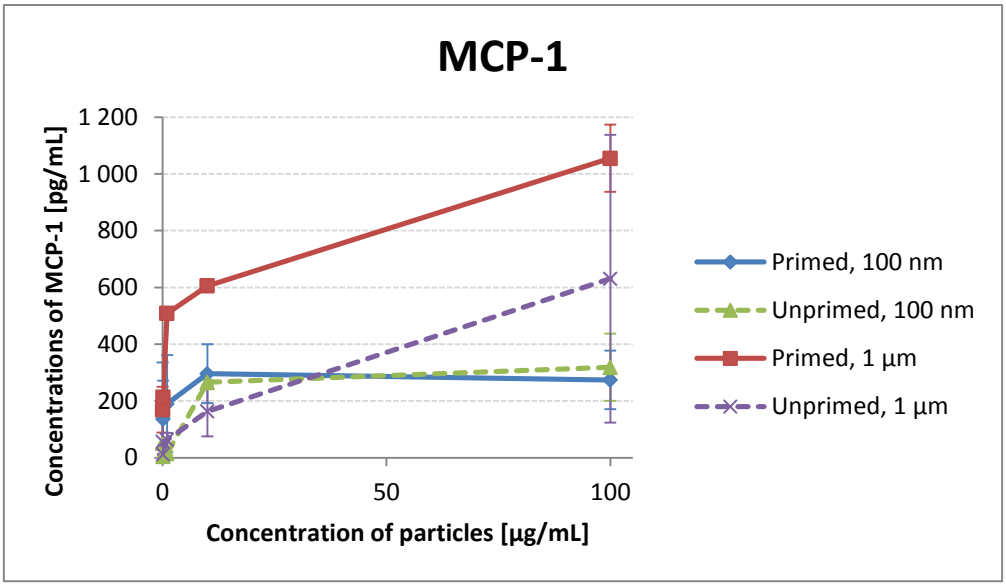

Figure N.4 Secretion of MCP-1 from monocytes, analyzed with Bio-plex (n=3).

N.2 Results from whole blood samples

All seventeen cytokines from the Bio-plex showed similar dose-response relationship from the whole blood samples. Among these, only IL-1β, IL-2, IL-6 and TNF-α gave any significance in the response, and are therefore presented in chapter 3 and attachment M. The remaining thirteen cytokines are presented here.

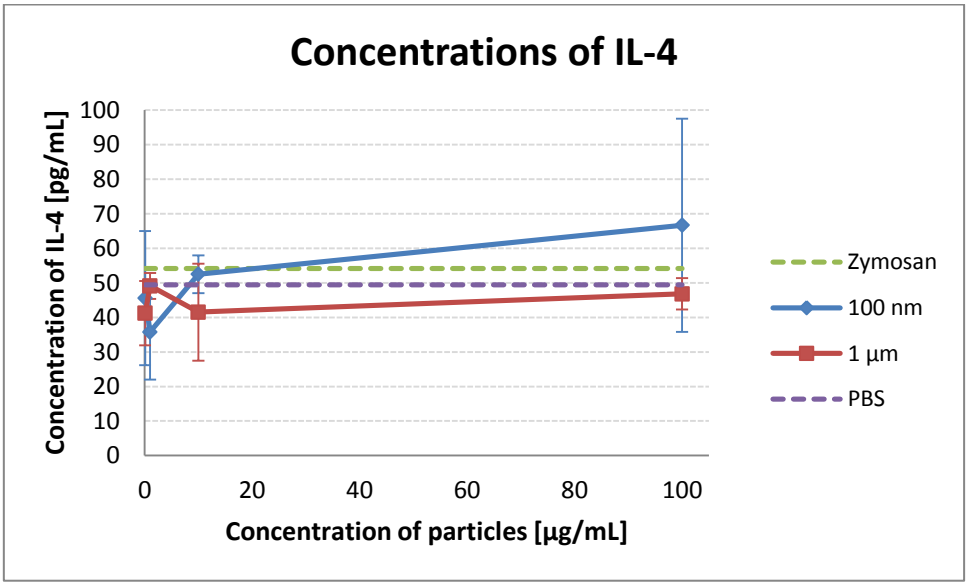

Figure N.5 Secretion of IL-4 from whole blood, analyzed with Bio-plex (n=3).

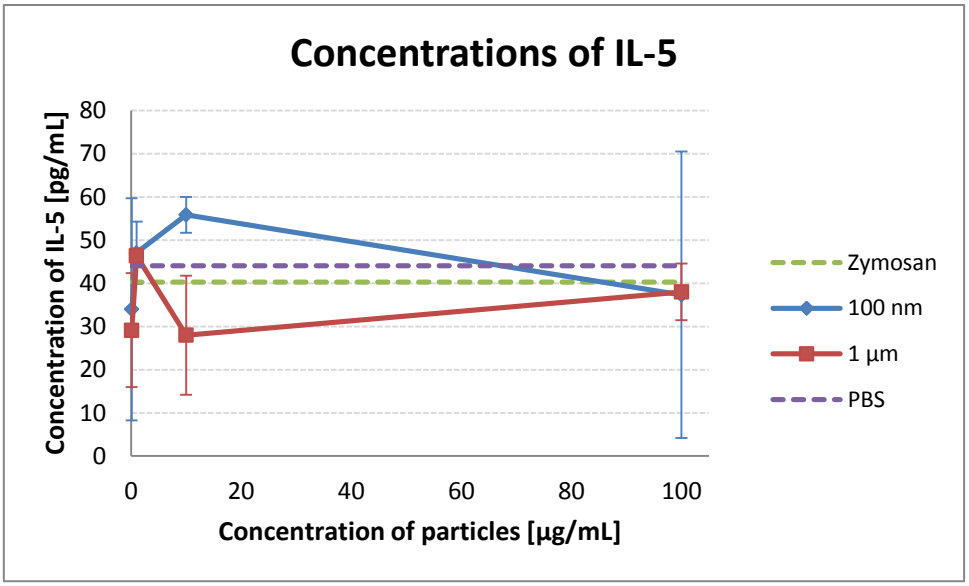

Figure N.6 Secretion of IL-5 from whole blood, analyzed with Bio-plex (n=3).

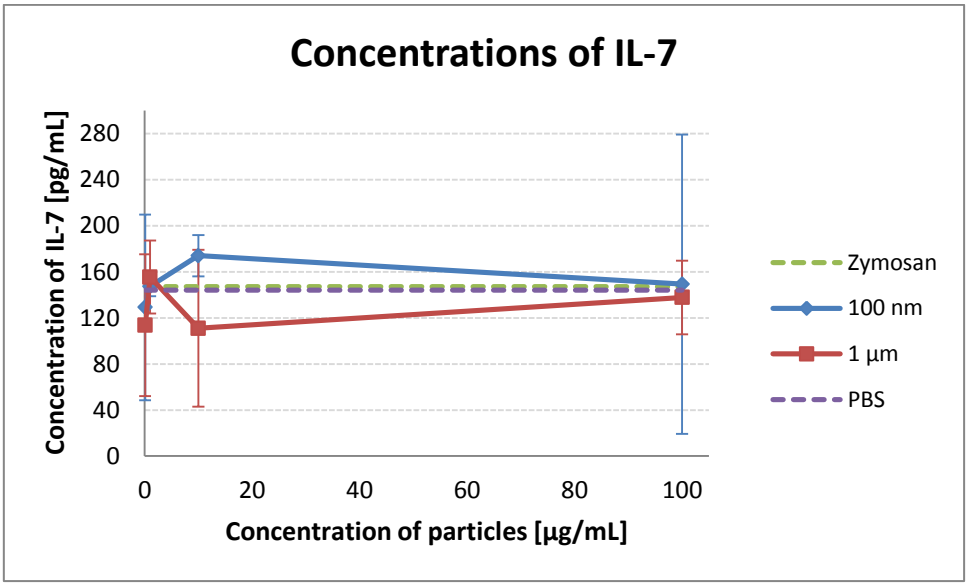

Figure N.7 Secretion of IL-7 from whole blood, analyzed with Bio-plex (n=3).

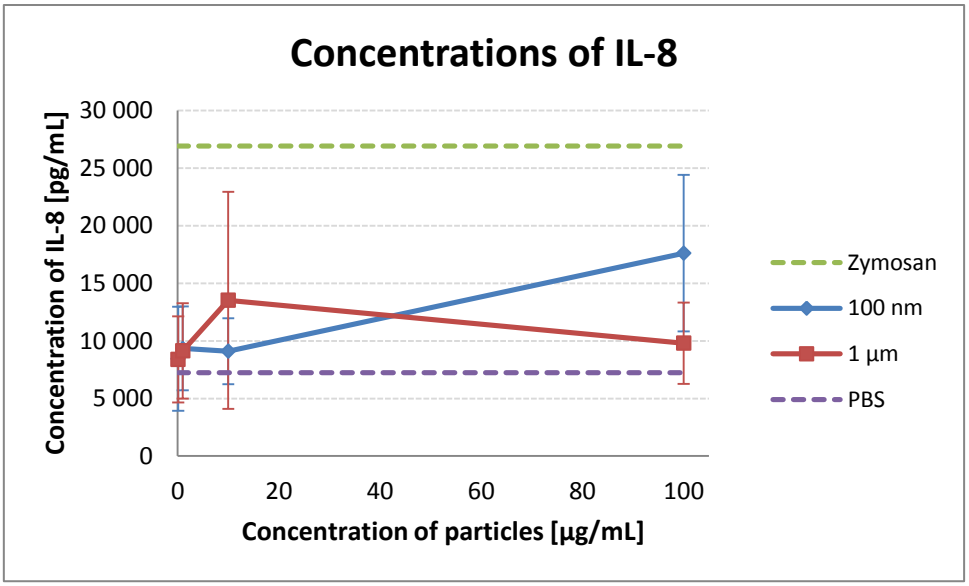

Figure N.8 Secretion of IL-8 from whole blood, analyzed with Bio-plex (n=3).

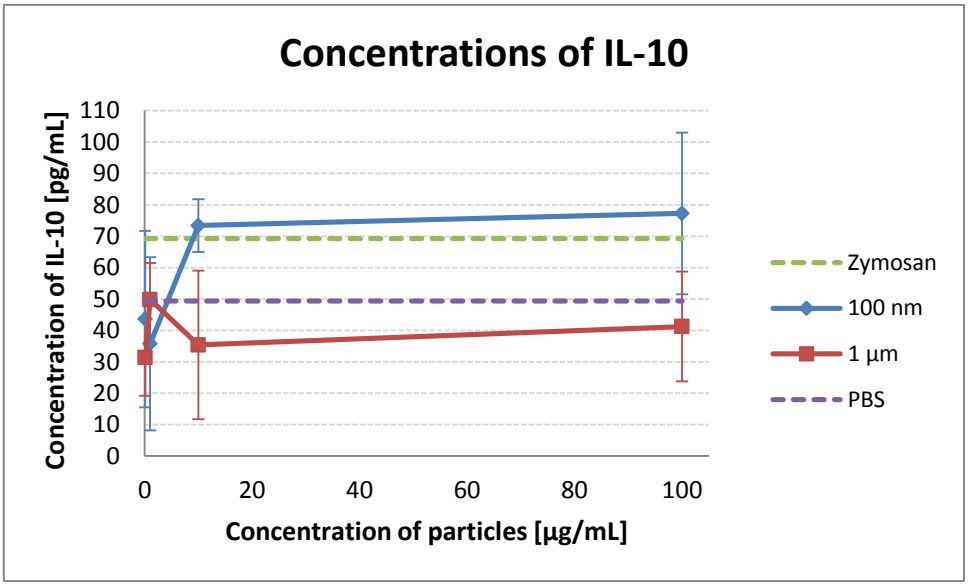

Figure N.9 Secretion of IL-10 from whole blood, analyzed with Bio-plex (n=3).

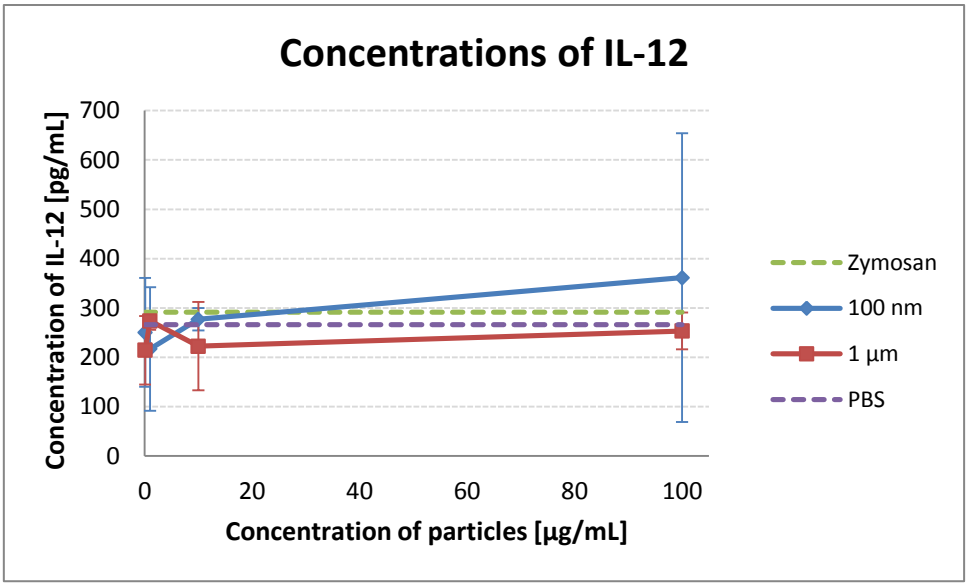

Figure N.10 Secretion of IL-12 from whole blood, analyzed with Bio-plex (n=3).

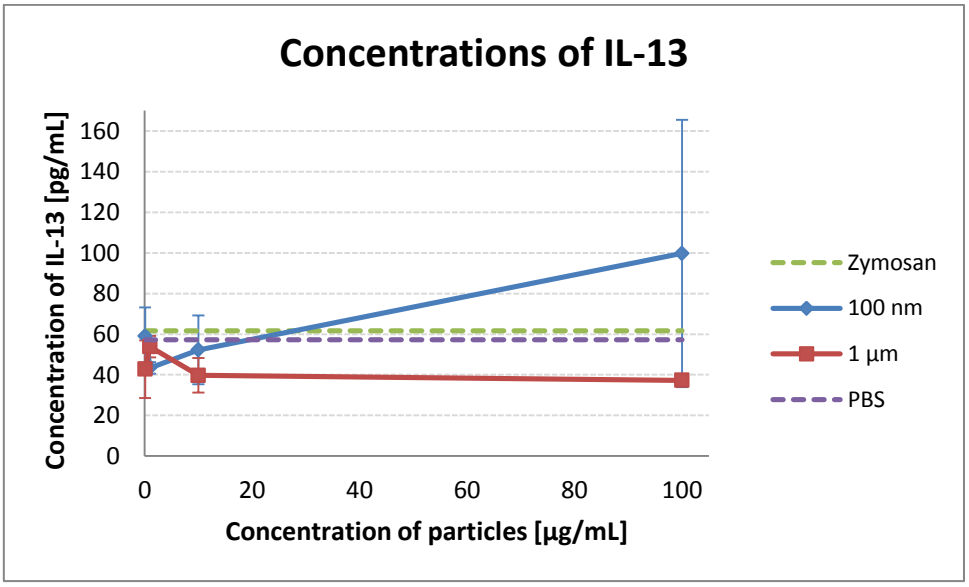

Figure N.11 Secretion of IL-13 from whole blood, analyzed with Bio-plex (n=3).

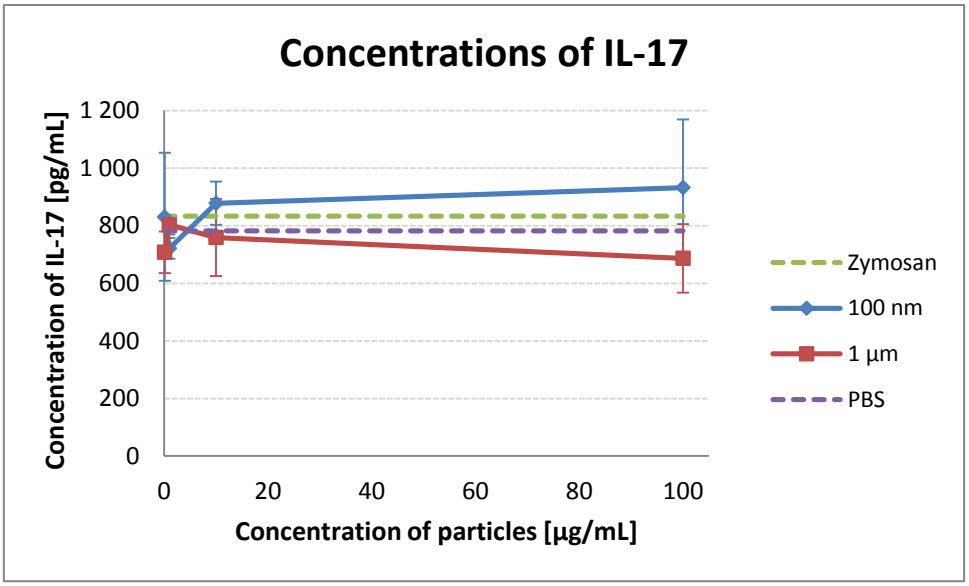

Figure N.12 Secretion of IL-17 from whole blood, analyzed with Bio-plex (n=3).

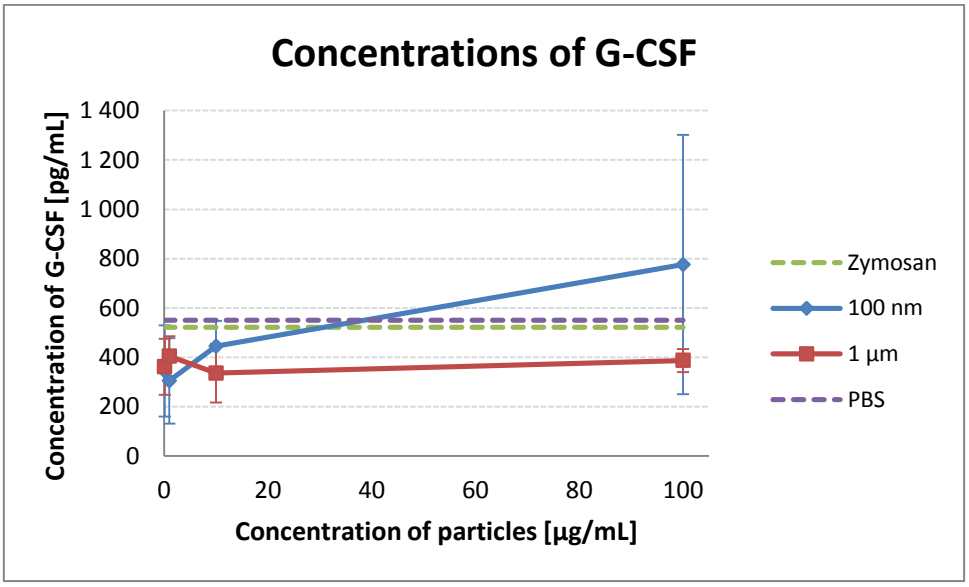

Figure N.13 Secretion of G-CSF from whole blood, analyzed with Bio-plex (n=3).

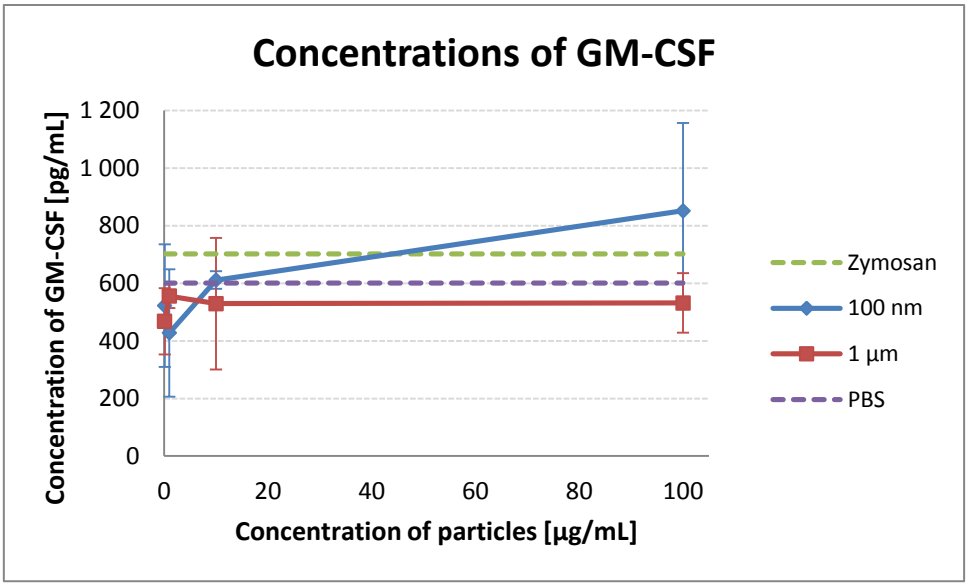

Figure N.14 Secretion of GM-CSF from whole blood, analyzed with Bio-plex (n=3).

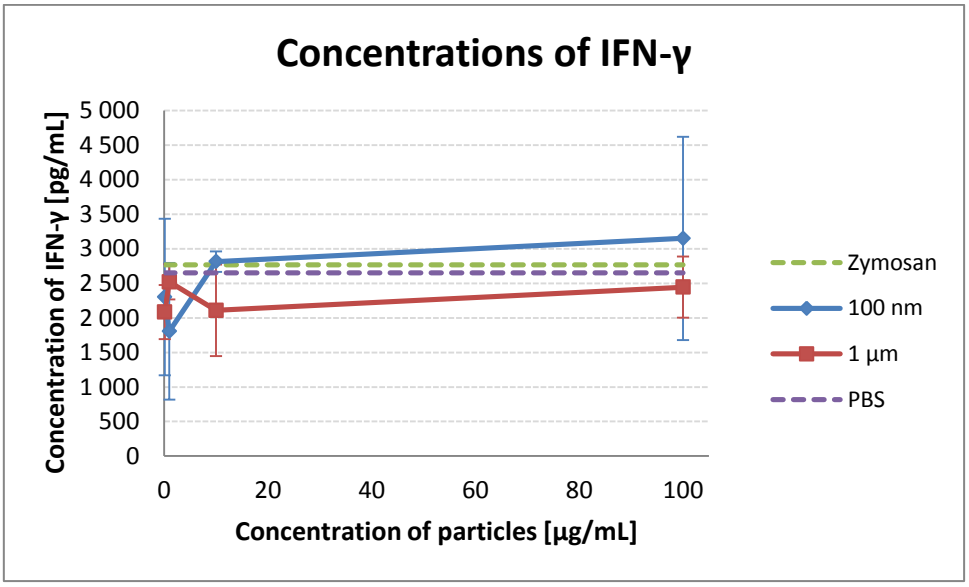

Figure N.15 Secretion of IFN-γ from whole blood, analyzed with Bio-plex (n=3).

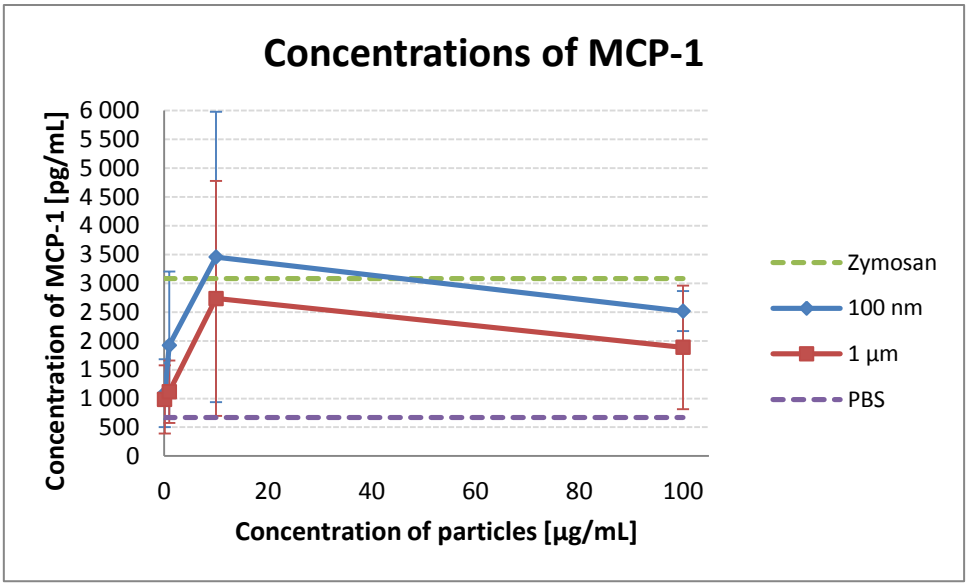

Figure N.16 Secretion of MCP-1 from whole blood, analyzed with Bio-plex (n=3).

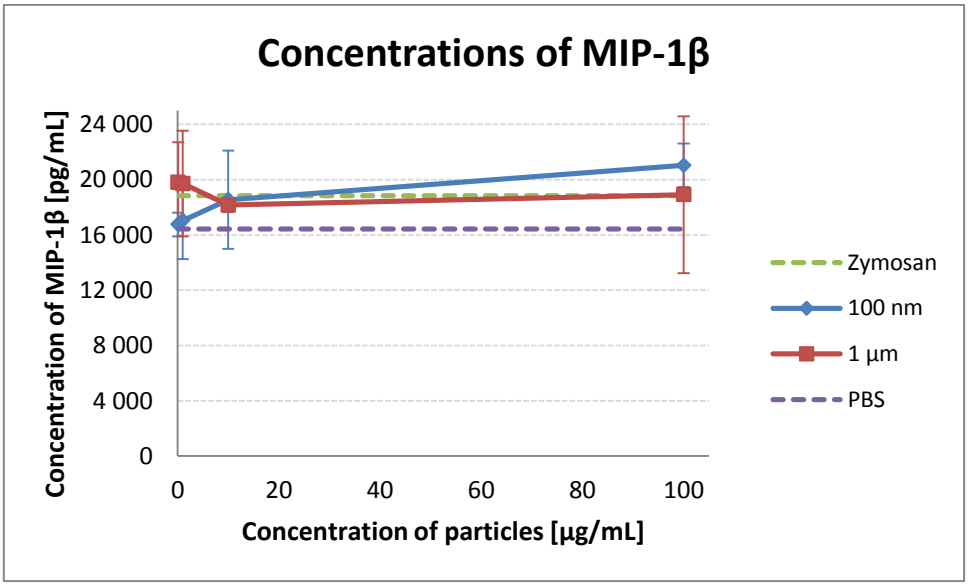

Figure N.17 Secretion of MIP-1β from whole blood, analyzed with Bio-plex (n=3).

Some cytokines show no differences in secretion of cytokines after stimulation with negative control (PBS) compared to positive control (Zymosan). This includes all cytokines except IL-8, IL-10 and MCP-1. This is interpreted as if there is no expression of these cytokines, whereas there is a non-significant expression of the remaining three cytokines. However, all results were included in this attachment to show that the secretion, no matter how little significant, show the same dose-response relationship as for those presented in chapter 3. In other words, the 100 nm particles result in higher cytokine secretion of all of the analyzed cytokines.

Attachment O – Datasheets for the submicron particles

The data sheets for both particles are included in this attachment.

chemicell GmbH
Eresburgstrasse 22-23
12103 Berlin
Germany

info@chemicell.com
chemicell.com

Product Information – nano-screenMAG-ARA

Product:	**nano-screenMAG-ARA**				
Article Number:	4415-1 (1 ml); 4415-5 (5 ml)				
Description:	Aqueous dispersion of magnetic fluorescent nanoparticles				
Application:	Weak cation exchanger; for covalent coupling of biomolecules (antibodies or proteins); see protocol A10				
Weight of Volume:	25 mg/ml				
Production Date:					
Lot:					
Core:	Magnetite				
Matrix:	Polysaccharide				
Size (hydrodynamic diameter):	100 nm	150 nm	200 nm		
Number of Particles:	~ 1.8 x 10^{15}/g	~ 5.2 x 10^{14}/g	~ 2.2 x 10^{14}/g		
Density:	~ 1.25 g/cm^3				
Type of Magnetization:	Superparamagnetic				
Functional Group:	Glucuronic acid - Carboxyl				
nano-screenMAG/ Fluorescence Color:	**B** **blue**	**G** **green**	**O** **orange**	**P** **pink**	**R** **red**
Excitation:	378 nm	476 nm	524 nm	547 nm	578 nm
Emission:	413 nm	490 nm	539 nm	581 nm	613 nm
Storage Buffer:	ddH_2O				
Autoclaved:	Yes				
Storage:	At 4 – 8 ℃. **Do not freeze!** **PROTECT FROM LIGHT!**				
Expiry date:	Two years after production date				

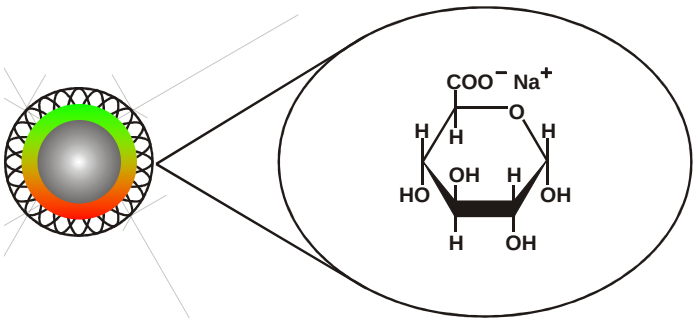

NOTE: The fluorescence of the nano-screenMAG particles is only detectable on the same side where the excitation takes place.

Please note that there is a difference in fluorescence observation between dissolved fluorescence molecules and solid fluorescence particles. Fluorescence spectrophotometer with a fluorescence detection unit with an angle of 90° to the excitation source will detect no or only weak fluorescence signals.

chemicell GmbH
Eresburgstrasse 22-23
12103 Berlin
Germany

info@chemicell.com
chemicell.com

Product Information – screenMAG-Carboxyl

Product:	**screenMAG-Carboxyl (Magnetic-Fluorescent Beads)**
Article Number:	2102-1 (1 ml); 2102-5 (5 ml)
Description:	Aqueous dispersion of magnetic fluorescent silica particles
Application:	For covalent coupling of biomolecules; see protocol A1
Lot Number:	0501/10
Production Date:	January 2010
Weight of Volume:	50 mg/ml
Core:	Maghemite
Matrix:	Silica, non-porous
Size (hydrodynamic diameter):	1.0 µm
Number of Particles:	1.8 x 10^{12}/g
Surface Area:	~ 50 m^2/g
Density:	~ 2.25 g/cm^3
Type of Magnetization:	Superparamagnetic
Functional Group:	Carboxyl (-COOH)
Carboxylation Degree:	~ 850 µmol COOH/g

screenMAG/	B	G	O	OP	RR	R
Fluorescence Color:	**blue**	**green**	**orange**	**orange**	**red**	**red**
Excitation:	400 nm	502 nm	526 nm	536 nm	540 nm	633 nm
Emission:	420 nm	525 nm	555 nm	617 nm	625 nm	672 nm

Autoclaved:	Yes
Storage Buffer / Solution:	ddH_2O
Storage:	At 4 – 8 °C. **Do not freeze!** **PROTECT FROM LIGHT!**
Expiry Date:	Two years after production date.
Note:	**For complete resuspension vortex thoroughly!**

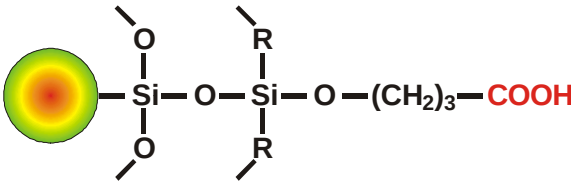

NOTE: The fluorescence of the screenMAG particles is only detectable on the same side where the excitation takes place.

Please note that there is a difference in fluorescence observation between dissolved fluorescence molecules and solid fluorescence particles. Fluorescence spectrophotometer with a fluorescence detection unit with an angle of 90° to the excitation source will detect no or only weak fluorescence signals.